



THE UNIVERSITY *of* EDINBURGH

Edinburgh Research Explorer



Search for the Higgs boson produced in association with a W boson and decaying to four b -quarks via two spin-zero particles in pp collisions at 13 TeV with the ATLAS detector

Search for the Higgs boson produced in association with a W boson and decaying to four b -quarks via two spin-zero particles in pp collisions at 13 TeV with the ATLAS detector

ATLAS Collaboration*

CERN, 1211 Geneva 23, Switzerland

Received: 28 June 2016 / Accepted: 6 October 2016 / Published online: 5 November 2016

© CERN for the benefit of the ATLAS collaboration 2016. This article is published with open access at Springerlink.com

Abstract This paper presents a dedicated search for exotic decays of the Higgs boson to a pair of new spin-zero particles, $H \rightarrow aa$, where the particle a decays to b -quarks and has a mass in the range of 20–60 GeV. The search is performed in events where the Higgs boson is produced in association with a W boson, giving rise to a signature of a lepton (electron or muon), missing transverse momentum, and multiple jets from b -quark decays. The analysis is based on the full dataset of pp collisions at $\sqrt{s} = 13$ TeV recorded in 2015 by the ATLAS detector at the CERN Large Hadron Collider, corresponding to an integrated luminosity of 3.2 fb^{-1} . No significant excess of events above the Standard Model prediction is observed, and a 95% confidence-level upper limit is derived for the product of the production cross section for $pp \rightarrow WH$ times the branching ratio for the decay $H \rightarrow aa \rightarrow 4b$. The upper limit ranges from 6.2 pb for an a -boson mass $m_a = 20$ GeV to 1.5 pb for $m_a = 60$ GeV.

1 Introduction

Following the discovery of the Higgs boson by the ATLAS and CMS Collaborations [1, 2] at the Large Hadron Collider (LHC), a comprehensive programme of measurements of the properties of this particle is underway. These measurements could uncover deviations from expected Standard Model (SM) branching ratios or allow for the possibility of decays into non-SM particles. Existing measurements constrain the non-SM or “exotic” branching ratio of the Higgs boson decays to less than approximately 30% at 95% confidence level (CL) [3–5]. Exotic decays are predicted by many theories of physics beyond the SM [6], including those with an extended Higgs sector such as the Next-to-Minimal Supersymmetric Standard Model (NMSSM) [7–11], several models of dark matter [12–16], models with a first-order elec-

troweak phase transition [17, 18], and theories with neutral naturalness [19–21].

One of the simplest possibilities is that the Higgs boson decays to a pair of new spin-zero particles, a , which in turn decay to a pair of SM particles, mainly fermions [6].¹ These kinds of models have been used to explain the recent observations of a gamma-ray excess from the galactic centre by the Fermi Large Area Telescope (FermiLAT) [22, 23]. Several searches have been performed for $H \rightarrow aa$. The D0 and ATLAS Collaborations have searched for a signal of $H \rightarrow aa \rightarrow 2\mu 2\tau$ in the a -boson mass ranges $3.7 \text{ GeV} \leq m_a \leq 19 \text{ GeV}$ and $3.7 \text{ GeV} \leq m_a \leq 50 \text{ GeV}$, respectively [24, 25]. The D0 and CMS Collaborations have searched for the signature $H \rightarrow aa \rightarrow 4\mu$ in the range $2m_\mu \leq m_a \leq 2m_\tau$ [24, 26]. In this analysis, the a -boson is assumed to have a negligibly small lifetime. Several other searches have been performed by the ATLAS, CMS and LHCb Collaborations for signatures that may correspond to a long-lived a -boson: displaced decays of jets or displaced decays of collimated leptons [27–32].

The result presented in this paper covers an unexplored decay mode in searches for $H \rightarrow aa$ by considering $a \rightarrow bb$. The a -boson can be either a scalar or a pseudoscalar under parity transformations, since the decay mode considered in this search is not sensitive to the difference in coupling. An example of a model with predominant $a \rightarrow bb$ decays is one where the new scalar mixes with the SM Higgs boson and inherits its Yukawa couplings [6]. This search focuses on the $pp \rightarrow WH$ process, with $W \rightarrow \ell\nu$ ($\ell = e, \mu$) and $H \rightarrow 2a \rightarrow 4b$ in the range $20 \text{ GeV} < m_a < 60 \text{ GeV}$. The resulting signature has a single lepton accompanied by a high multiplicity of jets originating from a bottom quark (b -jets). Since the b -jets are produced from the decay of the Higgs boson, they tend to have low transverse momentum (p_T) compared to m_H and can be overlapping, especially for

* e-mail: atlas.publications@cern.ch

¹ Throughout this paper, the symbol for a particle may be used to represent both the particle and its antiparticle.

light a -bosons. Events with an electron or muon, including those produced via leptonically decaying τ -leptons, are considered. The WH process is chosen for this search because the charged lepton in the final state provides a powerful handle to efficiently trigger and identify these events against the more ubiquitous background process of strong production of four b -jets. Several kinematic variables, including the reconstructed masses in the decay $H \rightarrow 2a \rightarrow 4b$, are used to identify signal events. The background estimation techniques, systematic uncertainties and statistical treatment closely follow those used in other ATLAS searches with similar signatures [33–36].

2 ATLAS detector

The ATLAS detector [37] covers nearly the entire solid angle² around the collision point. It consists of an inner tracking detector surrounded by a thin superconducting solenoid magnet producing a 2 T axial magnetic field, electromagnetic and hadronic calorimeters, and an external muon spectrometer incorporating three large toroid magnet assemblies. The inner detector consists of a high-granularity silicon pixel detector, including the newly installed insertable B-layer [38], and a silicon microstrip tracker, together providing precision tracking in the pseudorapidity range $|\eta| < 2.5$, complemented by a transition radiation tracker providing tracking and electron identification information for $|\eta| < 2.0$. The electromagnetic (EM) sampling calorimeter uses lead as the absorber material and liquid argon (LAr) as the active medium, and is divided into barrel ($|\eta| < 1.475$) and end-cap ($1.375 < |\eta| < 3.2$) regions. Hadron calorimetry is also based on the sampling technique, with either scintillator tiles or LAr as the active medium, and with steel, copper, or tungsten as the absorber material. The scintillator tile calorimeter is divided into barrel ($|\eta| < 1.0$) and end-cap ($0.8 < |\eta| < 1.7$) regions, and the LAr hadronic calorimeter includes an end-cap ($1.5 < |\eta| < 3.2$) and a forward ($3.1 < |\eta| < 4.9$) region. The muon spectrometer measures the deflection of muons with $|\eta| < 2.7$ using multiple layers of high-precision tracking chambers in a toroidal field of approximately 0.5 T and 1 T in the central and end-cap regions of ATLAS, respectively. The muon spectrometer is also instrumented with separate trigger chambers covering $|\eta| < 2.4$. A two-level trigger system, consisting of a custom-hardware level followed by a software-based level,

is used to reduce the event rate to a maximum of around 1 kHz for offline storage [39].

3 Event samples and object selection

The search presented in this paper is based on the proton–proton (pp) collision dataset collected by the ATLAS detector at the LHC at $\sqrt{s} = 13$ TeV with 25 ns bunch spacing during 2015. The full dataset corresponds to an integrated luminosity of 3.2 fb^{-1} . The data for this search were collected using the single-electron or single-muon triggers with the lowest transverse momentum thresholds available [39].

Electron candidates are reconstructed by associating an inner-detector track with an isolated energy deposit in the EM calorimeter [40,41]. Candidates are identified using the tight quality criteria and are required to have $p_T > 25$ GeV and $|\eta| < 2.47$, excluding the transition region between the barrel and end-cap EM calorimeters, $1.37 < |\eta| < 1.52$. Muon candidates are reconstructed by combining matching tracks in the inner detector and the muon spectrometer [42], and are required to satisfy the medium quality criteria and to have $p_T > 25$ GeV and $|\eta| < 2.4$. Events are required to have exactly one reconstructed electron or muon that is matched within a cone of size $\Delta R \equiv \sqrt{(\Delta\eta)^2 + (\Delta\phi)^2} = 0.15$ to the lepton candidate reconstructed by the trigger algorithms.

In order to distinguish leptons produced in the decays of W bosons from those produced in the decays of heavy-flavour hadrons, all lepton candidates are required to be consistent with originating from the primary interaction vertex, chosen as the vertex with the highest sum of the p_T^2 of its associated tracks. Furthermore, since lepton candidates arising from background sources, such as decays of hadrons, are typically embedded in jets, all lepton candidates are required to be isolated from other particles in the event. This is achieved by imposing a maximal allowed value on the energy deposited in the calorimeter and/or the momentum of inner-detector tracks within a cone of $\Delta R = 0.2$ around the direction of the lepton candidate's momentum. The isolation criteria, dependent on p_T and η , are applied to produce a nominal efficiency of at least 90% for electrons and muons from $Z \rightarrow \ell^+ \ell^-$ decays after all other identification criteria are applied [42].

Jets are reconstructed from clusters [43] of energy in the calorimeters using the anti- k_t clustering algorithm [44,45] with radius parameter $R = 0.4$. Jets are required to have $p_T > 20$ GeV and $|\eta| < 2.5$, and they are calibrated using energy- and η -dependent corrections. A track-based veto is used to suppress contributions from jets arising from additional pp interactions (pile-up) [46]. Jets consistent with the hadronisation of a b -quark are identified using information from track impact parameters and secondary vertices, which are combined in a multivariate discriminant [47]. The efficiency to identify b -quark jets (b -tagging) is approximately

² ATLAS uses a right-handed coordinate system with its origin at the nominal interaction point (IP) in the centre of the detector and the z -axis coinciding with the axis of the beam pipe. The x -axis points from the IP to the centre of the LHC ring, and the y -axis points upward. Cylindrical coordinates (r, ϕ) are used in the transverse plane, ϕ being the azimuthal angle around the beam pipe. The pseudorapidity is defined in terms of the polar angle θ as $\eta = -\ln \tan(\theta/2)$.

77% for a factor of 126 in rejection against light-quark and gluon jets, about 5 against jets originating from c -quarks, and about 10 against hadronically decaying τ -leptons, as determined in a simulated sample of top-quark pair ($t\bar{t}$) events [47–49]. Jets tagged by this multivariate discriminant, independently of the flavour of the quark that initiated it, are called b -tagged jets throughout the text, while the term b -jet is reserved for those jets originating from b -quark decays, as determined from simulation.

Jets are required to be separated from the lepton candidates by ΔR larger than 0.2 or 0.4 for electrons or muons, respectively. Electrons separated from the nearest jet by $0.2 < \Delta R < 0.4$ are considered part of the jet and not a lepton candidate. The transverse momentum imbalance \vec{E}_T^{miss} , the magnitude of which (E_T^{miss}) is commonly referred to as missing transverse momentum, is defined as the negative vector sum of the transverse momenta of calibrated selected objects, such as electrons, muons and jets. The transverse momenta of charged-particle tracks compatible with the primary vertex and not matched to any of those objects are also included in the negative vector sum [50,51].

4 Signal and background modelling

Simulated event samples are used to study the characteristics of the signal and to calculate its acceptance, and are also used for most of the SM background estimation. Signal samples of associated Higgs boson production with a W boson, $pp \rightarrow WH$, are generated with POWHEG-BOX v2-r3033 [52–55] using the CT10 parton distribution functions (PDFs) [56] at next-to-leading order (NLO). A Higgs boson mass of $m_H = 125 \text{ GeV}$ is assumed and the sample is normalised to the next-to-next-to-leading-order (NNLO) cross section recommended by the Higgs cross-section working group $\sigma_{\text{SM}}(WH) = 1.37 \text{ pb}$ [57]. The Higgs boson decay to two spin-zero a -bosons and the subsequent decay of each a -boson to a pair of b -quarks are simulated with PYTHIA v8.186 [58]. The a -boson decay is done in the narrow-width approximation and the coupling to the b -quarks is assumed to be that of a pseudoscalar. However, since the polarisation of the quarks is not observable, this search is insensitive to the specific parity hypothesis. PYTHIA v8.186 is used for the showering, hadronisation, and underlying-event (UE) simulation with the A14 set of tuned parameters (tune) [59]. The mass of the a -boson is varied for different signal hypotheses in the range $20 \text{ GeV} \leq m_a \leq 60 \text{ GeV}$, in 10 GeV mass steps. Different branching-ratio hypotheses are obtained by scaling the signal sample normalisation.

Samples of $t\bar{t}$ are also produced using the NLO POWHEG-BOX v2-r3026 generator with the CT10 PDFs. A top-quark mass (m_t) of 172.5 GeV is assumed. The POWHEG-BOX model parameter h_{damp} , which controls matrix element to

parton shower (PS) matching and effectively regulates the high- p_T radiation, is set to $h_{\text{damp}} = m_t$. This setting was found to best describe the $t\bar{t}$ -system p_T at $\sqrt{s} = 7 \text{ TeV}$ [60]. The baseline $t\bar{t}$ sample is interfaced to PYTHIA v6.428 [61] with the Perugia 2012 tune [62]. Alternative $t\bar{t}$ samples are generated using POWHEG-BOX v2-r3026 interfaced to HERWIG++ v2.7 [63] or MADGRAPH5_aMC@NLO [64] interfaced to HERWIG++. The effects of initial- and final-state radiation (ISR/FSR) are explored using two alternative POWHEG-BOX v2-r3026+PYTHIA v6.428 samples. The first has h_{damp} set to $2m_t$, the renormalisation and factorisation scales set to half the nominal value and uses the Perugia 2012 radHi UE tune, giving more radiation. The second sample uses the Perugia 2012 radLo UE tune, has $h_{\text{damp}} = m_t$ and has the renormalisation and factorisation scales set to twice the nominal value, giving less radiation [65]. The $t\bar{t}$ samples are normalised to the NNLO theoretical cross section of $832_{-51}^{+46} \text{ pb}$, obtained with TOP++ v2.0 [66–72].

The simulated $t\bar{t}$ events are categorised depending on the parton-level flavour content of additional particle jets³ not originating from the decay of the $t\bar{t}$ system. Events containing at least one additional particle jet matched to a b -hadron are labelled as $t\bar{t}$. Events containing at least one additional particle jet matched to a c -hadron and no b -hadron are labelled as $b\bar{b}$. The $t\bar{t}$ and $b\bar{b}$ categories are generically referred to as $t\bar{t}$ +HF events (with HF standing for “heavy flavour”). Remaining events are labelled $t\bar{t}$ +light-jets (referred to as $t\bar{t}$ +light) and also include events with no additional particle jets.

The associated heavy-flavour jets in $t\bar{t}$ +HF are modelled in POWHEG-BOX+PYTHIA via the PS evolution and are simulated with a five-flavour scheme. The $t\bar{t}$ modelling is improved by reweighting the top-quark p_T , $t\bar{t}$ -system p_T , and kinematic properties of the associated particle jets not originating from the top-quark decay [33] to agree with a $t\bar{t}$ sample generated at NLO with SHERPA+OPENLOOPS [73,74]. This SHERPA+OPENLOOPS sample is simulated with the four-flavour scheme (4FS) using SHERPA v2.1.1 [73] and the CT10 PDF set.

Samples of single-top-quark backgrounds corresponding to the Wt and s -channel production mechanisms are generated with POWHEG-BOX v2-r2819 [75,76] using the CT10 PDF set. Overlaps between the $t\bar{t}$ and Wt final states are handled using the “diagram removal” scheme [77]. Samples of t -channel single-top-quark events are generated using the POWHEG-BOX [78] NLO generator that uses the 4FS. The single-top-quark samples are normalised to the approximate NNLO theoretical cross sections [79–81]. The parton

³ Particle jets are reconstructed by clustering stable particles, excluding muons and neutrinos, using the anti- k_t algorithm with a radius parameter $R = 0.4$. Muons and neutrinos are excluded to better reproduce the jet reconstruction based on calorimeter clusters.

shower, hadronisation and underlying event are modelled using either PYTHIA v6.428 with the Perugia 2012 tune or HERWIG++ v2.7 with the UE-EE-5 [82] tune.

Samples of W/Z +jets events are generated with the SHERPA v2.1.1 generator. The matrix-element calculation is performed up to two partons at NLO and up to four partons at leading order (LO) using COMIX [83] and OPENLOOPS [74] and uses the CT10 PDFs. Both the W +jets and Z +jets samples are normalised to their respective inclusive NNLO theoretical cross section calculated with FEWZ [84].

Samples of diboson production $WW/WZ/ZZ$ +jets events are generated with the NLO generator SHERPA v2.1.1. Samples of $t\bar{t} + \gamma/W/Z$ events, including $t\bar{t} + WW$, are generated with up to two additional partons using MADGRAPH5_aMC@NLO and interfaced to PYTHIA v8.186. Samples of $t\bar{t} + H$ events are generated using MADGRAPH5_aMC@NLO and interfaced to HERWIG++ v2.7.

The main signal and background samples use the EVTGEN v1.2.0 [85] program to simulate the decay of heavy-flavour hadrons, except for those generated with SHERPA. All are then processed with the full simulation of the ATLAS detector [86] based on GEANT4 [87]. The alternative $t\bar{t}$ samples used to estimate systematic uncertainties are based on a fast simulation of the calorimeter response [88]. Events are generated with pile-up that is simulated with PYTHIA v8.186 [58] and are reweighted so that the distribution of the multiplicity of pile-up interactions matches the distribution observed in the data. Simulated event samples are processed using the same reconstruction algorithms and analysis chain as the data.

As described in Sect. 5, backgrounds are estimated by fitting predictions derived from simulation to data in several background-enriched samples. The only background prediction not derived from simulation is the multijet background, which contributes to the selected data sample when a jet is mis-reconstructed as a lepton and satisfies the identification criteria. In the electron channel, it consists of non-prompt electrons from heavy-flavour decays, from unidentified photon conversions or from jets with a high fraction of energy deposited in the EM calorimeter. In the muon channel, it consists of heavy-flavour decays and in-flight decays of light mesons.

The multijet background contribution is evaluated from data using the “matrix method” [34, 89, 90], which uses differences between the isolation properties of background (fake/non-prompt) leptons and signal (prompt) leptons from W boson decays. The estimate uses a sample enriched in multijet background events obtained by applying the full event selection except for loosening the lepton isolation requirement. Each event with a lepton candidate that satisfies at least the loosened isolation requirement is scaled by a weight that depends on whether this lepton candidate also satisfies the tighter isolation requirement. The weights are determined

from the efficiencies for fake/non-prompt and prompt leptons satisfying the loosened isolation requirement to also satisfy the tighter one [90]. These efficiencies are measured in data control samples enriched in either fake/non-prompt leptons, mostly multijet events, or prompt leptons, mostly $Z \rightarrow \ell^+\ell^-$ events. The shape of each multijet background distribution is derived by applying the same method to the sample obtained with an identical selection as described in Sect. 5, but lowering the b -tagged-jet multiplicity requirement to two. This strategy reduces the statistical uncertainty of the multijet background estimate, improving the stability of the fitting method described in Sect. 5.2.

5 Analysis strategy

The $H \rightarrow 2a \rightarrow 4b$ decay chain is expected to have multiple b -tagged jets, often three or four, satisfying the object selection. The dominant background arises from $t\bar{t}$ events. Preselected events are required to have exactly one electron or muon and at least three jets, of which at least two must be b -tagged. Events are required to satisfy $E_T^{\text{miss}} > 25$ GeV and the transverse mass⁴ must fulfil $m_T^W > 50$ GeV, in order to be consistent with W boson decays. Events are categorised into eight channels depending on the number of jets (3, 4 and ≥ 5) and the number of b -tagged jets (2, 3 and ≥ 4). These analysis channels are referred to as (n_j, m_b) indicating n selected jets including m b -tagged jets.

The categories most sensitive to the $H \rightarrow 2a \rightarrow 4b$ decay chain are (3j, 3b), (4j, 3b) and (4j, 4b). In these channels, background $t\bar{t}$ events can only satisfy the selection criteria if accompanied by additional b -tagged jets. In the case of (3j, 3b) or (4j, 3b), the main sources of $t\bar{t}$ background are events with jets mis-identified as b -jets, particularly from $W \rightarrow cs$ decays, where the c -jet is mis-identified, and from $W \rightarrow \tau\nu$, where the τ -lepton decays hadronically and is likewise mis-identified. In the case of (4j, 4b), the $t\bar{t}$ background includes more events with genuine b -quarks from gluon splitting to $b\bar{b}$ pairs. The main purpose of the five other jet and b -tagged-jet multiplicity channels is to constrain the $t\bar{t}$ +jets background prediction and the related systematic uncertainties (see Sect. 6) through a profile likelihood fit to data (see Sect. 5.2).

The $t\bar{t}$ +light background is dominant in the sample of events with exactly two or three b -tagged jets. The background processes $b\bar{b}$ and $t\bar{t}$ become more important as the jet and b -tagged-jet multiplicities increase. In particular, the $t\bar{t}$ background dominates for events with ≥ 5 jets and ≥ 4 b -tagged jets.

⁴ The transverse mass is defined as $m_T^W \equiv \sqrt{2E_T^{\text{miss}} p_T^\ell (1 - \cos \Delta\phi)}$, where p_T^ℓ is the transverse momentum of the lepton and $\Delta\phi$ is the azimuthal angle between the lepton and \vec{E}_T^{miss} directions.

5.1 Signal and background discrimination

In order to improve the sensitivity of the search, several kinematic variables are identified to distinguish between signal and background, and are combined into a boosted decision tree (BDT) multivariate discriminant [91] that uses the AdaBoost algorithm [92]. The BDT is trained to discriminate between signal events with an a -boson mass of 60 GeV and $t\bar{t}$ events. As described below, the variables chosen as input for the BDT do not depend strongly on the value of m_a and provide excellent separation between signal and background, so training each mass hypothesis separately with these variables would only slightly improve the sensitivity of the search. The training is performed separately for each of the channels (3j, 3b), (4j, 3b) and (4j, 4b) since the signal and background kinematics differ between them.

Signal events are characterised by the presence of a resonance resulting from the Higgs boson decay $H \rightarrow 2a \rightarrow 4b$. Two variables are used to reconstruct particles from the signal decay chain. The first is the reconstructed invariant mass of the b -tagged jets, m_{bbb} or m_{bbbb} , defined for events with three or four b -tagged jets respectively, which peaks around the Higgs boson mass for signal events. In the case of three b -tagged jets, the peak is due to events where two b -quarks are merged in a single jet or one of the b -quarks is very soft in an asymmetric decay and has a small impact on the kinematics. The second discriminating variable for events with four b -tagged jets is the minimum difference between the invariant masses of bb pairs (Δm_{\min}^{bb}). For signal events, two pairs of b -quarks originate from a pair of a -bosons, so for the correct jet pairing, $m_{bb} \approx m_a$, and the difference between the invariant masses of the bb pairs is smaller for signal than for $t\bar{t}$ background events.

Additional kinematic variables exhibit differences between signal and background. The H_T variable, defined as the scalar sum of p_T for all jets in the event, is a measure of the total hadronic energy in the event, which is typically larger for $t\bar{t}$ than for WH events. The transverse momentum of the W boson, p_T^W , constructed from the vector sum of the \vec{E}_T^{miss} and the lepton \vec{p}_T , is slightly higher for signal WH events, where the W boson recoils against the Higgs boson, than for background $t\bar{t}$ events. Another variable used is the average

angular separation between all pairs of b -tagged jets, referred to as $\Delta R_{\text{av}}^{bb}$. For background $t\bar{t}$ events, the b -tagged jets originate from the decays of the two top quarks and tend to be spatially more separated than for the signal. A related variable is the minimum ΔR separation between any b -tagged jet and the lepton, $\Delta R_{\min}^{\ell b}$. In $t\bar{t}$ background events, the lepton is typically closer to a b -tagged jet than in signal events, since the lepton and the nearest b -tagged jet often originate from the same top-quark decay. In the case of the signal, the Higgs boson and hence the b -jets recoil against the W boson, which the lepton comes from.

Finally, two variables are used to identify particles from the dominant $t\bar{t}$ background decay chain. The first variable is used in the (4j, 3b) channel to distinguish between $t\bar{t}$ events with two b -tagged jets from the top-quark decays and $t\bar{t}$ events with a third b -tagged jet from a mis-identified charm or light jet from the hadronically decaying W boson. The invariant mass of two b -tagged jets, selected as the pair with the smallest ΔR separation, and the non- b -tagged jet, m_{bbj} , reconstructs the hadronically decaying top quark, peaking around the top-quark mass for these background events. The second variable, used in the (4j, 4b) channel, is a variant of the m_{T2} observable, defined as the minimum “mother” particle mass compatible with all the transverse momenta and mass-shell constraints [93], that identifies events with several invisible particles. In the case of the $t\bar{t}$ background events, in addition to the E_T^{miss} from the neutrino from a leptonic W boson decay, invisible particles may arise from a τ -lepton decay or from a lost jet from a W boson. In these cases, the m_{T2} has an endpoint at the top-quark mass, which is not the case for the signal.

Table 1 indicates which variables are used to train each of the three BDT discriminants for the (3j, 3b), (4j, 3b), and (4j, 4b) categories. Figures 1, 2 and 3 show the expected distributions of the kinematical variables obtained after using the statistical procedure and the systematic uncertainties described in Sects. 5.2 and 6, respectively. These variables are used in the BDT discriminants for signal and background for all events that satisfy the event selection criteria, and are shown in Figs. 1, 2 and 3 inclusively in number of jets and b -tagged jets. The distributions are dominated by events with the minimum number of b -tagged jets. In this comparison, the jets in each event are ordered by value of the b -tagging discrim-

Table 1 List of variables used in the three signal regions as inputs to the BDT multivariate discriminant and used in the five control regions. The variables are described in the text

Region	m_{bbb}	m_{bbbb}	Δm_{\min}^{bb}	H_T	p_T^W	$\Delta R_{\text{av}}^{bb}$	$\Delta R_{\min}^{\ell b}$	m_{bbj}	m_{T2}
Signal									
(3j, 3b)	✓			✓	✓	✓	✓		
(4j, 3b)	✓			✓	✓	✓		✓	
(4j, 4b)		✓	✓	✓		✓			✓
Control				✓					

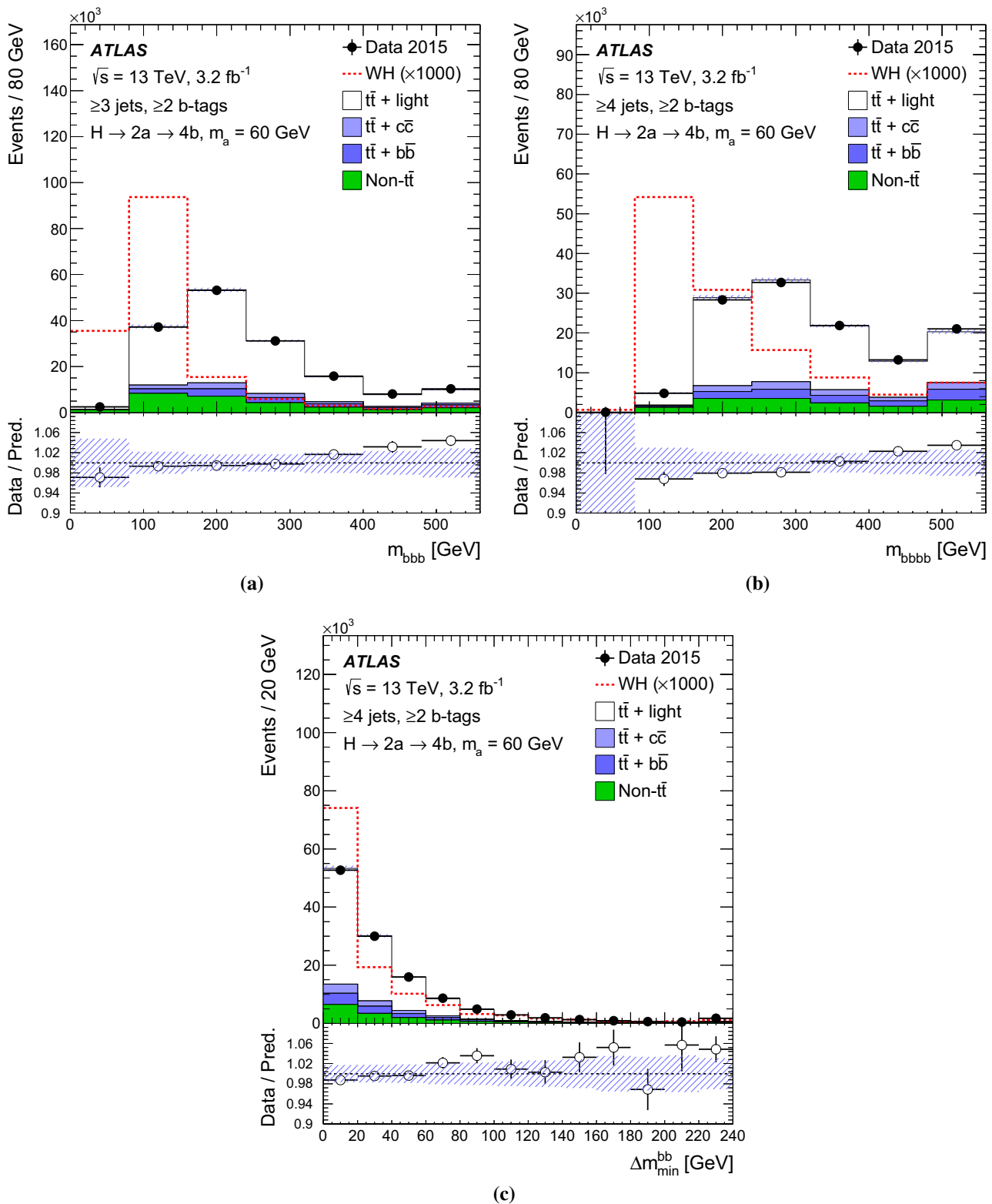


Fig. 1 Comparison of data with the SM background predictions for the distributions of **a** m_{bbb} , **b** m_{bbbb} and **c** Δm_{\min}^{bb} in the sample that is inclusive in number of jets and b -tagged jets. Distributions for the signal model ($WH, H \rightarrow 2a \rightarrow 4b$), with $m_a = 60 \text{ GeV}$, normalised to the SM $pp \rightarrow WH$ cross section, assuming $\text{BR}(H \rightarrow aa) \times \text{BR}(a \rightarrow bb)^2 = 1$ and scaled by a factor of 1000, are overlaid. The

hashed area represents the total uncertainty in the background. Comparisons use events with ≥ 3 jets, except when at least four jets are necessary to define the variable, in which case events with ≥ 4 jets are used. The last bin contains the overflow. Markers are not drawn if they are outside the y-axis range

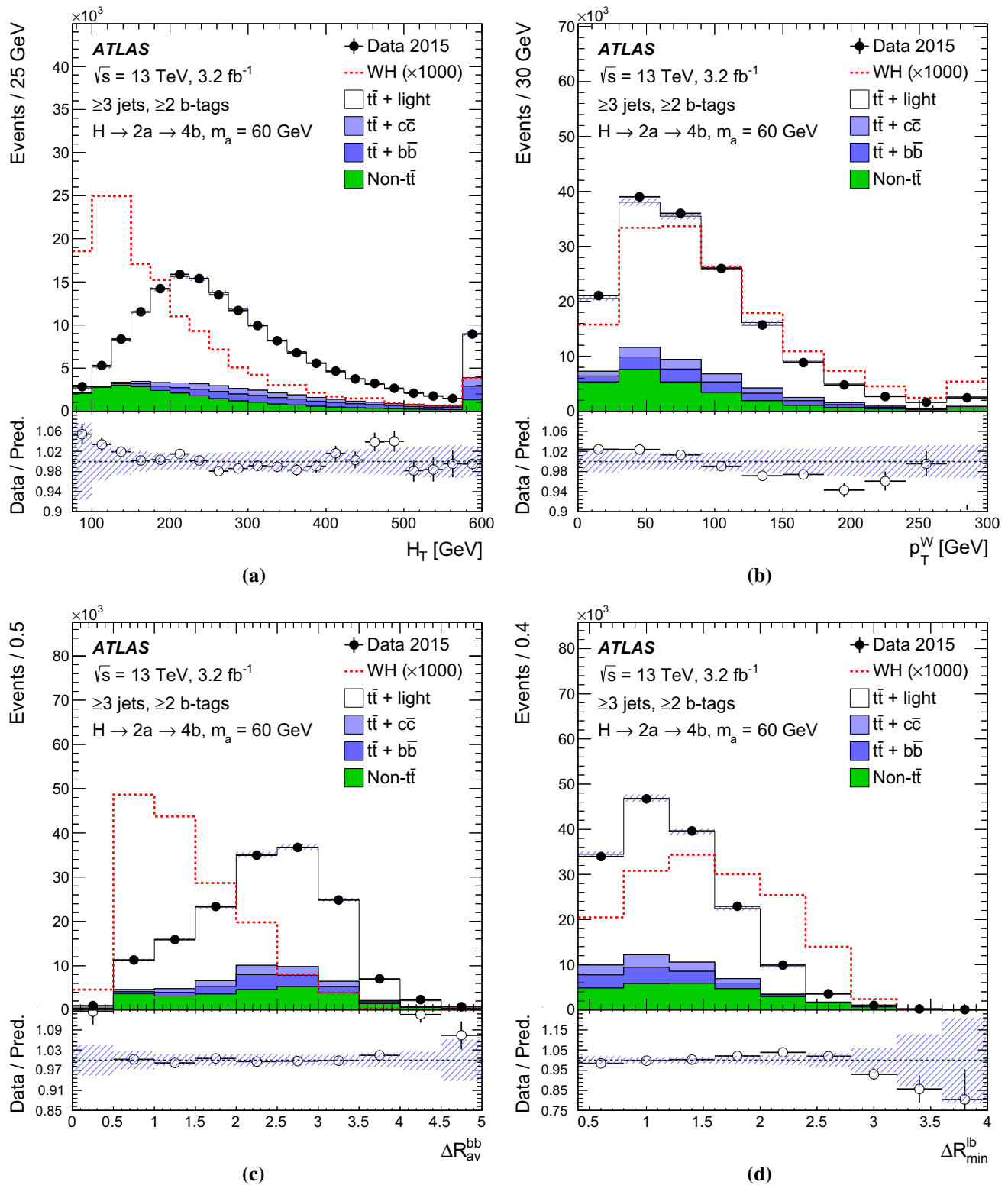


Fig. 2 Comparison of data with the SM background predictions for the distributions of **a** H_T , **b** p_T^W , **c** ΔR_{av}^{bb} and **d** ΔR_{min}^{lb} in the sample that is inclusive in number of jets and b -tagged jets. Distributions for the signal model (WH , $H \rightarrow 2a \rightarrow 4b$), with $m_a = 60$ GeV, normalised to the

SM $pp \rightarrow WH$ cross section, assuming $\text{BR}(H \rightarrow aa) \times \text{BR}(a \rightarrow bb)^2 = 1$ and scaled by a factor of 1000, are overlaid. The hashed area represents the total uncertainty in the background. The last bin contains the overflow

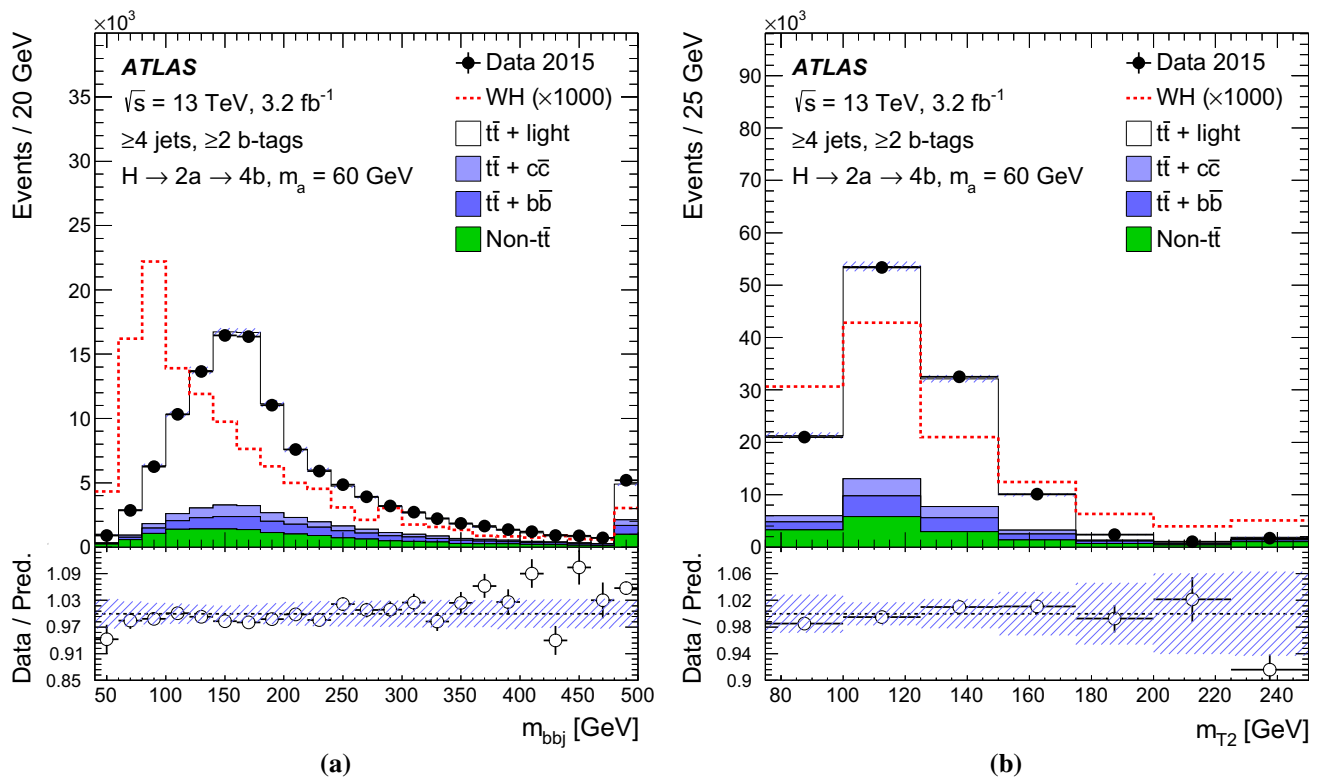


Fig. 3 Comparison of data with the SM background predictions for the distributions of **a** m_{bbj} and **b** m_{T2} in the sample that is inclusive in number of jets and b -tagged jets. Distributions for the signal model (WH , $H \rightarrow 2a \rightarrow 4b$), with $m_a = 60$ GeV, normalised to the SM

$pp \rightarrow WH$ cross section, assuming $\text{BR}(H \rightarrow aa) \times \text{BR}(a \rightarrow bb)^2 = 1$ and scaled by a factor of 1000, are overlaid. The hashed area represents the total uncertainty in the background. The last bin contains the overflow

inant and those with the highest score are used to calculate the input variables of the BDT, even if they do not satisfy the b -tagging criteria used in this analysis. The distributions are similar to those obtained in each analysis channel and indicate that each variable individually has some signal and background discrimination power. The tail in the m_{bbbb} distribution for signal events, shown in Fig. 1, is mainly formed by events with jets mis-associated to the a -boson decay. The tail is greatly reduced in the signal regions with the tighter requirement on the number of b -tagged jets. Figure 4 shows the BDT discriminant for signal and background events that satisfy the event selection criteria inclusively in number of jets and b -tagged jets. These distributions are used to validate the BDT modelling in background-enriched samples with kinematic properties that are similar to those in the signal regions.

5.2 Fitting procedure

The distributions of the final discriminants in the eight analysis channels considered are combined to test the presence of a signal. The BDT discriminant, described in Sect. 5.1, is used for the channels enriched with signal, (3j, 3b), (4j, 3b) and

(4j, 4b), while the H_T distribution is used in the five control channels. The statistical analysis is based on a binned likelihood function constructed as a product of Poisson probability terms over all bins considered in the search.

The likelihood function, L , depends on the parameter of interest, the signal-strength μ , defined as:

$$\mu = \sigma(WH) \times \text{BR}(H \rightarrow aa) \times \text{BR}(a \rightarrow bb)^2, \quad (1)$$

where $\sigma(WH)$ is the production cross section for $pp \rightarrow WH$.

Systematic uncertainties in the signal and background predictions (see Sect. 6) are accounted for in the likelihood function as a set of nuisance parameters, θ . These parameters are implemented as Gaussian priors in the case of shape uncertainties and log-normal priors for uncertainties affecting the normalisation, with width parameters corresponding to the size of the respective uncertainties. Statistical uncertainties in the background estimates in each bin of the discriminant distributions are also taken into account via dedicated nuisance parameters in the fit.

The background-only hypothesis is tested by fitting the background predictions to the observed data, setting $\mu = 0$

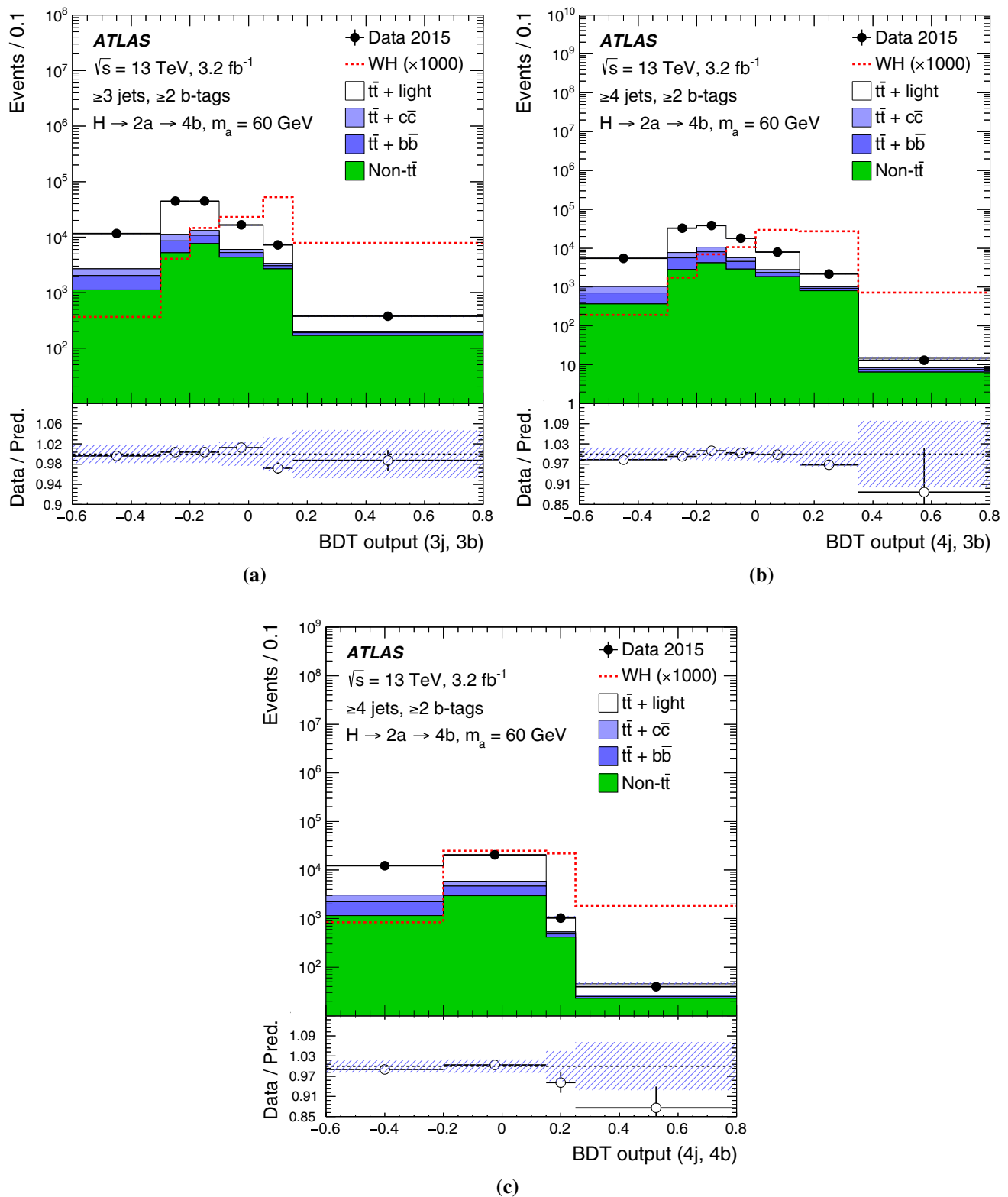


Fig. 4 Comparison of data with the SM background predictions for the distributions of **a** BDT (3j, 3b), **b** BDT (4j, 3b), and **c** BDT (4j, 4b) in the sample that is inclusive in number of jets and b -tagged jets. Distributions for the signal model ($WH, H \rightarrow 2a \rightarrow 4b$), with $m_a = 60 \text{ GeV}$, normalised to the SM $pp \rightarrow WH$ cross section, assuming $\text{BR}(H \rightarrow aa) \times \text{BR}(a \rightarrow bb)^2 = 1$ and scaled by a factor of 1000,

are overlaid. The hashed area represents the total uncertainty in the background. Comparisons use events with ≥ 3 jets, except when at least four jets are necessary to define the BDT discriminant, in which case events with ≥ 4 jets are used. The BDT output is determined in the range $[-1, 1]$. The first and last bin contain the underflow and overflow, respectively

Table 2 Summary of the impact of the considered systematic uncertainties (in %) on the normalisation of the signal ($m_a = 60$ GeV) and the main backgrounds for the (4j, 4b) channel after the fit. The total uncertainty can differ from the sum in quadrature of individual sources due to correlations between them

Systematic uncertainty [%]	$WH, H \rightarrow 2a \rightarrow 4b$	$t\bar{t} + \text{light}$	$t\bar{t} + c\bar{c}$	$t\bar{t} + b\bar{b}$
Luminosity	4	4	4	4
Lepton efficiencies	1	1	1	1
Jet efficiencies	6	4	4	4
Jet energy resolution	5	1	3	1
Jet energy scale	4	2	4	3
b -tagging efficiency	17	5	5	9
c -tagging efficiency	1	6	12	4
Light-jet-tagging efficiency	2	29	5	3
Theoretical cross sections	–	5	5	5
$t\bar{t}$: modelling	–	6	45	26
$t\bar{t}$ +HF: normalisation	–	–	35	18
$t\bar{t}$ +HF: modelling	–	–	–	5
Signal modelling	7	–	–	–
Total	21	31	54	21

and maximising the likelihood over θ . The best-fit μ is obtained by performing a binned likelihood fit to the data under the signal-plus-background hypothesis, i.e. maximising the likelihood function $L(\mu, \theta)$ over μ and θ . The nuisance parameters θ allow variations of the predicted signal and background according to the corresponding systematic uncertainties, and their fitted values correspond to the deviations from the nominal predictions that globally provide the best fit to the data. This procedure allows a reduction of the impact of systematic uncertainties on the search sensitivity by taking advantage of the highly populated background-dominated channels included in the likelihood fit.

6 Systematic uncertainties

Several sources of systematic uncertainty are considered that affect the normalisation or the shape of the signal and background contributions to the final discriminant distributions. Each source of systematic uncertainty is considered to be uncorrelated with other sources, but correlated across processes and channels where appropriate. This section describes the sources of systematic uncertainty considered in this search.

Luminosity and pile-up The uncertainty in the integrated luminosity is 5%, affecting the overall normalisation of all processes estimated from the simulation. It is derived, following a methodology similar to that detailed in Ref. [94], from a calibration of the luminosity scale using x – y beam-separation scans performed in August 2015. The uncertainty associated with the modelling of pile-up arises mainly from differences between the expected and observed fraction of the visible pp cross section.

Reconstructed objects Uncertainties associated with leptons arise from the reconstruction, identification and trigger

efficiencies, as well as lepton momentum scales and resolutions. These efficiencies are measured using tag-and-probe techniques on $Z \rightarrow \ell^+\ell^-$ data and simulated events. The small differences found are corrected in the simulation. Negligible uncertainties arise from the corrections applied to adjust the lepton momentum scales and resolutions in simulation to match those in data. The combined effect of all these uncertainties results in an overall normalisation uncertainty in the signal and background of less than 1%.

Uncertainties associated with jets arise from the efficiency of jet reconstruction and identification, as well as the jet energy scale and resolution. The largest contribution comes from the jet energy scale uncertainty, which depends on jet p_T and η . It affects the normalisation of signal and backgrounds by approximately 5% in the most sensitive search channels. Uncertainties associated with energy scales and resolutions of leptons and jets are propagated to E_T^{miss} . An uncertainty in the contribution from charged-particle tracks is also included in the E_T^{miss} uncertainty [51]. Additional uncertainties originating from the modelling of the underlying event are negligibly small.

Several uncertainties are associated with the identification of the jet flavour, in particular the modelling of the b -, c -, and light-jet-tagging efficiencies in the simulation, which are corrected to match the efficiencies measured in data [47–49]. These uncertainties are derived from studies performed with data at $\sqrt{s} = 8$ TeV and are extrapolated to 13 TeV. They depend on the jet p_T and the light-jet-tagging additionally depends on the jet η . The sources of systematic uncertainty in the tagging efficiencies are taken as uncorrelated between b -jets, c -jets, and light-jets. They have their largest impact in the (4j, 4b) channel, resulting in 4% uncertainty in the $t\bar{t}$ background normalisation associated with the uncertainty in the b -jet-tagging scale factors, 8% uncertainty in the $b\bar{b}$ background normalisation associated with the uncer-

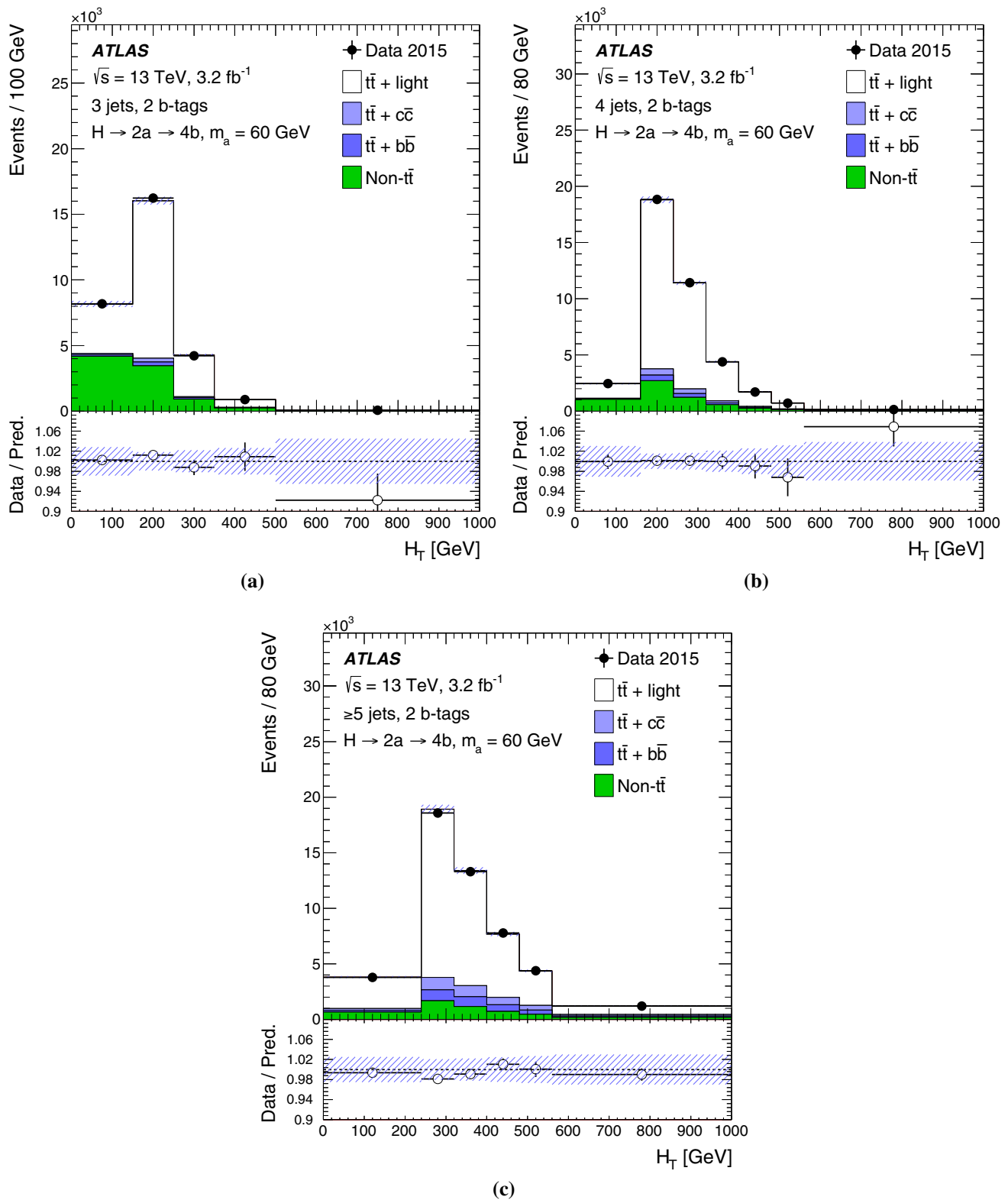


Fig. 5 Comparison between the data and prediction for the distribution of the H_T variable used in the control regions with two b -tagged jets. These distributions are after the fit is performed on data under

the background-only hypothesis. The *hashed area* represents the total uncertainty in the background. The last bin contains the overflow

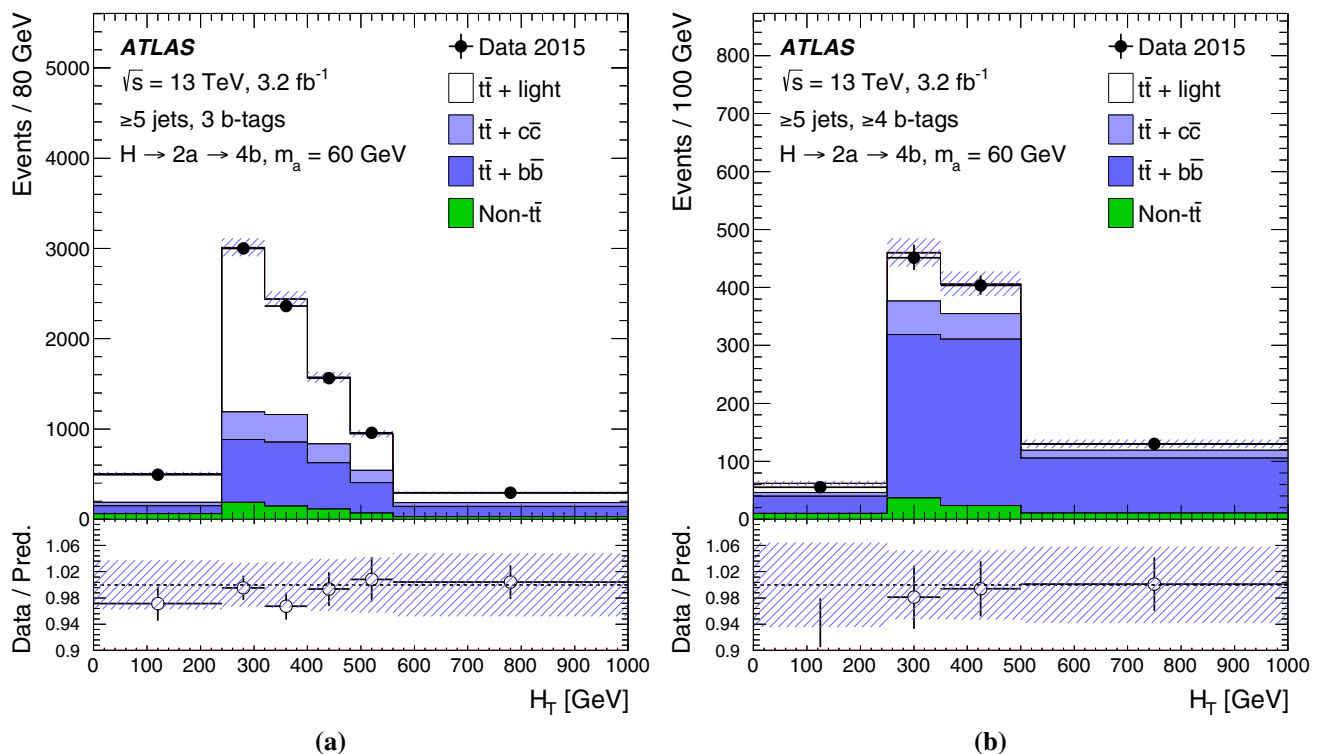


Fig. 6 Comparison between the data and prediction for the distribution of the H_T variable used in the control regions with three and four b -tagged jets. These distributions are after the fit is performed on data under the background-only hypothesis. The last bin contains the overflow

tainty in the c -jet-tagging scale factors, and 45% uncertainty in the normalisation of the $t\bar{t}$ +light background normalisation associated with the uncertainty in the light-jet-tagging scale factors.

Background modelling: Several sources of systematic uncertainty affecting the modelling of $t\bar{t}$ +jets are considered. An uncertainty of approximately 6% is assumed for the $t\bar{t}$ production cross section [72], including contributions from variations of the factorisation and renormalisation scales, and uncertainties arising from the PDFs, α_S , and the top-quark mass.

A 50% uncertainty is assigned to the normalisation of the $t\bar{t}$ background. This uncertainty is derived from a comparison of the $t\bar{t}$ production cross sections predicted by POWHEG-BOX+PYTHIA and by SHERPA+OPENLOOPS at NLO (see Sect. 4) [33]. An additional 50% uncertainty is assigned to the component of the $t\bar{t}$ background that contains exactly one b -hadron not originating from a top-quark decay matched to a particle jet. The same systematic uncertainty of 50% is applied to the normalisation of the $b\bar{b}$ background in the absence of an NLO prediction for this process. The uncertainties in the $t\bar{t}$ components and $b\bar{b}$ are treated as uncorrelated.

Systematic uncertainties affecting the shape of the $t\bar{t}$ background account for the choice of generator, the choice of parton shower and hadronisation models, and the effects

of initial- and final-state radiation. The uncertainties are derived from comparisons between the nominal simulation and alternative samples produced with POWHEG-BOX or MADGRAPH5_aMC@NLO interfaced to PYTHIA or HERWIG++ (see Sect. 4) and are treated as uncorrelated across $t\bar{t}$ +jets backgrounds. Additional uncertainties are evaluated to account for the use of SHERPA+OPENLOOPS NLO to model the $t\bar{t}$ background. In particular, uncertainties are assessed for the PDFs, as well as the choice of shower recoil model and scale. An additional uncertainty accounts for limited knowledge of the component of the $t\bar{t}$ background originating from multiple parton interactions, which is not included in the NLO prediction. These systematic uncertainties are estimated following the methods described in Ref. [33].

The uncertainties in the predictions for the total cross sections for the other background processes are applied as normalisation uncertainties and are: 5% for each of the W/Z +jets and diboson processes, +5%/−4% for single-top-quark production, 15% for $t\bar{t} + \gamma/W/Z$ and +9%/−12% for $t\bar{t}H$ [79–81, 95–99]. An additional uncertainty of 24% is added in quadrature for each additional jet to account for the extrapolation to higher jet multiplicities, based on a comparison among different algorithms for merging LO matrix-element and parton shower simulations [100]. An uncertainty is applied to the modelling of the single-top-

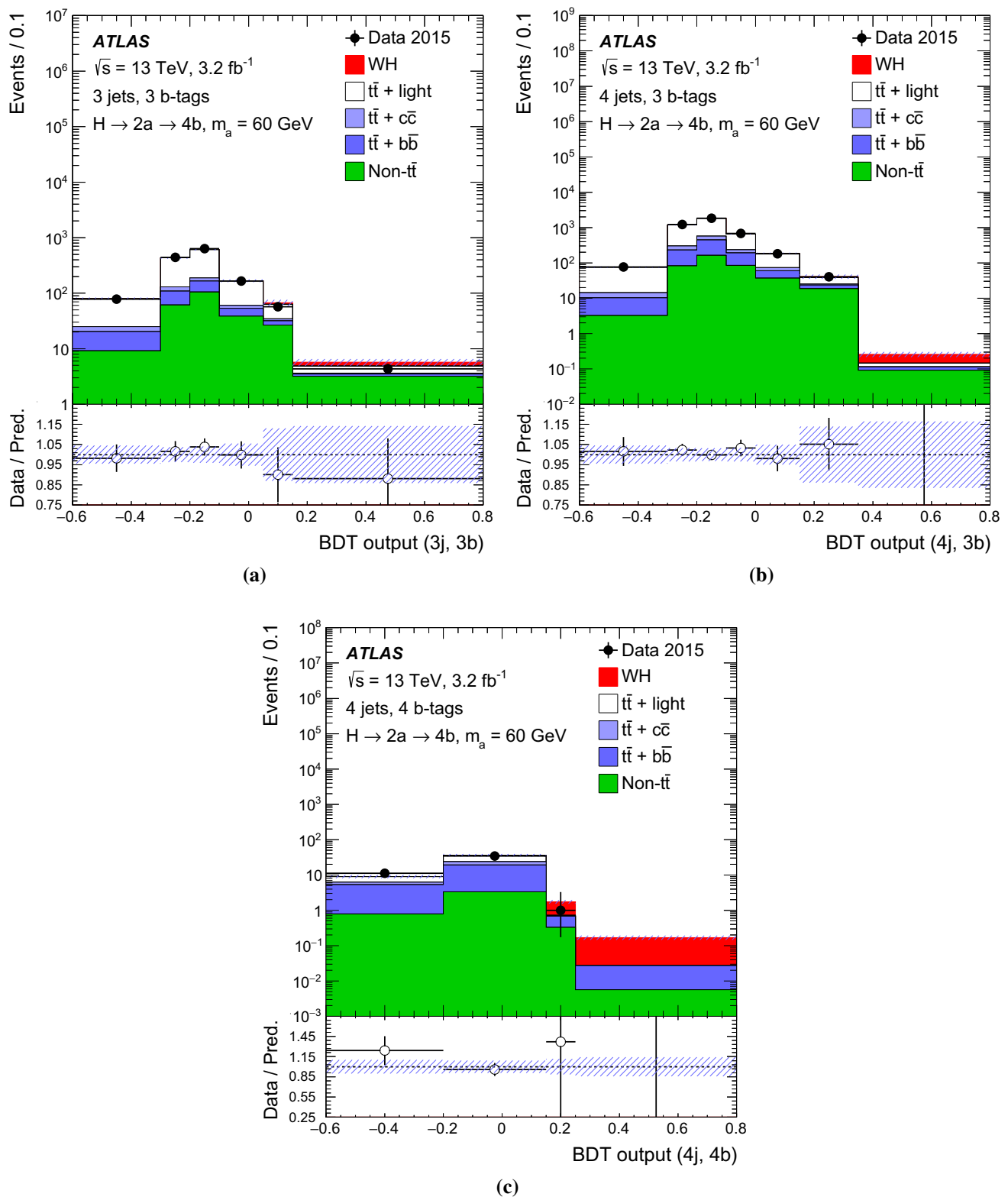


Fig. 7 Comparison between the data and prediction for the distribution of the BDT discriminant used in the signal regions. These distributions are after the fit is performed on data under the background-only hypothesis. The hashed area represents the total uncertainty in the background. The distributions for the signal model ($WH, H \rightarrow 2a \rightarrow 4b$), with

$m_a = 60 \text{ GeV}$, are normalised to the SM $pp \rightarrow WH$ cross section, assuming $\text{BR}(H \rightarrow aa) \times \text{BR}(a \rightarrow bb)^2 = 1$. The BDT output is determined in the range $[-1, 1]$. The first and last bin contain the underflow and overflow, respectively. Markers are not drawn if they are outside the y-axis range

Table 3 Expected event yields of the SM background processes in the three signal regions after performing the fit with the background-only hypothesis. The observed data and the number of expected signal events are also indicated. The signal yields are quoted for some representative values of m_a and assume the SM $pp \rightarrow WH$ cross section,

Process	(3j, 3b)	(4j, 3b)	(4j, 4b)
$t\bar{t}$ + light	1089 ± 76	2940 ± 180	53 ± 16
$t\bar{t}$ + $c\bar{c}$	70 ± 28	280 ± 110	21 ± 11
$t\bar{t}$ + $b\bar{b}$	172 ± 55	610 ± 160	74 ± 15
$t\bar{t}$ + $\gamma/W/Z$	0.8 ± 0.1	4 ± 1	0.4 ± 0.1
W + jets	93 ± 31	129 ± 40	2 ± 1
Z + jets	18 ± 12	14 ± 10	–
Single-top-quark	135 ± 13	208 ± 17	8 ± 1
Multijet	48 ± 20	67 ± 28	4 ± 2
Dibosons	4 ± 1	9 ± 1	0.6 ± 0.4
$t\bar{t}$ + H	0.7 ± 0.1	4 ± 1	0.8 ± 0.2
Total	1640 ± 58	4270 ± 130	165 ± 15
Data	1646	4302	166
$WH, H \rightarrow 2a \rightarrow 4b$			
$m_a = 60$ GeV	10 ± 2	9 ± 1	3 ± 1
$m_a = 40$ GeV	11 ± 2	10 ± 2	2 ± 1
$m_a = 20$ GeV	6 ± 1	5 ± 1	0.7 ± 0.2

quark background to account for the choice of scheme to handle the overlaps between the $t\bar{t}$ and Wt final states. Small uncertainties arising from scale variations, which change the amount of initial-state radiation and thus the event kinematics, are also considered.

Uncertainties in the estimate of the multijet background come from the limited number of events in the data sample without the isolation requirement and from uncertainties in the measured non-prompt and prompt lepton efficiencies. The normalisation uncertainty assigned to this background is 60%, as derived by comparing the multijet background prediction to data in control regions obtained by inverting the requirements on the E_T^{miss} and on m_T^W . An uncertainty in the shape of the predicted background distribution covers the difference between the prediction obtained by reducing the required number of b -tagged jets and the prediction at high b -tagged-jet multiplicity (see Sect. 4).

Signal modelling Several sources of systematic uncertainty affect the theoretical modelling of the signal acceptance. Uncertainties originate from the choice of PDFs, the factorization and renormalization scales, and the parton shower, hadronisation and underlying event models.

As described in Sect. 5.2, a binned maximum-likelihood fit is performed on the distributions of the final discriminant in the eight channels considered. The fit constrains systematic uncertainties from several sources thanks to the large number of events in the analysis channels considered and

$\sigma_{\text{SM}}(WH) = 1.37$ pb [57], and $\text{BR}(H \rightarrow aa) \times \text{BR}(a \rightarrow bb)^2 = 1$. The uncertainties include statistical and systematic components (systematic uncertainties are discussed in Sect. 6). The total uncertainty can differ from the sum in quadrature of individual sources due to correlations between them

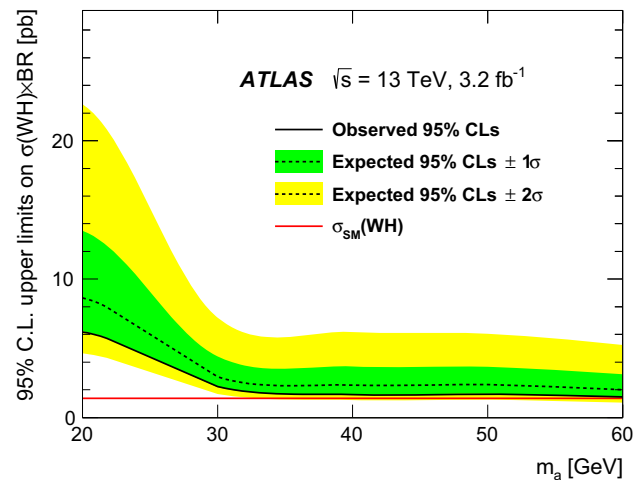


Fig. 8 Upper limit at 95% CL on $\sigma(WH) \times \text{BR}$, where $\text{BR} = \text{BR}(H \rightarrow aa) \times \text{BR}(a \rightarrow bb)^2$, versus m_a . The observed (CL_s) values (solid black line) are compared to the expected (median) (CL_s) values under the background-only hypothesis (dotted black line). The surrounding shaded bands correspond to the 68 and 95% CL intervals around the expected (CL_s) values, denoted by $\pm 1\sigma$ and $\pm 2\sigma$, respectively. The solid red line indicates the SM $pp \rightarrow WH$ cross section, assuming $\text{BR}(H \rightarrow aa) \times \text{BR}(a \rightarrow bb)^2 = 1$. Markers are not drawn if they are outside the y-axis range

the variations in the background composition across channels. The channels with two b -tagged jets constrain the main uncertainties affecting the $t\bar{t}$ +light background prediction, while the channels with ≥ 5 jets and ≥ 3 b -tagged jets are

sensitive to the dominant uncertainties affecting the $t\bar{t}$ +HF background prediction.

After performing the fit, the leading sources of systematic uncertainty are the modelling of the $t\bar{t}$ +jets background and b -, c - and light-jet-tagging efficiencies. Table 2 summarises the systematic uncertainties by indicating their impact on the normalisation of the signal and the main backgrounds in the (4j, 4b) channel. The uncertainties for the other signal channels (3j, 3b) and (4j, 3b) are reduced to about 7% for the $t\bar{t}$ +light contribution, mainly due to the reduced dependence on the light-jet-tagging efficiency, and to about 12% for the signal, primarily because of the reduced b -tagging efficiency uncertainty due to the lower b -tagged-jet multiplicity requirement.

7 Results

The best fit of the background predictions to data in the binned maximum-likelihood fit is shown in Figures 5, 6 and 7. Table 3 shows the resulting yields and uncertainties for the signal regions after the fit. The SM background yields obtained after performing the fit are in agreement with the results from a fit using only the H_T distributions in the control regions.

In the absence of a significant excess of data above the background prediction, upper limits are calculated for μ , defined in Eq. (1). The modified frequentist method (CL_s) [101] and asymptotic formulae [102] are used. Figure 8 shows the upper limits obtained at 95% CL. The mass hypothesis m_a is tested in steps of 10 GeV between 20 and 60 GeV. The observed (expected) 95% CL upper limits on μ range from 6.2 (8.6) pb, assuming $m_a = 20$ GeV, to 1.5 (2.0) pb, assuming $m_a = 60$ GeV. Assuming the SM $pp \rightarrow WH$ cross section, it is not possible to set limits on the branching fraction with the amount of data used. The reduced sensitivity for the light a -boson hypothesis is due to a lower acceptance caused by overlapping b -jets. The event yields indicated in Table 3 correspond to the sum of all BDT bins, while the fit is most sensitive in the highest BDT bins, where the data are slightly below the prediction, and hence the observed limit is slightly lower than the expected one.

8 Conclusion

This paper presents a dedicated search for exotic decays of the Higgs boson to a pair of new spin-zero particles, $H \rightarrow aa$, where the new a -boson decays to b -quarks. The search focuses on the process $pp \rightarrow WH$ where the Higgs boson is produced in association with a W boson. The analysis uses the pp collision dataset at $\sqrt{s} = 13\text{TeV}$ recorded by the ATLAS detector at the LHC in 2015, cor-

responding to an integrated luminosity of $3.2 \pm 0.2\text{fb}^{-1}$. The search for $H \rightarrow 2a \rightarrow 4b$ is performed in the mass range $20\text{ GeV} \leq m_a \leq 60\text{ GeV}$. The analysis uses several kinematic variables combined in a multivariate discriminant in signal regions and uses control regions to reduce the uncertainties in the backgrounds. No significant excess of data is observed relative to the SM predictions. Upper limits are derived for the product of the production cross section for $pp \rightarrow WH$ times the branching ratio for the decay $H \rightarrow 2a \rightarrow 4b$. The upper limit ranges from 6.2 pb for an a -boson mass $m_a = 20\text{ GeV}$ to 1.5 pb for $m_a = 60\text{ GeV}$.

Acknowledgements We thank CERN for the very successful operation of the LHC, as well as the support staff from our institutions without whom ATLAS could not be operated efficiently. We acknowledge the support of ANPCyT, Argentina; YerPhI, Armenia; ARC, Australia; BMWFW and FWF, Austria; ANAS, Azerbaijan; SSTC, Belarus; CNPq and FAPESP, Brazil; NSERC, NRC and CFI, Canada; CERN; CONICYT, Chile; CAS, MOST and NSFC, China; COLCIENCIAS, Colombia; MSMT CR, MPO CR and VSC CR, Czech Republic; DNRF and DNSRC, Denmark; IN2P3-CNRS, CEA-DSM/IRFU, France; GNSF, Georgia; BMBF, HGF, and MPG, Germany; GSRT, Greece; RGC, Hong Kong SAR, China; ISF, I-CORE and Benoziyo Center, Israel; INFN, Italy; MEXT and JSPS, Japan; CNRST, Morocco; FOM and NWO, Netherlands; RCN, Norway; MNiSW and NCN, Poland; FCT, Portugal; MNE/IFA, Romania; MES of Russia and NRC KI, Russian Federation; JINR; MESTD, Serbia; MSSR, Slovakia; ARRS and MIZŠ, Slovenia; DST/NRF, South Africa; MINECO, Spain; SRC and Wallenberg Foundation, Sweden; SERI, SNSF and Cantons of Bern and Geneva, Switzerland; MOST, Taiwan; TAEK, Turkey; STFC, United Kingdom; DOE and NSF, United States of America. In addition, individual groups and members have received support from BCKDF, the Canada Council, CANARIE, CRC, Compute Canada, FQRNT, and the Ontario Innovation Trust, Canada; EPLANET, ERC, FP7, Horizon 2020 and Marie Skłodowska-Curie Actions, European Union; Investissements d'Avenir Labex and Idex, ANR, Région Auvergne and Fondation Partager le Savoir, France; DFG and AvH Foundation, Germany; Herakleitos, Thales and Aristeia programmes co-financed by EU-ESF and the Greek NSRF; BSF, GIF and Minerva, Israel; BRF, Norway; Generalitat de Catalunya, Generalitat Valenciana, Spain; the Royal Society and Leverhulme Trust, United Kingdom. The crucial computing support from all WLCG partners is acknowledged gratefully, in particular from CERN, the ATLAS Tier-1 facilities at TRIUMF (Canada), NDGF (Denmark, Norway, Sweden), CC-IN2P3 (France), KIT/GridKA (Germany), INFN-CNAF (Italy), NL-T1 (Netherlands), PIC (Spain), ASGC (Taiwan), RAL (UK) and BNL (USA), the Tier-2 facilities worldwide and large non-WLCG resource providers. Major contributors of computing resources are listed in Ref. [103].

Open Access This article is distributed under the terms of the Creative Commons Attribution 4.0 International License (<http://creativecommons.org/licenses/by/4.0/>), which permits unrestricted use, distribution, and reproduction in any medium, provided you give appropriate credit to the original author(s) and the source, provide a link to the Creative Commons license, and indicate if changes were made. Funded by SCOAP³.

References

1. ATLAS Collaboration, Observation of a new particle in the search for the Standard Model Higgs boson with the ATLAS detector at

- the LHC. Phys. Lett. B **716** (2012). doi:[10.1016/j.physletb.2012.08.020](https://doi.org/10.1016/j.physletb.2012.08.020). arXiv:[1207.7214](https://arxiv.org/abs/1207.7214) [hep-ex]
2. CMS Collaboration, Observation of a new boson at a mass of 125 GeV with the CMS experiment at the LHC. Phys. Lett. B **716**, 30 (2012). doi:[10.1016/j.physletb.2012.08.021](https://doi.org/10.1016/j.physletb.2012.08.021). arXiv:[1207.7235](https://arxiv.org/abs/1207.7235) [hep-ex]
3. ATLAS Collaboration, Measurements of the Higgs boson production and decay rates and coupling strengths using pp collision data at $\sqrt{s} = 7$ and 8 TeV in the ATLAS experiment. Eur. Phys. J. C **76**, 6 (2016). doi:[10.1140/epjc/s10052-015-3769-y](https://doi.org/10.1140/epjc/s10052-015-3769-y). arXiv:[1507.04548](https://arxiv.org/abs/1507.04548) [hep-ex]
4. CMS Collaboration, Precise determination of the mass of the Higgs boson and tests of compatibility of its couplings with the standard model predictions using proton collisions at 7 and 8 TeV. Eur. Phys. J. C **75**, 212 (2015). doi:[10.1140/epjc/s10052-015-3351-7](https://doi.org/10.1140/epjc/s10052-015-3351-7). arXiv:[1412.8662](https://arxiv.org/abs/1412.8662) [hep-ex]
5. ATLAS and CMS Collaborations Measurements of the Higgs boson production and decay rates and constraints on its couplings from a combined ATLAS and CMS analysis of the LHC pp collision data at $\sqrt{s} = 7$ and 8 TeV (2016). arXiv:[1606.02266](https://arxiv.org/abs/1606.02266) [hep-ex]
6. D. Curtin et al., Exotic decays of the 125 GeV Higgs boson. Phys. Rev. D **90**, 075004 (2014). doi:[10.1103/PhysRevD.90.075004](https://doi.org/10.1103/PhysRevD.90.075004). arXiv:[1312.4992](https://arxiv.org/abs/1312.4992) [hep-ph]
7. B.A. Dobrescu, K.T. Matchev, Light axion within the next-to-minimal supersymmetric standard model. JHEP **09**, 031 (2000). doi:[10.1088/1126-6708/2000/09/031](https://doi.org/10.1088/1126-6708/2000/09/031). arXiv:[hep-ph/0008192](https://arxiv.org/abs/hep-ph/0008192)
8. U. Ellwanger et al., Towards a no lose theorem for NMSSM Higgs discovery at the LHC (2003). arXiv:[hep-ph/0305109](https://arxiv.org/abs/hep-ph/0305109)
9. R. Dermisek, J.F. Gunion, Escaping the large fine tuning and little hierarchy problems in the next to minimal supersymmetric model and $h \rightarrow aa$ decays. Phys. Rev. Lett. **95**, 041801 (2005). doi:[10.1103/PhysRevLett.95.041801](https://doi.org/10.1103/PhysRevLett.95.041801). arXiv:[hep-ph/0502105](https://arxiv.org/abs/hep-ph/0502105)
10. S. Chang et al., Nonstandard higgs boson decays. Ann. Rev. Nucl. Part. Sci. **58**, 75–98 (2008). doi:[10.1146/annurev.nucl.58.110707.171200](https://doi.org/10.1146/annurev.nucl.58.110707.171200). arXiv:[0801.4554](https://arxiv.org/abs/0801.4554) [hep-ph]
11. D.E. Morrissey, A. Pierce, Modified higgs boson phenomenology from gauge or gaugino mediation in the NMSSM. Phys. Rev. D **78**, 075029 (2008). doi:[10.1103/PhysRevD.78.075029](https://doi.org/10.1103/PhysRevD.78.075029). arXiv:[0807.2259](https://arxiv.org/abs/0807.2259) [hep-ph]
12. V. Silveira, A. Zee, Scalar phantoms. Phys. Lett. B **161**, 136 (1985). doi:[10.1016/0370-2693\(85\)90624-0](https://doi.org/10.1016/0370-2693(85)90624-0)
13. M. Pospelov, A. Ritz, M.B. Voloshin, Secluded WIMP dark matter. Phys. Lett. B **662**, 53–61 (2008). doi:[10.1016/j.physletb.2008.02.052](https://doi.org/10.1016/j.physletb.2008.02.052). arXiv:[0711.4866](https://arxiv.org/abs/0711.4866) [hep-ph]
14. P. Draper et al., Dark light higgs. Phys. Rev. Lett. **106**, 121805 (2011). doi:[10.1103/PhysRevLett.106.121805](https://doi.org/10.1103/PhysRevLett.106.121805). arXiv:[1009.3963](https://arxiv.org/abs/1009.3963) [hep-ph]
15. S. Ipek, D. McKeen, A.E. Nelson, A renormalizable model for the galactic center gamma ray excess from dark matter annihilation. Phys. Rev. D **90**, 055021 (2014). doi:[10.1103/PhysRevD.90.055021](https://doi.org/10.1103/PhysRevD.90.055021). arXiv:[1404.3716](https://arxiv.org/abs/1404.3716) [hep-ph]
16. A. Martin, J. Shelton, J. Unwin, Fitting the galactic center gamma-ray excess with cascade annihilations. Phys. Rev. D **90**, 103513 (2014). doi:[10.1103/PhysRevD.90.103513](https://doi.org/10.1103/PhysRevD.90.103513). arXiv:[1405.0272](https://arxiv.org/abs/1405.0272) [hep-ph]
17. S. Profumo, M.J. Ramsey-Musolf, G. Shaughnessy, Singlet higgs phenomenology and the electroweak phase transition. JHEP **08**, 010 (2007). doi:[10.1088/1126-6708/2007/08/010](https://doi.org/10.1088/1126-6708/2007/08/010). arXiv:[0705.2425](https://arxiv.org/abs/0705.2425) [hep-ph]
18. N. Blinov et al., Electroweak baryogenesis from exotic electroweak symmetry breaking. Phys. Rev. D **92**, 035012 (2015). doi:[10.1103/PhysRevD.92.035012](https://doi.org/10.1103/PhysRevD.92.035012). arXiv:[1504.05195](https://arxiv.org/abs/1504.05195) [hep-ph]
19. G. Burdman et al., Folded supersymmetry and the LEP paradox. JHEP **02**, 009 (2007). doi:[10.1088/1126-6708/2007/02/009](https://doi.org/10.1088/1126-6708/2007/02/009). arXiv:[hep-ph/0609152](https://arxiv.org/abs/hep-ph/0609152)
20. N. Craig et al., Naturalness in the dark at the LHC. JHEP **07**, 105 (2015). doi:[10.1007/JHEP07\(2015\)105](https://doi.org/10.1007/JHEP07(2015)105). arXiv:[1501.05310](https://arxiv.org/abs/1501.05310) [hep-ph]
21. D. Curtin, C.B. Verhaaren, Discovering uncolored naturalness in exotic higgs decays. JHEP **12**, 072 (2015). doi:[10.1007/JHEP12\(2015\)072](https://doi.org/10.1007/JHEP12(2015)072). arXiv:[1506.06141](https://arxiv.org/abs/1506.06141) [hep-ph]
22. M. Ajello et al., Fermi-LAT observations of high-energy γ -ray emission toward the galactic center. Astrophys. J. **819**, 44 (2016). doi:[10.3847/0004-637X/819/1/44](https://doi.org/10.3847/0004-637X/819/1/44). arXiv:[1511.02938](https://arxiv.org/abs/1511.02938) [astro-ph.HE]
23. C. Boehm et al., Extended gamma-ray emission from Coy dark matter. JCAP **1405**, 009 (2014). doi:[10.1088/1475-7516/2014/05/009](https://doi.org/10.1088/1475-7516/2014/05/009). arXiv:[1401.6458](https://arxiv.org/abs/1401.6458) [hep-ph]
24. V. Abazov et al., Search for NMSSM Higgs bosons in the $h \rightarrow aa \rightarrow \mu\mu\mu\mu, \mu\mu\tau\tau$ channels using p anti-p collisions at $\sqrt{s} = 1.96$ TeV. Phys. Rev. Lett. **103**, 061801 (2009). doi:[10.1103/PhysRevLett.103.061801](https://doi.org/10.1103/PhysRevLett.103.061801). arXiv:[0905.3381](https://arxiv.org/abs/0905.3381) [hep-ex]
25. ATLAS Collaboration, Search for Higgs bosons decaying to aa in the $\mu\mu\tau\tau$ final state in pp collisions at $\sqrt{s} = 8$ TeV with the ATLAS experiment. Phys. Rev. D **92**, 052002 (2015). doi:[10.1103/PhysRevD.92.052002](https://doi.org/10.1103/PhysRevD.92.052002). arXiv:[1505.01609](https://arxiv.org/abs/1505.01609) [hep-ex]
26. CMS Collaboration, A search for pair production of new light bosons decaying into muons. Phys. Lett. B **752**, 146–168 (2016). doi:[10.1016/j.physletb.2015.10.067](https://doi.org/10.1016/j.physletb.2015.10.067). arXiv:[1506.00424](https://arxiv.org/abs/1506.00424) [hep-ex]
27. ATLAS Collaboration, Search for long-lived neutral particles decaying into lepton jets in proton–proton collisions at $\sqrt{s} = 8$ TeV with the ATLAS detector. JHEP **11**, 088 (2014). doi:[10.1007/JHEP11\(2014\)088](https://doi.org/10.1007/JHEP11(2014)088). arXiv:[1409.0746](https://arxiv.org/abs/1409.0746) [hep-ex]
28. CMS Collaboration, Search for long-lived particles that decay into final states containing two electrons or two muons in proton–proton collisions at $\sqrt{s} = 8$ TeV. Phys. Rev. D **91**, 052012 (2015). doi:[10.1103/PhysRevD.91.052012](https://doi.org/10.1103/PhysRevD.91.052012). arXiv:[1411.6977](https://arxiv.org/abs/1411.6977) [hep-ex]
29. ATLAS Collaboration, Search for long-lived, weakly interacting particles that decay to displaced hadronic jets in proton–proton collisions at $\sqrt{s} = 8$ TeV with the ATLAS detector. Phys. Rev. D **92**, 012010 (2015). doi:[10.1103/PhysRevD.92.012010](https://doi.org/10.1103/PhysRevD.92.012010). arXiv:[1504.03634](https://arxiv.org/abs/1504.03634) [hep-ex]
30. ATLAS Collaboration, Search for pair-produced long-lived neutral particles decaying in the ATLAS hadronic calorimeter in pp collisions at $\sqrt{s} = 8$ TeV. Phys. Lett. B **743**, 15 (2015). arXiv:[1510.04020](https://arxiv.org/abs/1510.04020) [hep-ex]
31. CMS Collaboration, Search for long-lived neutral particles decaying to quark–antiquark pairs in proton–proton collisions at $\sqrt{s} = 8$ TeV. Phys. Rev. D **91**, 012007 (2015). doi:[10.1103/PhysRevD.91.012007](https://doi.org/10.1103/PhysRevD.91.012007). arXiv:[1411.6530](https://arxiv.org/abs/1411.6530) [hep-ex]
32. LHCb Collaboration, Search for long-lived particles decaying to jet pairs. Eur. Phys. J. C **75**, 152 (2015). doi:[10.1140/epjc/s10052-015-3344-6](https://doi.org/10.1140/epjc/s10052-015-3344-6). arXiv:[1412.3021](https://arxiv.org/abs/1412.3021) [hep-ex]
33. ATLAS Collaboration, Search for the Standard Model Higgs boson produced in association with top quarks and decaying into $b\bar{b}$ in pp collisions at $\sqrt{s} = 8$ TeV with the ATLAS detector. Eur. Phys. J. C **75**, 349 (2015). doi:[10.1140/epjc/s10052-015-3543-1](https://doi.org/10.1140/epjc/s10052-015-3543-1). arXiv:[1503.05066](https://arxiv.org/abs/1503.05066) [hep-ex]
34. ATLAS Collaboration, Search for production of vector-like quark pairs and of four top quarks in the lepton-plus-jets final state in pp collisions at $\sqrt{s} = 8$ TeV with the ATLAS detector. JHEP **08**, 105 (2015). doi:[10.1007/JHEP08\(2015\)105](https://doi.org/10.1007/JHEP08(2015)105). arXiv:[1505.04306](https://arxiv.org/abs/1505.04306) [hep-ex]
35. ATLAS Collaboration, Search for flavour-changing neutral current top quark decays $t \rightarrow Hq$ in pp collisions at $\sqrt{s} = 8$ TeV with the ATLAS detector. JHEP **12**, 061 (2015). doi:[10.1007/JHEP12\(2015\)061](https://doi.org/10.1007/JHEP12(2015)061). arXiv:[1509.06047](https://arxiv.org/abs/1509.06047) [hep-ex]
36. ATLAS Collaboration, Search for charged Higgs bosons in the $H^\pm \rightarrow tb$ decay channel in pp collisions at $\sqrt{s} = 8$ TeV using the ATLAS detector. JHEP **03**, 127 (2016). doi:[10.1007/JHEP03\(2016\)127](https://doi.org/10.1007/JHEP03(2016)127). arXiv:[1512.03704](https://arxiv.org/abs/1512.03704) [hep-ex]

37. ATLAS Collaboration, The ATLAS experiment at the CERN Large Hadron Collider. JINST **3**, S08003 (2008). doi:[10.1088/1748-0221/3/08/S08003](https://doi.org/10.1088/1748-0221/3/08/S08003)
38. ATLAS Collaboration, ATLAS insertable b-layer technical design report. ATLAS-TDR-19 (2010). <http://cdsweb.cern.ch/record/1291633>
39. ATLAS Collaboration, 2015 start-up trigger menu and initial performance assessment of the ATLAS trigger using Run-2 data, ATL-DAQ-PUB-2016-001 (2016). <http://cdsweb.cern.ch/record/2136007>
40. ATLAS Collaboration, Electron reconstruction and identification efficiency measurements with the ATLAS detector using the 2011 LHC proton–proton collision data. Eur. Phys. J. C **74**, 2941 (2014). doi:[10.1140/epjc/s10052-014-2941-0](https://doi.org/10.1140/epjc/s10052-014-2941-0). arXiv:[1404.2240](https://arxiv.org/abs/1404.2240) [hep-ex]
41. ATLAS Collaboration, Electron efficiency measurements with the ATLAS detector using the 2012 LHC proton–proton collision data. ATLAS-CONF-2014-032 (2014). <http://cdsweb.cern.ch/record/1706245>
42. ATLAS Collaboration, Muon reconstruction performance of the ATLAS detector in proton–proton collision data at $\sqrt{s} = 13$ TeV. Eur. Phys. J. C **76**, 292 (2016). doi:[10.1140/epjc/s10052-016-4120-y](https://doi.org/10.1140/epjc/s10052-016-4120-y). arXiv:[1603.05598](https://arxiv.org/abs/1603.05598) [hep-ex]
43. ATLAS Collaboration, Topological cell clustering in the ATLAS calorimeters and its performance in LHC Run 1 (2016). arXiv:[1603.02934](https://arxiv.org/abs/1603.02934) [hep-ex]
44. M. Cacciari, G.P. Salam, Dispelling the N^3 myth for the k_t jet-finder. Phys. Lett. B **641**, 57 (2006). doi:[10.1016/j.physletb.2006.08.037](https://doi.org/10.1016/j.physletb.2006.08.037). arXiv:[0512210](https://arxiv.org/abs/0512210) [hep-ph]
45. M. Cacciari, G.P. Salam, G. Soyez, The anti- k_t jet clustering algorithm. JHEP **04**, 063 (2008). doi:[10.1088/1126-6708/2008/04/063](https://doi.org/10.1088/1126-6708/2008/04/063). arXiv:[0802.1189](https://arxiv.org/abs/0802.1189) [hep-ph]
46. ATLAS Collaboration, Performance of pile-up mitigation techniques for jets in pp collisions with the ATLAS detector. Nucl. Instrum. Meth. A **824**, 367 (2016). doi:[10.1016/j.nima.2015.10.039](https://doi.org/10.1016/j.nima.2015.10.039). arXiv:[1510.03823](https://arxiv.org/abs/1510.03823) [hep-ex]
47. ATLAS Collaboration, Expected performance of the ATLAS b-tagging algorithms in Run-2. ATL-PHYS-PUB-2015-022 (2015). <http://cdsweb.cern.ch/record/2037697>
48. ATLAS Collaboration, Performance of b -jet identification in the ATLAS experiment. JINST **11**, P04008 (2016). doi:[10.1088/1748-0221/11/04/P04008](https://doi.org/10.1088/1748-0221/11/04/P04008). arXiv:[1512.01094](https://arxiv.org/abs/1512.01094) [hep-ex]
49. ATLAS Collaboration, Commissioning of the ATLAS b -tagging algorithms using $t\bar{t}$ events in early Run-2 data. ATLAS-PHYS-PUB-2015-039 (2015). <http://cdsweb.cern.ch/record/2047871>
50. ATLAS Collaboration, Performance of missing transverse momentum reconstruction in proton–proton collisions at 7 TeV with ATLAS. Eur. Phys. J. C **72**, 1844 (2012). doi:[10.1140/epjc/s10052-011-1844-6](https://doi.org/10.1140/epjc/s10052-011-1844-6). arXiv:[1108.5602](https://arxiv.org/abs/1108.5602) [hep-ex]
51. ATLAS Collaboration, Performance of missing transverse momentum reconstruction for the ATLAS detector in the first proton–proton collisions at $\sqrt{s} = 13$ TeV. ATL-PHYS-PUB-2015-027 (2015). <http://cdsweb.cern.ch/record/2037904>
52. S. Frixione, P. Nason, G. Ridolfi, A positive-weight next-to-leading-order monte carlo for heavy flavour hadroproduction. JHEP **09**, 126 (2007). doi:[10.1088/1126-6708/2007/09/126](https://doi.org/10.1088/1126-6708/2007/09/126). arXiv:[0707.3088](https://arxiv.org/abs/0707.3088) [hep-ph]
53. P. Nason, A new method for combining NLO QCD with shower Monte Carlo algorithms. JHEP **11**, 040 (2004). doi:[10.1088/1126-6708/2004/11/040](https://doi.org/10.1088/1126-6708/2004/11/040). arXiv:[hep-ph/0409146](https://arxiv.org/abs/hep-ph/0409146) [hep-ph]
54. S. Frixione, P. Nason, C. Oleari, Matching NLO QCD computations with parton shower simulations: the POWHEG method. JHEP **11**, 070 (2007). doi:[10.1088/1126-6708/2007/11/070](https://doi.org/10.1088/1126-6708/2007/11/070). arXiv:[0709.2092](https://arxiv.org/abs/0709.2092) [hep-ph]
55. S. Alioli et al., A general framework for implementing NLO calculations in shower Monte Carlo programs: the POWHEG BOX. JHEP **06**, 043 (2010). doi:[10.1007/JHEP06\(2010\)043](https://doi.org/10.1007/JHEP06(2010)043). arXiv:[1002.2581](https://arxiv.org/abs/1002.2581) [hep-ph]
56. H.-L. Lai et al., New parton distributions for collider physics. Phys. Rev. D **82**, 074024 (2010). doi:[10.1103/PhysRevD.82.074024](https://doi.org/10.1103/PhysRevD.82.074024). arXiv:[1007.2241](https://arxiv.org/abs/1007.2241) [hep-ph]
57. J.R. Andersen et al., Handbook of LHC Higgs cross sections: 3. Higgs properties, ed. by S. Heinemeyer et al. (2013) doi:[10.5170/CERN-2013-004](https://doi.org/10.5170/CERN-2013-004). arXiv:[1307.1347](https://arxiv.org/abs/1307.1347) [hep-ph]
58. T. Sjöstrand, S. Mrenna, P. Skands, A. Brief, Introduction to Pythia 8.1. Comput. Phys. Commun. **178**, 852 (2008). doi:[10.1016/j.cpc.2008.01.036](https://doi.org/10.1016/j.cpc.2008.01.036). arXiv:[0710.3820](https://arxiv.org/abs/0710.3820) [hep-ph]
59. ATLAS Collaboration, ATLAS Run 1 Pythia8 tunes. ATL-PHYS-PUB-2014-021 (2014). <http://cdsweb.cern.ch/record/1966419>
60. ATLAS Collaboration, Comparison of Monte Carlo generator predictions to ATLAS measurements of top pair production at $\sqrt{s} = 7$ TeV. ATL-PHYS-PUB-2015-002 (2015). <http://cdsweb.cern.ch/record/1981319>
61. T. Sjöstrand, S. Mrenna, P.Z. Skands, PYTHIA 6.4 physics and manual. JHEP **05**, 026 (2006). doi:[10.1088/1126-6708/2006/05/026](https://doi.org/10.1088/1126-6708/2006/05/026). arXiv:[hep-ph/0603175](https://arxiv.org/abs/hep-ph/0603175) [hep-ph]
62. P.Z. Skands, Tuning Monte Carlo generators: the Perugia tunes. Phys. Rev. D **82**, 074018 (2010). doi:[10.1103/PhysRevD.82.074018](https://doi.org/10.1103/PhysRevD.82.074018). arXiv:[1005.3457](https://arxiv.org/abs/1005.3457) [hep-ph]
63. M. Bahr et al., Herwig++ physics and manual. Eur. Phys. J. C **58** (2008). doi:[10.1140/epjc/s10052-008-0798-9](https://doi.org/10.1140/epjc/s10052-008-0798-9). arXiv:[0803.0883](https://arxiv.org/abs/0803.0883) [hep-ph]
64. J. Alwall et al., The automated computation of tree-level and next-to-leading order differential cross sections, and their matching to parton shower simulations. JHEP **07**, 079 (2014). doi:[10.1007/JHEP07\(2014\)079](https://doi.org/10.1007/JHEP07(2014)079). arXiv:[1405.0301](https://arxiv.org/abs/1405.0301) [hep-ph]
65. ATLAS Collaboration, Comparison of Monte Carlo generator predictions from Powheg and Sherpa to ATLAS measurements of top pair production at 7 TeV. ATL-PHYS-PUB-2015-011 (2015). <http://cdsweb.cern.ch/record/2020602>
66. M. Cacciari et al., Top-pair production at hadron colliders with next-to-next-to-leading logarithmic soft-gluon resummation. Phys. Lett. B **710**, 612 (2012). doi:[10.1016/j.physletb.2012.03.013](https://doi.org/10.1016/j.physletb.2012.03.013). arXiv:[1111.5869](https://arxiv.org/abs/1111.5869) [hep-ph]
67. M. Beneke et al., Hadronic top-quark pair production with NNLL threshold resummation. Nucl. Phys. B **855**, 695–741 (2012). doi:[10.1016/j.nuclphysb.2011.10.021](https://doi.org/10.1016/j.nuclphysb.2011.10.021). arXiv:[1109.1536](https://arxiv.org/abs/1109.1536) [hep-ph]
68. P. Bärnreuther, M. Czakon, A. Mitov, Percent-level-precision physics at the Tevatron: next-to-next-to-leading order QCD corrections to $q\bar{q} \rightarrow t\bar{t} + X$. Phys. Rev. Lett. **109**, 132001 (2012). doi:[10.1103/PhysRevLett.109.132001](https://doi.org/10.1103/PhysRevLett.109.132001). arXiv:[1204.5201](https://arxiv.org/abs/1204.5201) [hep-ph]
69. M. Czakon, A. Mitov, NNLO corrections to top-pair production at hadron colliders: the all-fermionic scattering channels. JHEP **12**, 054 (2012). doi:[10.1007/JHEP12\(2012\)054](https://doi.org/10.1007/JHEP12(2012)054). arXiv:[1207.0236](https://arxiv.org/abs/1207.0236) [hep-ph]
70. M. Czakon, A. Mitov, NNLO corrections to top pair production at hadron colliders: the quark–gluon reaction. JHEP **01**, 080 (2013). doi:[10.1007/JHEP01\(2013\)080](https://doi.org/10.1007/JHEP01(2013)080). arXiv:[1210.6832](https://arxiv.org/abs/1210.6832) [hep-ph]
71. M. Czakon, P. Fiedler, A. Mitov, Total top-quark pair-production cross section at hadron colliders through $O(\alpha_s^4)$. Phys. Rev. Lett. **110**, 252004 (2013). doi:[10.1103/PhysRevLett.110.252004](https://doi.org/10.1103/PhysRevLett.110.252004). arXiv:[1303.6254](https://arxiv.org/abs/1303.6254) [hep-ph]
72. M. Czakon, A. Mitov, Top++: a program for the calculation of the top-pair cross-section at hadron colliders. Comput. Phys. Commun. **185**, 2930 (2014). doi:[10.1016/j.cpc.2014.06.021](https://doi.org/10.1016/j.cpc.2014.06.021). arXiv:[1112.5675](https://arxiv.org/abs/1112.5675) [hep-ph]
73. T. Gleisberg et al., Event generation with SHERPA 1.1. JHEP **02**, 007 (2009). doi:[10.1088/1126-6708/2009/02/007](https://doi.org/10.1088/1126-6708/2009/02/007). arXiv:[0811.4622](https://arxiv.org/abs/0811.4622) [hep-ph]
74. F. Cascioli, P. Maierhofer, S. Pozzorini, Scattering amplitudes with open loops. Phys. Rev. Lett. **108**, 111601 (2012). doi:[10.1103/PhysRevLett.108.111601](https://doi.org/10.1103/PhysRevLett.108.111601). arXiv:[1111.5206](https://arxiv.org/abs/1111.5206) [hep-ph]

75. S. Alioli et al., NLO single-top production matched with shower in POWHEG: s- and t-channel contributions. *JHEP* **09**, 111 (2009). doi:[10.1007/JHEP02\(2010\)011](https://doi.org/10.1007/JHEP02(2010)011). doi:[10.1088/1126-6708/2009/09/111](https://doi.org/10.1088/1126-6708/2009/09/111). (Erratum: *JHEP* **02**, 011). arXiv:0907.4076 [hep-ph]
76. E. Re, Single-top Wt-channel production matched with parton showers using the POWHEG method. *Eur. Phys. J. C* **71**, 1547 (2011). doi:[10.1140/epjc/s10052-011-1547-z](https://doi.org/10.1140/epjc/s10052-011-1547-z). arXiv:1009.2450 [hep-ph]
77. S. Frixione et al., Single-top production in MC@NLO. *JHEP* **03**, 092 (2006). doi:[10.1088/1126-6708/2006/03/092](https://doi.org/10.1088/1126-6708/2006/03/092). arXiv:hep-ph/0512250
78. R. Frederix, E. Re, P. Torrielli, Single-top t-channel hadroproduction in the four-flavour scheme with POWHEG and aMC@NLO. *JHEP* **09**, 130 (2012). doi:[10.1007/JHEP09\(2012\)130](https://doi.org/10.1007/JHEP09(2012)130). arXiv:1207.5391 [hep-ph]
79. N. Kidonakis, Next-to-next-to-leading-order collinear and soft gluon corrections for t-channel single top quark production. *Phys. Rev. D* **83**, 091503 (2011). doi:[10.1103/PhysRevD.83.091503](https://doi.org/10.1103/PhysRevD.83.091503). arXiv:1103.2792 [hep-ph]
80. N. Kidonakis, Two-loop soft anomalous dimensions for single top quark associated production with a W- or H-. *Phys. Rev. D* **82**, 054018 (2010). doi:[10.1103/PhysRevD.82.054018](https://doi.org/10.1103/PhysRevD.82.054018). arXiv:1005.4451 [hep-ph]
81. N. Kidonakis, NNLL resummation for s-channel single top quark production. *Phys. Rev. D* **81**, 054028 (2010). doi:[10.1103/PhysRevD.81.054028](https://doi.org/10.1103/PhysRevD.81.054028). arXiv:1001.5034 [hep-ph]
82. M.H. Seymour, A. Siodmok, Constraining MPI models using σ_{eff} and recent tevatron and LHC underlying event data. *JHEP* **10**, 113 (2013). doi:[10.1007/JHEP10\(2013\)113](https://doi.org/10.1007/JHEP10(2013)113). arXiv:1307.5015 [hep-ph]
83. T. Gleisberg, S. Höche, Comix, a new matrix element generator. *JHEP* **12**, 039 (2008). doi:[10.1088/1126-6708/2008/12/039](https://doi.org/10.1088/1126-6708/2008/12/039). arXiv:0808.3674 [hep-ph]
84. C. Anastasiou et al., High precision QCD at hadron colliders: electroweak gauge boson rapidity distributions at NNLO. *Phys. Rev. D* **69**, 094008 (2004). doi:[10.1103/PhysRevD.69.094008](https://doi.org/10.1103/PhysRevD.69.094008). arXiv:hep-ph/0312266
85. D.J. Lange, The EvtGen particle decay simulation package. *Nucl. Instrum. Meth. A* **462**, 152–155 (2001). doi:[10.1016/S0168-9002\(01\)00089-4](https://doi.org/10.1016/S0168-9002(01)00089-4)
86. ATLAS Collaboration, The ATLAS simulation infrastructure. *Eur. Phys. J. C* **70**, 823 (2010). doi:[10.1140/epjc/s10052-010-1429-9](https://doi.org/10.1140/epjc/s10052-010-1429-9). arXiv:1005.4568 [physics.ins-det]
87. S. Agostinelli et al., GEANT4: a simulation toolkit. *Nucl. Instr. Meth. A* **506**, 250 (2003). doi:[10.1016/S0168-9002\(03\)01368-8](https://doi.org/10.1016/S0168-9002(03)01368-8)
88. ATLAS Collaboration, The simulation principle and performance of the ATLAS fast calorimeter simulation FastCaloSim. ATLAS-PHYS-PUB-2010-013 (2010). <http://cdsweb.cern.ch/record/1300517>
89. ATLAS Collaboration, Measurement of the top quark-pair production cross section with ATLAS in pp collisions at $\sqrt{s} = 7$ TeV. *Eur. Phys. J. C* **71**, 1577 (2011). doi:[10.1140/epjc/s10052-011-1577-6](https://doi.org/10.1140/epjc/s10052-011-1577-6). arXiv:1012.1792 [hep-ex]
90. ATLAS Collaboration, Estimation of non-prompt and fake lepton backgrounds in final states with top quarks produced in proton–proton collisions at $\sqrt{s} = 8$ TeV with the ATLAS detector. ATLAS-CONF-2014-058 (2014). <http://cdsweb.cern.ch/record/1951336>
91. F. Pedregosa et al., Scikit-learn: machine learning in python. *J. Mach. Learn. Res.* **12**, 2825–2830 (2011)
92. Y. Freund, R.E. Schapire, A decision-theoretic generalization of on-line learning and an application to boosting. *J. Comput. Syst. Sci.* **55**, 119 (1997). doi:[10.1006/jcss.1997.1504](https://doi.org/10.1006/jcss.1997.1504)
93. M. Burns et al., Using subsystem MT2 for complete mass determinations in decay chains with missing energy at hadron colliders. *JHEP* **03**, 143 (2009). doi:[10.1088/1126-6708/2009/03/143](https://doi.org/10.1088/1126-6708/2009/03/143). arXiv:0810.5576 [hep-ph]
94. ATLAS Collaboration, Improved luminosity determination in pp collisions at $\sqrt{s} = 7$ TeV using the ATLAS detector at the LHC. *Eur. Phys. J. C* **73**, 2518 (2013). doi:[10.1140/epjc/s10052-013-2518-3](https://doi.org/10.1140/epjc/s10052-013-2518-3). arXiv:1302.4393 [hep-ex]
95. J.M. Campbell, R.K. Ellis, An update on vector boson pair production at hadron colliders. *Phys. Rev. D* **60**, 113006 (1999). doi:[10.1103/PhysRevD.60.113006](https://doi.org/10.1103/PhysRevD.60.113006). arXiv:hep-ph/9905386
96. J.M. Campbell, R.K. Ellis, $t\bar{t}W^{\pm}$ production and decay at NLO. *JHEP* **07**, 052 (2012). doi:[10.1007/JHEP07\(2012\)052](https://doi.org/10.1007/JHEP07(2012)052). arXiv:1204.5678 [hep-ph]
97. M.V. Garzelli et al., $t\bar{t}W^{\pm}$ and $t\bar{t}Z$ hadroproduction at NLO accuracy in QCD with Parton shower and hadronization effects. *JHEP* **11**, 056 (2012). doi:[10.1007/JHEP11\(2012\)056](https://doi.org/10.1007/JHEP11(2012)056). arXiv:1208.2665 [hep-ph]
98. S. Dittmaier et al., Handbook of LHC Higgs cross sections: 1. inclusive observables (2011). doi:[10.5170/CERN-2011-002](https://doi.org/10.5170/CERN-2011-002). arXiv:1101.0593 [hep-ph]
99. ATLAS Collaboration, Modelling of the $t\bar{t}H$ and $t\bar{t}V$ ($V = W, Z$) processes for $\sqrt{s} = 13$ TeV ATLAS analyses. ATL-PHYS-PUB-2016-005 (2016). <http://cdsweb.cern.ch/record/2120826>
100. J. Alwall et al., Comparative study of various algorithms for the merging of parton showers and matrix elements in hadronic collisions. *Eur. Phys. J. C* **53**, 473–500 (2008). doi:[10.1140/epjc/s10052-007-0490-5](https://doi.org/10.1140/epjc/s10052-007-0490-5). arXiv:0706.2569 [hep-ph]
101. A.L. Read, Presentation of search results: the CL(s) technique. *J. Phys. G* **28**, 2693 (2002). doi:[10.1088/0954-3899/28/10/313](https://doi.org/10.1088/0954-3899/28/10/313)
102. G. Cowan et al., Asymptotic formulae for likelihood-based tests of new physics. *Eur. Phys. J. C* **71**, 1554 (2011). (Erratum: *Eur. Phys. J. C* **73**, 2501 (2013)). doi:[10.1140/epjc/s10052-011-1554-0](https://doi.org/10.1140/epjc/s10052-011-1554-0). doi:[10.1140/epjc/s10052-013-2501-z](https://doi.org/10.1140/epjc/s10052-013-2501-z). arXiv:1007.1727 [physics.data-an]
103. ATLAS Collaboration, ATLAS computing acknowledgements 2016–2017, ATL-GEN-PUB-2016-002 (2016). <https://cds.cern.ch/record/2202407>

ATLAS Collaboration

M. Aaboud^{136d}, G. Aad⁸⁷, B. Abbott¹¹⁴, J. Abdallah⁶⁵, O. Abidinov¹², B. Abeloos¹¹⁸, R. Aben¹⁰⁸, O. S. AbouZeid¹³⁸, N. L. Abraham¹⁵², H. Abramowicz¹⁵⁶, H. Abreu¹⁵⁵, R. Abreu¹¹⁷, Y. Abulaiti^{149a,149b}, B. S. Acharya^{168a,168b,a}, L. Adamczyk^{40a}, D. L. Adams²⁷, J. Adelman¹⁰⁹, S. Adomeit¹⁰¹, T. Adye¹³², A. A. Affolder⁷⁶, T. Agatonovic-Jovin¹⁴, J. Agricola⁵⁶, J. A. Aguilar-Saavedra^{127a,127f}, S. P. Ahlen²⁴, F. Ahmadov^{67,b}, G. Aielli^{134a,134b}, H. Akerstedt^{149a,149b}, T. P. A. Åkesson⁸³, A. V. Akimov⁹⁷, G. L. Alberghi^{22a,22b}, J. Albert¹⁷³, S. Albrand⁵⁷, M. J. Alconada Verzini⁷³, M. Aleksa³², I. N. Aleksandrov⁶⁷, C. Alexa^{28b}, G. Alexander¹⁵⁶, T. Alexopoulos¹⁰, M. Alhroob¹¹⁴, B. Ali¹²⁹, M. Aliev^{75a,75b}, G. Alimonti^{93a}, J. Alison³³, S. P. Alkire³⁷, B. M. M. Allbrooke¹⁵², B. W. Allen¹¹⁷, P. P. Allport¹⁹, A. Aloisio^{105a,105b}, A. Alonso³⁸, F. Alonso⁷³, C. Alpigiani¹³⁹, M. Alstady⁸⁷, B. Alvarez Gonzalez³², D. Álvarez Piqueras¹⁷¹, M. G. Alvigi^{105a,105b}, B. T. Amadio¹⁶, K. Amako⁶⁸, Y. Amaral Coutinho^{26a}, C. Amelung²⁵, D. Amidei⁹¹, S. P. Amor Dos Santos^{127a,127c}, A. Amorim^{127a,127b}, S. Amoroso³², G. Amundsen²⁵, C. Anastopoulos¹⁴², L. S. Ancu⁵¹, N. Andari¹⁹, T. Andeen¹¹, C. F. Anders^{60b}, G. Anders³², J. K. Anders⁷⁶, K. J. Anderson³³, A. Andreazza^{93a,93b}, V. Andrei^{60a}, S. Angelidakis⁹, I. Angelozzi¹⁰⁸, P. Anger⁴⁶, A. Angerami³⁷, F. Anghinolfi³², A. V. Anisenkov^{110,c}, N. Anjos¹³, A. Annovi^{125a,125b}, C. Antel^{60a}, M. Antonelli⁴⁹, A. Antonov^{99,*}, F. Anulli^{133a}, M. Aoki⁶⁸, L. Aperio Bella¹⁹, G. Arabidze⁹², Y. Arai⁶⁸, J. P. Araque^{127a}, A. T. H. Arce⁴⁷, F. A. Arduh⁷³, J.-F. Arguin⁹⁶, S. Argyropoulos⁶⁵, M. Arik^{20a}, A. J. Armbruster¹⁴⁶, L. J. Armitage⁷⁸, O. Arnaez³², H. Arnold⁵⁰, M. Arratia³⁰, O. Arslan²³, A. Artamonov⁹⁸, G. Artoni¹²¹, S. Artz⁸⁵, S. Asai¹⁵⁸, N. Asbah⁴⁴, A. Ashkenazi¹⁵⁶, B. Åsman^{149a,149b}, L. Asquith¹⁵², K. Assamagan²⁷, R. Astalos^{147a}, M. Atkinson¹⁷⁰, N. B. Atlay¹⁴⁴, K. Augsten¹²⁹, G. Avolio³², B. Axen¹⁶, M. K. Ayoub¹¹⁸, G. Azuelos^{96,d}, M. A. Baak³², A. E. Baas^{60a}, M. J. Baca¹⁹, H. Bachacou¹³⁷, K. Bachas^{75a,75b}, M. Backes¹⁵¹, M. Backhaus³², P. Bagiacchi^{133a,133b}, P. Bagnaia^{133a,133b}, Y. Bai^{35a}, J. T. Baines¹³², O. K. Baker¹⁸⁰, E. M. Baldwin^{110,c}, P. Balek¹⁷⁶, T. Balestri¹⁵¹, F. Balli¹³⁷, W. K. Balunas¹²³, E. Banas⁴¹, Sw. Banerjee^{177,e}, A. A. E. Bannoura¹⁷⁹, L. Barak³², E. L. Barberio⁹⁰, D. Barberis^{52a,52b}, M. Barbero⁸⁷, T. Barillari¹⁰², M.-S. Barisits³², T. Barklow¹⁴⁶, N. Barlow³⁰, S. L. Barnes⁸⁶, B. M. Barnett¹³², R. M. Barnett¹⁶, Z. Barnovska-Blenessy⁵, A. Baroncelli^{135a}, G. Barone²⁵, A. J. Barr¹²¹, L. Barranco Navarro¹⁷¹, F. Barreiro⁸⁴, J. Barreiro Guimarães da Costa^{35a}, R. Bartoldus¹⁴⁶, A. E. Barton⁷⁴, P. Bartos^{147a}, A. Basalaev¹²⁴, A. Bassalat^{118,f}, R. L. Bates⁵⁵, S. J. Batista¹⁶², J. R. Batley³⁰, M. Battaglia¹³⁸, M. Bause^{133a,133b}, F. Bauer¹³⁷, H. S. Bawa^{146,g}, J. B. Beacham¹¹², M. D. Beattie⁷⁴, T. Beau⁸², P. H. Beauchemin¹⁶⁶, P. Bechtel²³, H. P. Beck^{18,h}, K. Becker¹²¹, M. Becker⁸⁵, M. Beckingham¹⁷⁴, C. Becot¹¹¹, A. J. Beddall^{20d}, A. Beddall^{20b}, V. A. Bednyakov⁶⁷, M. Bedognetti¹⁰⁸, C. P. Bee¹⁵¹, L. J. Beemster¹⁰⁸, T. A. Beermann³², M. Begel²⁷, J. K. Behr⁴⁴, C. Belanger-Champagne⁸⁹, A. S. Bell⁸⁰, G. Bella¹⁵⁶, L. Bellagamba^{22a}, A. Bellerive³¹, M. Bellomo⁸⁸, K. Belotskiy⁹⁹, O. Beltramello³², N. L. Belyaev⁹⁹, O. Benary^{156,*}, D. Bencheikroun^{136a}, M. Bender¹⁰¹, K. Bendtz^{149a,149b}, N. Benekos¹⁰, Y. Benhammou¹⁵⁶, E. Benhar Nocchioli¹⁸⁰, J. Benitez⁶⁵, D. P. Benjamin⁴⁷, J. R. Bensinger²⁵, S. Bentvelsen¹⁰⁸, L. Beresford¹²¹, M. Beretta⁴⁹, D. Berge¹⁰⁸, E. Bergeas Kuutmann¹⁶⁹, N. Berger⁵, J. Beringer¹⁶, S. Berlendis⁵⁷, N. R. Bernard⁸⁸, C. Bernius¹¹¹, F. U. Bernlochner²³, T. Berry⁷⁹, P. Berta¹³⁰, C. Bertella⁸⁵, G. Bertoli^{149a,149b}, F. Bertolucci^{125a,125b}, I. A. Bertram⁷⁴, C. Bertsche⁴⁴, D. Bertsche¹¹⁴, G. J. Besjes³⁸, O. Bessidskaia Bylund^{149a,149b}, M. Bessner⁴⁴, N. Besson¹³⁷, C. Betancourt⁵⁰, A. Bethani⁵⁷, S. Bethke¹⁰², A. J. Bevan⁷⁸, R. M. Bianchi¹²⁶, L. Bianchini²⁵, M. Bianco³², O. Biebel¹⁰¹, D. Biedermann¹⁷, R. Bielski⁸⁶, N. V. Biesuz^{125a,125b}, M. Biglietti^{135a}, J. Bilbao De Mendizabal⁵¹, T. R. V. Billoud⁹⁶, H. Bilokon⁴⁹, M. Bindi⁵⁶, S. Binet¹¹⁸, A. Bingul^{20b}, C. Bini^{133a,133b}, S. Biondi^{22a,22b}, T. Bisanz⁵⁶, D. M. Bjergaard⁴⁷, C. W. Black¹⁵³, J. E. Black¹⁴⁶, K. M. Black²⁴, D. Blackburn¹³⁹, R. E. Blair⁶, J. -B. Blanchard¹³⁷, T. Blazek^{147a}, I. Bloch⁴⁴, C. Blocker²⁵, W. Blum^{85,*}, U. Blumenschein⁵⁶, S. Blunier^{34a}, G. J. Bobbink¹⁰⁸, V. S. Bobrovnikov^{110,c}, S. S. Bocchetta⁸³, A. Bocci⁴⁷, C. Bock¹⁰¹, M. Boehler⁵⁰, D. Boerner¹⁷⁹, J. A. Bogaerts³², D. Bogavac¹⁴, A. G. Bogdanchikov¹¹⁰, C. Bohm^{149a}, V. Boisvert⁷⁹, P. Bokan¹⁴, T. Bold^{40a}, A. S. Boldyrev^{168a,168c}, M. Bomben⁸², M. Bona⁷⁸, M. Boonekamp¹³⁷, A. Borisov¹³¹, G. Borissov⁷⁴, J. Bortfeldt³², D. Bortoletto¹²¹, V. Bortolotto^{62a,62b,62c}, K. Bos¹⁰⁸, D. Boscherini^{22a}, M. Bosman¹³, J. D. Bossio Sola²⁹, J. Boudreau¹²⁶, J. Bouffard², E. V. Bouhova-Thacker⁷⁴, D. Boumedienne³⁶, C. Bourdarios¹¹⁸, S. K. Boutle⁵⁵, A. Boveia³², J. Boyd³², I. R. Boyko⁶⁷, J. Bracinik¹⁹, A. Brandt⁸, G. Brandt⁵⁶, O. Brandt^{60a}, U. Bratzler¹⁵⁹, B. Brau⁸⁸, J. E. Brau¹¹⁷, H. M. Braun^{179,*}, W. D. Breaden Madden⁵⁵, K. Brendlinger¹²³, A. J. Brennan⁹⁰, L. Brenner¹⁰⁸, R. Brenner¹⁶⁹, S. Bressler¹⁷⁶, T. M. Bristow⁴⁸, D. Britton⁵⁵, D. Britzger⁴⁴, F. M. Brochu³⁰, I. Brock²³, R. Brock⁹², G. Brooijmans³⁷, T. Brooks⁷⁹, W. K. Brooks^{34b}, J. Brosamer¹⁶, E. Brost¹⁰⁹, J. H. Broughton¹⁹, P. A. Bruckman de Renstrom⁴¹, D. Bruncko^{147b}, R. Bruneliere⁵⁰, A. Bruni^{22a}, G. Bruni^{22a}, L. S. Bruni¹⁰⁸, B. H. Brunt³⁰, M. Bruschi^{22a}, N. Bruscino²³, P. Bryant³³, L. Bryngemark⁸³, T. Buanes¹⁵, Q. Buat¹⁴⁵, P. Buchholz¹⁴⁴, A. G. Buckley⁵⁵, I. A. Budagov⁶⁷, F. Buehrer⁵⁰, M. K. Bugge¹²⁰, O. Bulekov⁹⁹, D. Bullock⁸, H. Burckhart³², S. Burdin⁷⁶, C. D. Burgard⁵⁰, B. Burghgrave¹⁰⁹, K. Burka⁴¹, S. Burke¹³², I. Burmeister⁴⁵, J. T. P. Burr¹²¹, E. Busato³⁶, D. Büscher⁵⁰, V. Büscher⁸⁵, P. Bussey⁵⁵, J. M. Butler²⁴, C. M. Buttar⁵⁵, J. M. Butterworth⁸⁰, P. Butti¹⁰⁸, W. Buttinger²⁷, A. Buzatu⁵⁵, A. R. Buzykaev^{110,c}, S. Cabrera Urbán¹⁷¹,

- D. Caforio¹²⁹, V. M. Cairo^{39a,39b}, O. Cakir^{4a}, N. Calace⁵¹, P. Calafiura¹⁶, A. Calandri⁸⁷, G. Calderini⁸², P. Calfayan¹⁰¹, G. Callea^{39a,39b}, L. P. Caloba^{26a}, S. Calvente Lopez⁸⁴, D. Calvet³⁶, S. Calvet³⁶, T. P. Calvet⁸⁷, R. Camacho Toro³³, S. Camarda³², P. Camarri^{134a,134b}, D. Cameron¹²⁰, R. Caminal Armadans¹⁷⁰, C. Camincher⁵⁷, S. Campana³², M. Campanelli⁸⁰, A. Camplani^{93a,93b}, A. Campoverde¹⁴⁴, V. Canale^{105a,105b}, A. Canepa^{164a}, M. Cano Bret¹⁴¹, J. Cantero¹¹⁵, T. Cao⁴², M. D. M. Capeans Garrido³², I. Caprini^{28b}, M. Caprini^{28b}, M. Capua^{39a,39b}, R. Caputo⁸⁵, R. M. Carbone³⁷, R. Cardarelli^{134a}, F. Cardillo⁵⁰, I. Carli¹³⁰, T. Carli³², G. Carlino^{105a}, L. Carminati^{93a,93b}, S. Caron¹⁰⁷, E. Carquin^{34b}, G. D. Carrillo-Montoya³², J. R. Carter³⁰, J. Carvalho^{127a,127c}, D. Casadei¹⁹, M. P. Casado^{13,i}, M. Casolino¹³, D. W. Casper¹⁶⁷, E. Castaneda-Miranda^{148a}, R. Castelijns¹⁰⁸, A. Castelli¹⁰⁸, V. Castillo Gimenez¹⁷¹, N. F. Castro^{127a,j}, A. Catinaccio³², J. R. Catmore¹²⁰, A. Cattai³², J. Caudron²³, V. Cavaliere¹⁷⁰, E. Cavallaro¹³, D. Cavalli^{93a}, M. Cavalli-Sforza¹³, V. Cavasinni^{125a,125b}, F. Ceradini^{135a,135b}, L. Cerda Alberich¹⁷¹, B. C. Cerio⁴⁷, A. S. Cerqueira^{26b}, A. Cerri¹⁵², L. Cerrito^{134a,134b}, F. Cerutti¹⁶, M. Cerv³², A. Cervelli¹⁸, S. A. Cetin^{20c}, A. Chafaq^{136a}, D. Chakraborty¹⁰⁹, S. K. Chan⁵⁸, Y. L. Chan^{62a}, P. Chang¹⁷⁰, J. D. Chapman³⁰, D. G. Charlton¹⁹, A. Chatterjee⁵¹, C. C. Chau¹⁶², C. A. Chavez Barajas¹⁵², S. Che¹¹², S. Cheatham⁷⁴, A. Chegwiddden⁹², S. Chekanov⁶, S. V. Chekulaev^{164a}, G. A. Chelkov^{67,k}, M. A. Chelstowska⁹¹, C. Chen⁶⁶, H. Chen²⁷, K. Chen¹⁵¹, S. Chen^{35b}, S. Chen¹⁵⁸, X. Chen^{35c}, Y. Chen⁶⁹, H. C. Cheng⁹¹, H. J. Cheng^{35a}, Y. Cheng³³, A. Cheplakov⁶⁷, E. Cheremushkina¹³¹, R. Cherkaoui El Moursli^{136e}, V. Chernyatin^{27,*}, E. Cheu⁷, L. Chevalier¹³⁷, V. Chiarella⁴⁹, G. Chiarelli^{125a,125b}, G. Chiodini^{75a}, A. S. Chisholm¹⁹, A. Chitan^{28b}, M. V. Chizhov⁶⁷, K. Choi⁶³, A. R. Chomont³⁶, S. Chouridou⁹, B. K. B. Chow¹⁰¹, V. Christodoulou⁸⁰, D. Chromek-Burckhart³², J. Chudoba¹²⁸, A. J. Chuinard⁸⁹, J. J. Chwastowski⁴¹, L. Chytka¹¹⁶, G. Ciapetti^{133a,133b}, A. K. Ciftci^{4a}, D. Cinca⁴⁵, V. Cindro⁷⁷, I. A. Cioara²³, C. Ciocca^{22a,22b}, A. Ciochio¹⁶, F. Ciotto^{105a,105b}, Z. H. Citron¹⁷⁶, M. Citterio^{93a}, M. Ciubancan^{28b}, A. Clark⁵¹, B. L. Clark⁵⁸, M. R. Clark³⁷, P. J. Clark⁴⁸, R. N. Clarke¹⁶, C. Clement^{149a,149b}, Y. Coadou⁸⁷, M. Cobal^{168a,168c}, A. Cocco⁵¹, J. Cochran⁶⁶, L. Colasurdo¹⁰⁷, B. Cole³⁷, A. P. Colijn¹⁰⁸, J. Collot⁵⁷, T. Colombo³², G. Compostella¹⁰², P. Conde Muiño^{127a,127b}, E. Coniavitis⁵⁰, S. H. Connell^{148b}, I. A. Connelly⁷⁹, V. Consorti⁵⁰, S. Constantinescu^{28b}, G. Conti³², F. Conventi^{105a,1}, M. Cooke¹⁶, B. D. Cooper⁸⁰, A. M. Cooper-Sarkar¹²¹, K. J. R. Cormier¹⁶², T. Cornelissen¹⁷⁹, M. Corradi^{133a,133b}, F. Corriveau^{89,m}, A. Corso-Radu¹⁶⁷, A. Cortes-Gonzalez³², G. Cortiana¹⁰², G. Costa^{93a}, M. J. Costa¹⁷¹, D. Costanzo¹⁴², G. Cottin³⁰, G. Cowan⁷⁹, B. E. Cox⁸⁶, K. Cranmer¹¹¹, S. J. Crawley⁵⁵, G. Cree³¹, S. Crépe-Renaudin⁵⁷, F. Crescioli⁸², W. A. Cribbs^{149a,149b}, M. Crispin Ortuzar¹²¹, M. Cristinziani²³, V. Croft¹⁰⁷, G. Crosetti^{39a,39b}, A. Cueto⁸⁴, T. Cuhadar Donszelmann¹⁴², J. Cummings¹⁸⁰, M. Curatolo⁴⁹, J. Cúth⁸⁵, H. Cziri¹⁴⁴, P. Czodrowski³, G. D'amen^{22a,22b}, S. D'Auria⁵⁵, M. D'Onofrio⁷⁶, M. J. Da Cunha Sargedadas De Sousa^{127a,127b}, C. Da Via⁸⁶, W. Dabrowski^{40a}, T. Dado^{147a}, T. Dai⁹¹, O. Dale¹⁵, F. Dallaire⁹⁶, C. Dallapiccola⁸⁸, M. Dam³⁸, J. R. Dandoy³³, N. P. Dang⁵⁰, A. C. Daniells¹⁹, N. S. Dann⁸⁶, M. Danninger¹⁷², M. Dano Hoffmann¹³⁷, V. Dao⁵⁰, G. Darbo^{52a}, S. Darmora⁸, J. Dassoulas³, A. Dattagupta¹¹⁷, W. Davey²³, C. David¹⁷³, T. Davidek¹³⁰, M. Davies¹⁵⁶, P. Davison⁸⁰, E. Dawe⁹⁰, I. Dawson¹⁴², R. K. Daya-Ishmukhametova⁸⁸, K. De⁸, R. de Asmundis^{105a}, A. De Benedetti¹¹⁴, S. De Castro^{22a,22b}, S. De Cecco⁸², N. De Groot¹⁰⁷, P. de Jong¹⁰⁸, H. De la Torre⁸⁴, F. De Lorenzi⁶⁶, A. De Maria⁵⁶, D. De Pedis^{133a}, A. De Salvo^{133a}, U. De Sanctis¹⁵², A. De Santo¹⁵², J. B. De Vivie De Regie¹¹⁸, W. J. Dearnaley⁷⁴, R. Debbé²⁷, C. Debenedetti¹³⁸, D. V. Dedovich⁶⁷, N. Dehghanian³, I. Deigaard¹⁰⁸, M. Del Gaudio^{39a,39b}, J. Del Peso⁸⁴, T. Del Prete^{125a,125b}, D. Delgove¹¹⁸, F. Deliot¹³⁷, C. M. Delitzsch⁵¹, A. Dell'Acqua³², L. Dell'Asta²⁴, M. Dell'Orso^{125a,125b}, M. Della Pietra^{105a,1}, D. della Volpe⁵¹, M. Delmastro⁵, P. A. Delsart⁵⁷, D. A. DeMarco¹⁶², S. Demers¹⁸⁰, M. Demichev⁶⁷, A. Demilly⁸², S. P. Denisov¹³¹, D. Denysiuk¹³⁷, D. Derendarz⁴¹, J. E. Derkaoui^{136d}, F. Derue⁸², P. Dervan⁷⁶, K. Desch²³, C. Deterre⁴⁴, K. Dette⁴⁵, P. O. Deviveiros³², A. Dewhurst¹³², S. Dhaliwal²⁵, A. Di Ciaccio^{134a,134b}, L. Di Ciaccio⁵, W. K. Di Clemente¹²³, C. Di Donato^{133a,133b}, A. Di Girolamo³², B. Di Girolamo³², B. Di Micco^{135a,135b}, R. Di Nardo³², A. Di Simone⁵⁰, R. Di Sipio¹⁶², D. Di Valentino³¹, C. Diaconu⁸⁷, M. Diamond¹⁶², F. A. Dias⁴⁸, M. A. Diaz^{34a}, E. B. Diehl⁹¹, J. Dietrich¹⁷, S. Diglio⁸⁷, A. Dimitrievska¹⁴, J. Dingfelder²³, P. Dita^{28b}, S. Dita^{28b}, F. Dittus³², F. Djama⁸⁷, T. Djobava^{53b}, J. I. Djuvsland^{60a}, M. A. B. do Vale^{26c}, D. Dobos³², M. Dobre^{28b}, C. Doglioni⁸³, J. Dolejsi¹³⁰, Z. Dolezal¹³⁰, M. Donadelli^{26d}, S. Donati^{125a,125b}, P. Dondero^{122a,122b}, J. Donini³⁶, J. Dopke¹³², A. Doria^{105a}, M. T. Dova⁷³, A. T. Doyle⁵⁵, E. Drechsler⁵⁶, M. Dris¹⁰, Y. Du¹⁴⁰, J. Duarte-Campderros¹⁵⁶, E. Duchovni¹⁷⁶, G. Duckeck¹⁰¹, O. A. Ducu^{96,n}, D. Duda¹⁰⁸, A. Dudarev³², A. Chr. Dudder⁸⁵, E. M. Duffield¹⁶, L. Duflo¹¹⁸, M. Dührssen³², M. Dumancic¹⁷⁶, M. Dunford^{60a}, H. Duran Yildiz^{4a}, M. Düren⁵⁴, A. Durglishvili^{53b}, D. Duschinger⁴⁶, B. Dutta⁴⁴, M. Dyndal⁴⁴, C. Eckardt⁴⁴, K. M. Ecker¹⁰², R. C. Edgar⁹¹, N. C. Edwards⁴⁸, T. Eifert³², G. Eigen¹⁵, K. Einsweiler¹⁶, T. Ekelof¹⁶⁹, M. El Kacimi^{136c}, V. Ellajosyula⁸⁷, M. Ellert¹⁶⁹, S. Elles⁵, F. Ellinghaus¹⁷⁹, A. A. Elliot¹⁷³, N. Ellis³², J. Elmsheuser²⁷, M. Elsing³², D. Emelianov¹³², Y. Enari¹⁵⁸, O. C. Endner⁸⁵, J. S. Ennis¹⁷⁴, J. Erdmann⁴⁵, A. Ereditato¹⁸, G. Ernis¹⁷⁹, J. Ernst², M. Ernst²⁷, S. Errede¹⁷⁰, E. Ertel⁸⁵, M. Escalier¹¹⁸, H. Esch⁴⁵, C. Escobar¹²⁶, B. Esposito⁴⁹, A. I. Etienne¹³⁷, E. Etzion¹⁵⁶, H. Evans⁶³, A. Ezhilov¹²⁴, F. Fabbri^{22a,22b}, L. Fabbri^{22a,22b}, G. Facini³³, R. M. Fakhrutdinov¹³¹, S. Falciano^{133a}, R. J. Falla⁸⁰, J. Faltova³²

- Y. Fang^{35a}, M. Fanti^{93a,93b}, A. Farbin⁸, A. Farilla^{135a}, C. Farina¹²⁶, E. M. Farina^{122a,122b}, T. Farooque¹³, S. Farrell¹⁶, S. M. Farrington¹⁷⁴, P. Farthouat³², F. Fassi^{136e}, P. Fassnacht³², D. Fassouliotis⁹, M. Faucci Giannelli⁷⁹, A. Favareto^{52a,52b}, W. J. Fawcett¹²¹, L. Fayard¹¹⁸, O. L. Fedin^{124,o}, W. Fedorko¹⁷², S. Feigl¹²⁰, L. Feligioni⁸⁷, C. Feng¹⁴⁰, E. J. Feng³², H. Feng⁹¹, A. B. Fenjuk¹³¹, L. Feremenga⁸, P. Fernandez Martinez¹⁷¹, S. Fernandez Perez¹³, J. Ferrando⁵⁵, A. Ferrari¹⁶⁹, P. Ferrari¹⁰⁸, R. Ferrari^{122a}, D. E. Ferreira de Lima^{60b}, A. Ferrer¹⁷¹, D. Ferrere⁵¹, C. Ferretti⁹¹, A. Ferretto Parodi^{52a,52b}, F. Fiedler⁸⁵, A. Filipčić⁷⁷, M. Filipuzzi⁴⁴, F. Filthaut¹⁰⁷, M. Fincke-Keeler¹⁷³, K. D. Finelli¹⁵³, M. C. N. Fiolhais^{127a,127c}, L. Fiorini¹⁷¹, A. Firan⁴², A. Fischer², C. Fischer¹³, J. Fischer¹⁷⁹, W. C. Fisher⁹², N. Flaschel⁴⁴, I. Fleck¹⁴⁴, P. Fleischmann⁹¹, G. T. Fletcher¹⁴², R. R. M. Fletcher¹²³, T. Flick¹⁷⁹, A. Floderus⁸³, L. R. Flores Castillo^{62a}, M. J. Flowerdew¹⁰², G. T. Forcolin⁸⁶, A. Formica¹³⁷, A. Forti⁸⁶, A. G. Foster¹⁹, D. Fournier¹¹⁸, H. Fox⁷⁴, S. Fracchia¹³, P. Francavilla⁸², M. Franchini^{22a,22b}, D. Francis³², L. Franconi¹²⁰, M. Franklin⁵⁸, M. Frate¹⁶⁷, M. Fraternali^{122a,122b}, D. Freeborn⁸⁰, S. M. Fressard-Batraneanu³², F. Friedrich⁴⁶, D. Froidevaux³², J. A. Frost¹²¹, C. Fukunaga¹⁵⁹, E. Fullana Torregrosa⁸⁵, T. Fusayasu¹⁰³, J. Fuster¹⁷¹, C. Gabaldon⁵⁷, O. Gabizon¹⁷⁹, A. Gabrielli^{22a,22b}, A. Gabrielli¹⁶, G. P. Gach^{40a}, S. Gadatsch³², S. Gadomski⁵¹, G. Gagliardi^{52a,52b}, L. G. Gagnon⁹⁶, P. Gagnon⁶³, C. Galea¹⁰⁷, B. Galhardo^{127a,127c}, E. J. Gallas¹²¹, B. J. Gallop¹³², P. Gallus¹²⁹, G. Galster³⁸, K. K. Gan¹¹², J. Gao⁵⁹, Y. Gao⁴⁸, Y. S. Gao^{146,g}, F. M. Garay Walls⁴⁸, C. García¹⁷¹, J. E. García Navarro¹⁷¹, M. Garcia-Sciveres¹⁶, R. W. Gardner³³, N. Garelli¹⁴⁶, V. Garonne¹²⁰, A. Gascon Bravo⁴⁴, K. Gasnikova⁴⁴, C. Gatti⁴⁹, A. Gaudiello^{52a,52b}, G. Gaudio^{122a}, L. Gauthier⁹⁶, I. L. Gavrilenko⁹⁷, C. Gay¹⁷², G. Gaycken²³, E. N. Gazis¹⁰, Z. Gecse¹⁷², C. N. P. Gee¹³², Ch. Geich-Gimbel²³, M. Geisen⁸⁵, M. P. Geisler^{60a}, C. Gemme^{52a}, M. H. Genest⁵⁷, C. Geng^{59,p}, S. Gentile^{133a,133b}, C. Gentsos¹⁵⁷, S. George⁷⁹, D. Gerbaudo¹³, A. Gershon¹⁵⁶, S. Ghasemi¹⁴⁴, H. Ghazlane^{136b}, M. Ghneimat²³, B. Giacobbe^{22a}, S. Giagu^{133a,133b}, P. Giannetti^{125a,125b}, B. Gibbard²⁷, S. M. Gibson⁷⁹, M. Gignac¹⁷², M. Gilchriese¹⁶, T. P. S. Gillam³⁰, D. Gillberg³¹, G. Gilles¹⁷⁹, D. M. Gingrich^{3,d}, N. Giokaris⁹, M. P. Giordani^{168a,168c}, F. M. Giorgi^{22a}, F. M. Giorgi¹⁷, P. F. Giraud¹³⁷, P. Giromini⁵⁸, D. Giugni^{93a}, F. Giuli¹²¹, C. Giuliani¹⁰², M. Giulini^{60b}, B. K. Gjelsten¹²⁰, S. Gkaitatzis¹⁵⁷, I. Gkialas¹⁵⁷, E. L. Gkougkousis¹¹⁸, L. K. Gladilin¹⁰⁰, C. Glasman⁸⁴, J. Glatzer⁵⁰, P. C. F. Glaysheer⁴⁸, A. Glazov⁴⁴, M. Goblirsch-Kolb²⁵, J. Godlewski⁴¹, S. Goldfarb⁹⁰, T. Golling⁵¹, D. Golubkov¹³¹, A. Gomes^{127a,127b,127d}, R. Gonçalves^{127a}, J. Goncalves Pinto Firmino Da Costa¹³⁷, G. Gonella⁵⁰, L. Gonella¹⁹, A. Gongadze⁶⁷, S. González de la Hoz¹⁷¹, G. Gonzalez Parra¹³, S. Gonzalez-Sevilla⁵¹, L. Goossens³², P. A. Gorbounov⁹⁸, H. A. Gordon²⁷, I. Gorelov¹⁰⁶, B. Gorini³², E. Gorini^{75a,75b}, A. Gorišek⁷⁷, E. Gornicki⁴¹, A. T. Goshaw⁴⁷, C. Gössling⁴⁵, M. I. Gostkin⁶⁷, C. R. Goudet¹¹⁸, D. Goujdami^{136c}, A. G. Goussiou¹³⁹, N. Govender^{148b,q}, E. Gozani¹⁵⁵, L. Graber⁵⁶, I. Grabowska-Bold^{40a}, P. O. J. Gradin⁵⁷, P. Grafström^{22a,22b}, J. Gramling⁵¹, E. Gramstad¹²⁰, S. Grancagnolo¹⁷, V. Gratchev¹²⁴, P. M. Gravila^{28e}, H. M. Gray³², E. Graziani^{135a}, Z. D. Greenwood^{81,r}, C. Greife²³, K. Gregersen⁸⁰, I. M. Gregor⁴⁴, P. Grenier¹⁴⁶, K. Grevtsov⁵, J. Griffiths⁸, A. A. Grillo¹³⁸, K. Grimm⁷⁴, S. Grinstein^{13,s}, Ph. Gris³⁶, J. -F. Grivaz¹¹⁸, S. Groh⁸⁵, J. P. Grohs⁴⁶, E. Gross¹⁷⁶, J. Grosse-Knetter⁵⁶, G. C. Grossi⁸¹, Z. J. Grout⁸⁰, L. Guan⁹¹, W. Guan¹⁷⁷, J. Guenther⁶⁴, F. Guescini⁵¹, D. Guest¹⁶⁷, O. Gueta¹⁵⁶, E. Guido^{52a,52b}, T. Guillemin⁵, S. Guindon², U. Gul⁵⁵, C. Gumpert³², J. Guo¹⁴¹, Y. Guo^{59,p}, R. Gupta⁴², S. Gupta¹²¹, G. Gustavino^{133a,133b}, P. Gutierrez¹¹⁴, N. G. Gutierrez Ortiz⁸⁰, C. Gutsche⁴⁶, C. Guyot¹³⁷, C. Gwenlan¹²¹, C. B. Gwilliam⁷⁶, A. Haas¹¹¹, C. Haber¹⁶, H. K. Hadavand⁸, N. Haddad^{136e}, A. Hadeef⁸⁷, S. Hageböck²³, Z. Hajduk⁴¹, H. Hakobyan^{181,*}, M. Haleem⁴⁴, J. Haley¹¹⁵, G. Halladjian⁹², G. D. Hallowell⁸⁷, K. Hamacher¹⁷⁹, P. Hamal¹¹⁶, K. Hamano¹⁷³, A. Hamilton^{148a}, G. N. Hamity¹⁴², P. G. Hamnett⁴⁴, L. Han⁵⁹, K. Hanagaki^{68,t}, K. Hanawa¹⁵⁸, M. Hance¹³⁸, B. Haney¹²³, P. Hanke^{60a}, R. Hanna¹³⁷, J. B. Hansen³⁸, J. D. Hansen³⁸, M. C. Hansen²³, P. H. Hansen³⁸, K. Hara¹⁶⁵, A. S. Hard¹⁷⁷, T. Harenberg¹⁷⁹, F. Hariri¹¹⁸, S. Harkusha⁹⁴, R. D. Harrington⁴⁸, P. F. Harrison¹⁷⁴, F. Hartjes¹⁰⁸, N. M. Hartmann¹⁰¹, M. Hasegawa⁶⁹, Y. Hasegawa¹⁴³, A. Hasib¹¹⁴, S. Hassani¹³⁷, S. Haug¹⁸, R. Hauser⁹², L. Hauswald⁴⁶, M. Havranek¹²⁸, C. M. Hawkes¹⁹, R. J. Hawkings³², D. Hayakawa¹⁶⁰, D. Hayden⁹², C. P. Hays¹²¹, J. M. Hays⁷⁸, H. S. Hayward⁷⁶, S. J. Haywood¹³², S. J. Head¹⁹, T. Heck⁸⁵, V. Hedberg⁸³, L. Heelan⁸, S. Heim¹²³, T. Heim¹⁶, B. Heinemann¹⁶, J. J. Heinrich¹⁰¹, L. Heinrich¹¹¹, C. Heinz⁵⁴, J. Hejbal¹²⁸, L. Helary³², S. Hellman^{149a,149b}, C. Helsens³², J. Henderson¹²¹, R. C. W. Henderson⁷⁴, Y. Heng¹⁷⁷, S. Henkelmann¹⁷², A. M. Henriques Correia³², S. Henrot-Versille¹¹⁸, G. H. Herbert¹⁷, V. Herget¹⁷⁸, Y. Hernández Jiménez¹⁷¹, G. Herten⁵⁰, R. Hertenberger¹⁰¹, L. Hervas³², G. G. Hesketh⁸⁰, N. P. Hessey¹⁰⁸, J. W. Hetherly⁴², R. Hickling⁷⁸, E. Higón-Rodríguez¹⁷¹, E. Hill¹⁷³, J. C. Hill³⁰, K. H. Hiller⁴⁴, S. J. Hillier¹⁹, I. Hinchliffe¹⁶, E. Hines¹²³, R. R. Hinman¹⁶, M. Hirose⁵⁰, D. Hirschbuehl¹⁷⁹, J. Hobbs¹⁵¹, N. Hod^{164a}, M. C. Hodgkinson¹⁴², P. Hodgson¹⁴², A. Hoecker³², M. R. Hoferkamp¹⁰⁶, F. Hoenig¹⁰¹, D. Hohn²³, T. R. Holmes¹⁶, M. Homann⁴⁵, T. M. Hong¹²⁶, B. H. Hooberman¹⁷⁰, W. H. Hopkins¹¹⁷, Y. Horii¹⁰⁴, A. J. Horton¹⁴⁵, J.-Y. Hostachy⁵⁷, S. Hou¹⁵⁴, A. Hoummada^{136a}, J. Howarth⁴⁴, M. Hrabovsky¹¹⁶, I. Hristova¹⁷, J. Hrivnac¹¹⁸, T. Hryn'ova⁵, A. Hrynevich⁹⁵, C. Hsu^{148c}, P. J. Hsu^{154,u}, S. -C. Hsu¹³⁹, D. Hu³⁷, Q. Hu⁵⁹, S. Hu¹⁴¹, Y. Huang⁴⁴, Z. Hubacek¹²⁹, F. Hubaut⁸⁷, F. Huegging²³, T. B. Huffman¹²¹, E. W. Hughes³⁷, G. Hughes⁷⁴, M. Huhtinen³², P. Huo¹⁵¹, N. Huseynov^{67,b}, J. Huston⁹², J. Huth⁵⁸, G. Iacobucci⁵¹, G. Iakovidis²⁷, I. Ibragimov¹⁴⁴, L. Iconomidou-Fayard¹¹⁸, E. Ideal¹⁸⁰, Z. Idrissi^{136e},

- P. Iengo³², O. Igonkina^{108,y}, T. Iizawa¹⁷⁵, Y. Ikegami⁶⁸, M. Ikeno⁶⁸, Y. Ilchenko^{11,w}, D. Iliadis¹⁵⁷, N. Ilic¹⁴⁶, T. Ince¹⁰², G. Introzzi^{122a,122b}, P. Ioannou^{9,*}, M. Iodice^{135a}, K. Iordanidou³⁷, V. Ippolito⁵⁸, N. Ishijima¹¹⁹, M. Ishino¹⁵⁸, M. Ishitsuka¹⁶⁰, R. Ishmukhametov¹¹², C. Issever¹²¹, S. Istin^{20a}, F. Ito¹⁶⁵, J. M. Iturbe Ponce⁸⁶, R. Iuppa^{163a,163b}, W. Iwanski⁶⁴, H. Iwasaki⁶⁸, J. M. Izen⁴³, V. Izzo^{105a}, S. Jabbar³, B. Jackson¹²³, P. Jackson¹, V. Jain², K. B. Jakobi⁸⁵, K. Jakobs⁵⁰, S. Jakobsen³², T. Jakoubek¹²⁸, D. O. Jamin¹¹⁵, D. K. Jana⁸¹, E. Jansen⁸⁰, R. Jansky⁶⁴, J. Janssen²³, M. Janus⁵⁶, G. Jarlskog⁸³, N. Javadov^{67,b}, T. Javůrek⁵⁰, F. Jeanneau¹³⁷, L. Jeanty¹⁶, G. -Y. Jeng¹⁵³, D. Jennens⁹⁰, P. Jenni^{50,x}, C. Jeske¹⁷⁴, S. Jézéquel⁵, H. Ji¹⁷⁷, J. Jia¹⁵¹, H. Jiang⁶⁶, Y. Jiang⁵⁹, S. Jiggins⁸⁰, J. Jimenez Pena¹⁷¹, S. Jin^{35a}, A. Jinaru^{28b}, O. Jinnouchi¹⁶⁰, H. Jivan^{148c}, P. Johansson¹⁴², K. A. Johns⁷, W. J. Johnson¹³⁹, K. Jon-And^{149a,149b}, G. Jones¹⁷⁴, R. W. L. Jones⁷⁴, S. Jones⁷, T. J. Jones⁷⁶, J. Jongmanns^{60a}, P. M. Jorge^{127a,127b}, J. Jovicevic^{164a}, X. Ju¹⁷⁷, A. Juste Rozas^{13,s}, M. K. Köhler¹⁷⁶, A. Kaczmarek⁴¹, M. Kado¹¹⁸, H. Kagan¹¹², M. Kagan¹⁴⁶, S. J. Kahn⁸⁷, T. Kaji¹⁷⁵, E. Kajomovitz⁴⁷, C. W. Kalderon¹²¹, A. Kaluza⁸⁵, S. Kama⁴², A. Kamenshchikov¹³¹, N. Kanaya¹⁵⁸, S. Kaneti³⁰, L. Kanjir⁷⁷, V. A. Kantserov⁹⁹, J. Kanzaki⁶⁸, B. Kaplan¹¹¹, L. S. Kaplan¹⁷⁷, A. Kapliy³³, D. Kar^{148c}, K. Karakostas¹⁰, A. Karamaoun³, N. Karastathis¹⁰, M. J. Kareem⁵⁶, E. Karentzos¹⁰, M. Karnevskiy⁸⁵, S. N. Karpov⁶⁷, Z. M. Karpova⁶⁷, K. Karthik¹¹¹, V. Kartvelishvili⁷⁴, A. N. Karyukhin¹³¹, K. Kasahara¹⁶⁵, L. Kashif¹⁷⁷, R. D. Kass¹¹², A. Kastanas¹⁵, Y. Kataoka¹⁵⁸, C. Kato¹⁵⁸, A. Katre⁵¹, J. Katzy⁴⁴, K. Kawade¹⁰⁴, K. Kawagoe⁷², T. Kawamoto¹⁵⁸, G. Kawamura⁵⁶, V. F. Kazanin^{110,c}, R. Keeler¹⁷³, R. Kehoe⁴², J. S. Keller⁴⁴, J. J. Kempster⁷⁹, H. Keoshkerian¹⁶², O. Kepka¹²⁸, B. P. Kerševan⁷⁷, S. Kersten¹⁷⁹, R. A. Keyes⁸⁹, M. Khader¹⁷⁰, F. Khalil-zada¹², A. Khanov¹¹⁵, A. G. Kharlamov^{110,c}, T. J. Khoo⁵¹, V. Khovanskii⁹⁸, E. Khramov⁶⁷, J. Khubua^{53b,y}, S. Kido⁶⁹, C. R. Kilby⁷⁹, H. Y. Kim⁸, S. H. Kim¹⁶⁵, Y. K. Kim³³, N. Kimura¹⁵⁷, O. M. Kind¹⁷, B. T. King⁷⁶, M. King¹⁷¹, J. Kirk¹³², A. E. Kiryunin¹⁰², T. Kishimoto¹⁵⁸, D. Kisielewska^{40a}, F. Kiss⁵⁰, K. Kiuchi¹⁶⁵, O. Kivernyk¹³⁷, E. Kladiva^{147b}, M. H. Klein³⁷, M. Klein⁷⁶, U. Klein⁷⁶, K. Kleinknecht⁸⁵, P. Klimek¹⁰⁹, A. Klimentov²⁷, R. Klingenberg⁴⁵, J. A. Klinger¹⁴², T. Klioutchnikova³², E. -E. Kluge^{60a}, P. Kluit¹⁰⁸, S. Kluth¹⁰², J. Knapik⁴¹, E. Kneringer⁶⁴, E. B. F. G. Knoops⁸⁷, A. Knue⁵⁵, A. Kobayashi¹⁵⁸, D. Kobayashi¹⁶⁰, T. Kobayashi¹⁵⁸, M. Kobel⁴⁶, M. Kocian¹⁴⁶, P. Kodys¹³⁰, N. M. Koehler¹⁰², T. Koffas³¹, E. Koffeman¹⁰⁸, T. Koi¹⁴⁶, H. Kolanoski¹⁷, M. Kolb^{60b}, I. Koletsou⁵, A. A. Komar^{97,*}, Y. Komori¹⁵⁸, T. Kondo⁶⁸, N. Kondrashova⁴⁴, K. Köneke⁵⁰, A. C. König¹⁰⁷, T. Kono^{68,z}, R. Konoplich^{111,aa}, N. Konstantinidis⁸⁰, R. Kopeliansky⁶³, S. Koperny^{40a}, L. Köpke⁸⁵, A. K. Kopp⁵⁰, K. Korcyl⁴¹, K. Kordas¹⁵⁷, A. Korn⁸⁰, A. A. Korol^{110,c}, I. Korolkov¹³, E. V. Korolkova¹⁴², O. Kortner¹⁰², S. Kortner¹⁰², T. Kosek¹³⁰, V. V. Kostyukhin²³, A. Kotwal⁴⁷, A. Kourkouveli-Charalampidi^{122a,122b}, C. Kourkouvelis⁹, V. Kouskoura²⁷, A. B. Kowalewska⁴¹, R. Kowalewski¹⁷³, T. Z. Kowalski^{40a}, C. Kozakai¹⁵⁸, W. Kozanecki¹³⁷, A. S. Kozhin¹³¹, V. A. Kramarenko¹⁰⁰, G. Kramberger⁷⁷, D. Krasnopevtsev⁹⁹, M. W. Krasny⁸², A. Krasznahorkay³², A. Kravchenko²⁷, M. Kretz^{60c}, J. Kretzschmar⁷⁶, K. Kreutzfeldt⁵⁴, P. Krieger¹⁶², K. Krizka³³, K. Kroeninger⁴⁵, H. Kroha¹⁰², J. Kroll¹²³, J. Kroseberg²³, J. Krstic¹⁴, U. Kruchonak⁶⁷, H. Krüger²³, N. Krumnack⁶⁶, A. Kruse¹⁷⁷, M. C. Kruse⁴⁷, M. Kruskal²⁴, T. Kubota⁹⁰, H. Kucuk⁸⁰, S. Kuday^{4b}, J. T. Kuechler¹⁷⁹, S. Kuehn⁵⁰, A. Kugel^{60c}, F. Kuger¹⁷⁸, A. Kuhl¹³⁸, T. Kuhl⁴⁴, V. Kukhtin⁶⁷, R. Kukla¹³⁷, Y. Kulchitsky⁹⁴, S. Kuleshov^{34b}, M. Kuna^{133a,133b}, T. Kunigo⁷⁰, A. Kupco¹²⁸, H. Kurashige⁶⁹, Y. A. Kurochkin⁹⁴, V. Kus¹²⁸, E. S. Kuwertz¹⁷³, M. Kuze¹⁶⁰, J. Kvita¹¹⁶, T. Kwan¹⁷³, D. Kyriazopoulos¹⁴², A. La Rosa¹⁰², J. L. La Rosa Navarro^{26d}, L. La Rotonda^{39a,39b}, C. Lacasta¹⁷¹, F. Lacava^{133a,133b}, J. Lacey³¹, H. Lacker¹⁷, D. Lacour⁸², V. R. Lacuesta¹⁷¹, E. Ladygin⁶⁷, R. Lafaye⁵, B. Laforge⁸², T. Lagouri¹⁸⁰, S. Lai⁵⁶, S. Lammers⁶³, W. Lampl⁷, E. Lançon¹³⁷, U. Landgraf⁵⁰, M. P. J. Landon⁷⁸, M. C. Lanfermann⁵¹, V. S. Lang^{60a}, J. C. Lange¹³, A. J. Lankford¹⁶⁷, F. Lanni²⁷, K. Lantzsch²³, A. Lanza^{122a}, S. Laplace⁸², C. Lapoire³², J. F. Laporte¹³⁷, T. Lari^{93a}, F. Lasagni Manghi^{22a,22b}, M. Lassnig³², P. Laurelli⁴⁹, W. Lavrijsen¹⁶, A. T. Law¹³⁸, P. Laycock⁷⁶, T. Lazovich⁵⁸, M. Lazzaroni^{93a,93b}, B. Le⁹⁰, O. Le Dortz⁸², E. Le Guirriec⁸⁷, E. P. Le Quilleuc¹³⁷, M. LeBlanc¹⁷³, T. LeCompte⁶, F. Ledroit-Guillon⁵⁷, C. A. Lee²⁷, S. C. Lee¹⁵⁴, L. Lee¹, B. Lefebvre⁸⁹, G. Lefebvre⁸², M. Lefebvre¹⁷³, F. Legger¹⁰¹, C. Leggett¹⁶, A. Lehan⁷⁶, G. Lehmann Miotto³², X. Lei⁷, W. A. Leight³¹, A. G. Leister¹⁸⁰, M. A. L. Leite^{26d}, R. Leitner¹³⁰, D. Lellouch¹⁷⁶, B. Lemmer⁵⁶, K. J. C. Leney⁸⁰, T. Lenz²³, B. Lenzi³², R. Leone⁷, S. Leone^{125a,125b}, C. Leonidopoulos⁴⁸, S. Leontsinis¹⁰, G. Lerner¹⁵², C. Leroy⁹⁶, A. A. J. Lesage¹³⁷, C. G. Lester³⁰, M. Levchenko¹²⁴, J. Levêque⁵, D. Levin⁹¹, L. J. Levinson¹⁷⁶, M. Levy¹⁹, D. Lewis⁷⁸, A. M. Leyko²³, M. Leyton⁴³, B. Li^{59,p}, C. Li⁵⁹, H. Li¹⁵¹, H. L. Li³³, L. Li⁴⁷, L. Li¹⁴¹, Q. Li^{35a}, S. Li⁴⁷, X. Li⁸⁶, Y. Li¹⁴⁴, Z. Liang^{35a}, B. Liberti^{134a}, A. Liblong¹⁶², P. Lichard³², K. Lie¹⁷⁰, J. Liebal²³, W. Liebig¹⁵, A. Limosani¹⁵³, S. C. Lin^{154,ab}, T. H. Lin⁸⁵, B. E. Lindquist¹⁵¹, A. E. Lioni⁵¹, E. Lipeles¹²³, A. Lipniacka¹⁵, M. Lisovsky^{60b}, T. M. Liss¹⁷⁰, A. Lister¹⁷², A. M. Litke¹³⁸, B. Liu^{154,ac}, D. Liu¹⁵⁴, H. Liu⁹¹, H. Liu²⁷, J. Liu⁸⁷, J. B. Liu⁵⁹, K. Liu⁸⁷, L. Liu¹⁷⁰, M. Liu⁴⁷, M. Liu⁵⁹, Y. L. Liu⁵⁹, Y. Liu⁵⁹, M. Livan^{122a,122b}, A. Lleres⁵⁷, J. Llorente Merino^{35a}, S. L. Lloyd⁷⁸, F. Lo Sterzo¹⁵⁴, E. M. Lobodzinska⁴⁴, P. Loch⁷, W. S. Lockman¹³⁸, F. K. Loebinger⁸⁶, A. E. Loesch-Jensen³⁸, K. M. Loew²⁵, A. Loginov^{180,*}, T. Lohse¹⁷, K. Lohwasser⁴⁴, M. Lokajicek¹²⁸, B. A. Long²⁴, J. D. Long¹⁷⁰, R. E. Long⁷⁴, L. Longo^{75a,75b}, K. A. Looper¹¹², L. Lopes^{127a}, D. Lopez Mateos⁵⁸, B. Lopez Paredes¹⁴², I. Lopez Paz¹³, A. Lopez Solis⁸², J. Lorenz¹⁰¹, N. Lorenzo Martinez⁶³,

M. Losada²¹, P. J. Lösel¹⁰¹, X. Lou^{35a}, A. Lounis¹¹⁸, J. Love⁶, P. A. Love⁷⁴, H. Lu^{62a}, N. Lu⁹¹, H. J. Lubatti¹³⁹, C. Luci^{133a,133b}, A. Lucotte⁵⁷, C. Luedtke⁵⁰, F. Luehring⁶³, W. Lukas⁶⁴, L. Luminari^{133a}, O. Lundberg^{149a,149b}, B. Lund-Jensen¹⁵⁰, P. M. Luzi⁸², D. Lynn²⁷, R. Lysak¹²⁸, E. Lytken⁸³, V. Lyubushkin⁶⁷, H. Ma²⁷, L. L. Ma¹⁴⁰, Y. Ma¹⁴⁰, G. Maccarrone⁴⁹, A. Macchiolo¹⁰², C. M. Macdonald¹⁴², B. Maček⁷⁷, J. Machado Miguens^{123,127b}, D. Madaffari⁸⁷, R. Madar³⁶, H. J. Maddocks¹⁶⁹, W. F. Mader⁴⁶, A. Madsen⁴⁴, J. Maeda⁶⁹, S. Maeland¹⁵, T. Maeno²⁷, A. Maevskiy¹⁰⁰, E. Magradze⁵⁶, J. Mahlstedt¹⁰⁸, C. Maiani¹¹⁸, C. Maidantchik^{26a}, A. A. Maier¹⁰², T. Maier¹⁰¹, A. Maio^{127a,127b,127d}, S. Majewski¹¹⁷, Y. Makida⁶⁸, N. Makovec¹¹⁸, B. Malaescu⁸², Pa. Malecki⁴¹, V. P. Maleev¹²⁴, F. Malek⁵⁷, U. Mallik⁶⁵, D. Malon⁶, C. Malone¹⁴⁶, S. Maltezos¹⁰, S. Malyukov³², J. Mamuzic¹⁷¹, G. Mancini⁴⁹, B. Mandelli³², L. Mandelli^{93a}, I. Mandić⁷⁷, J. Maneira^{127a,127b}, L. Manhaes de Andrade Filho^{26b}, J. Manjarres Ramos^{164b}, A. Mann¹⁰¹, A. Manousos³², B. Mansoulie¹³⁷, J. D. Mansour^{35a}, R. Mantifel⁸⁹, M. Mantoani⁵⁶, S. Manzoni^{93a,93b}, L. Mapelli³², G. Marceca²⁹, L. March⁵¹, G. Marchiori⁸², M. Marcisovsky¹²⁸, M. Marjanovic¹⁴, D. E. Marley⁹¹, F. Marroquim^{26a}, S. P. Marsden⁸⁶, Z. Marshall¹⁶, S. Marti-Garcia¹⁷¹, B. Martin⁹², T. A. Martin¹⁷⁴, V. J. Martin⁴⁸, B. Martin dit Latour¹⁵, M. Martinez^{13,s}, V. I. Martinez Outschoorn¹⁷⁰, S. Martin-Haugh¹³², V. S. Martoiu^{28b}, A. C. Martyniuk⁸⁰, M. Marx¹³⁹, A. Marzin³², L. Masetti⁸⁵, T. Mashimo¹⁵⁸, R. Mashinistov⁹⁷, J. Masik⁸⁶, A. L. Maslennikov^{110,c}, I. Massa^{22a,22b}, L. Massa^{22a,22b}, P. Mastrandrea⁵, A. Mastroberardino^{39a,39b}, T. Masubuchi¹⁵⁸, P. Mättig¹⁷⁹, J. Mattmann⁸⁵, J. Maurer^{28b}, S. J. Maxfield⁷⁶, D. A. Maximov^{110,c}, R. Mazini¹⁵⁴, S. M. Mazza^{93a,93b}, N. C. Mc Fadden¹⁰⁶, G. Mc Goldrick¹⁶², S. P. Mc Kee⁹¹, A. McCann⁹¹, R. L. McCarthy¹⁵¹, T. G. McCarthy¹⁰², L. I. McClymont⁸⁰, E. F. McDonald⁹⁰, J. A. Mcfayden⁸⁰, G. Mchedlidze⁵⁶, S. J. McMahon¹³², R. A. McPherson^{173,m}, M. Medinnis⁴⁴, S. Meehan¹³⁹, S. Mehlhase¹⁰¹, A. Mehta⁷⁶, K. Meier^{60a}, C. Meineck¹⁰¹, B. Meirose⁴³, D. Melini¹⁷¹, B. R. Mellado Garcia^{148c}, M. Melo^{147a}, F. Meloni¹⁸, A. Mengarelli^{22a,22b}, S. Menke¹⁰², E. Meoni¹⁶⁶, S. Mergelmeyer¹⁷, P. Mermod⁵¹, L. Merola^{105a,105b}, C. Meroni^{93a}, F. S. Merritt³³, A. Messina^{133a,133b}, J. Metcalfe⁶, A. S. Mete¹⁶⁷, C. Meyer⁸⁵, C. Meyer¹²³, J-P. Meyer¹³⁷, J. Meyer¹⁰⁸, H. Meyer Zu Theenhausen^{60a}, F. Miano¹⁵², R. P. Middleton¹³², S. Miglioranza^{52a,52b}, L. Mijovic⁴⁸, G. Mikenberg¹⁷⁶, M. Mikestikova¹²⁸, M. Mikuz⁷⁷, M. Milesi⁹⁰, A. Milic⁶⁴, D. W. Miller³³, C. Mills⁴⁸, A. Milov¹⁷⁶, D. A. Milstead^{149a,149b}, A. A. Minaenko¹³¹, Y. Minami¹⁵⁸, I. A. Minashvili⁶⁷, A. I. Mincer¹¹¹, B. Mindur^{40a}, M. Mineev⁶⁷, Y. Ming¹⁷⁷, L. M. Mir¹³, K. P. Mistry¹²³, T. Mitani¹⁷⁵, J. Mitrevski¹⁰¹, V. A. Mitsou¹⁷¹, A. Miucci¹⁸, P. S. Miyagawa¹⁴², J. U. Mjörnmark⁸³, T. Moa^{149a,149b}, K. Mochizuki⁹⁶, S. Mohapatra³⁷, S. Molander^{149a,149b}, R. Moles-Valls²³, R. Monden⁷⁰, M. C. Mondragon⁹², K. Mönig⁴⁴, J. Monk³⁸, E. Monnier⁸⁷, A. Montalbano¹⁵¹, J. Montejo Berlingen³², F. Monticelli⁷³, S. Monzani^{93a,93b}, R. W. Moore³, N. Morange¹¹⁸, D. Moreno²¹, M. Moreno Llacer⁵⁶, P. Moretti^{52a}, S. Morgenstern³², D. Mori¹⁴⁵, T. Mori¹⁵⁸, M. Morii⁵⁸, M. Morinaga¹⁵⁸, V. Morisbak¹²⁰, S. Moritz⁸⁵, A. K. Morley¹⁵³, G. Mornacchi³², J. D. Morris⁷⁸, S. S. Mortensen³⁸, L. Morvaj¹⁵¹, M. Mosidze^{53b}, J. Moss^{146,ad}, K. Motohashi¹⁶⁰, R. Mount¹⁴⁶, E. Mountricha²⁷, S. V. Mouraviev^{97,*}, E. J. W. Moyse⁸⁸, S. Muanza⁸⁷, R. D. Mudd¹⁹, F. Mueller¹⁰², J. Mueller¹²⁶, R. S. P. Mueller¹⁰¹, T. Mueller³⁰, D. Muenstermann⁷⁴, P. Mullen⁵⁵, G. A. Mullier¹⁸, F. J. Munoz Sanchez⁸⁶, J. A. Murillo Quijada¹⁹, W. J. Murray^{132,174}, H. Musheghyan⁵⁶, M. Muškinja⁷⁷, A. G. Myagkov^{131,ae}, M. Myska¹²⁹, B. P. Nachman¹⁴⁶, O. Nackenhorst⁵¹, K. Nagai¹²¹, R. Nagai^{68,z}, K. Nagano⁶⁸, Y. Nagasaka⁶¹, K. Nagata¹⁶⁵, M. Nagel⁵⁰, E. Nagy⁸⁷, A. M. Nairz³², Y. Nakahama¹⁰⁴, K. Nakamura⁶⁸, T. Nakamura¹⁵⁸, I. Nakano¹¹³, H. Namasivayam⁴³, R. F. Naranjo Garcia⁴⁴, R. Narayan¹¹, D. I. Narrias Villar^{60a}, I. Naryshkin¹²⁴, T. Naumann⁴⁴, G. Navarro²¹, R. Nayyar⁷, H. A. Neal⁹¹, P. Yu. Nechaeva⁹⁷, T. J. Neep⁸⁶, A. Negri^{122a,122b}, M. Negrini^{22a}, S. Nektarijevic¹⁰⁷, C. Nellist¹¹⁸, A. Nelson¹⁶⁷, S. Nemecek¹²⁸, P. Nemethy¹¹¹, A. A. Nepomuceno^{26a}, M. Nessi^{32,af}, M. S. Neubauer¹⁷⁰, M. Neumann¹⁷⁹, R. M. Neves¹¹¹, P. Nevski²⁷, P. R. Newman¹⁹, D. H. Nguyen⁶, T. Nguyen Manh⁹⁶, R. B. Nickerson¹²¹, R. Nicolaidou¹³⁷, J. Nielsen¹³⁸, A. Nikiforov¹⁷, V. Nikolaenko^{131,ae}, I. Nikolic-Audit⁸², K. Nikolopoulos¹⁹, J. K. Nilsen¹²⁰, P. Nilsson²⁷, Y. Ninomiya¹⁵⁸, A. Nisati^{133a}, R. Nisius¹⁰², T. Nobe¹⁵⁸, M. Nomachi¹¹⁹, I. Nomidis³¹, T. Nooney⁷⁸, S. Norberg¹¹⁴, M. Nordberg³², N. Norjoharuddeen¹²¹, O. Novgorodova⁴⁶, S. Nowak¹⁰², M. Nozaki⁶⁸, L. Nozka¹¹⁶, K. Ntekas¹⁰, E. Nurse⁸⁰, F. Nuti⁹⁰, F. O'grady⁷, D. C. O'Neil¹⁴⁵, A. A. O'Rourke⁴⁴, V. O'Shea⁵⁵, F. G. Oakham^{31,d}, H. Oberlack¹⁰², T. Obermann²³, J. Ocariz⁸², A. Ochi⁶⁹, I. Ochoa³⁷, J. P. Ochoa-Ricoux^{34a}, S. Oda⁷², S. Odaka⁶⁸, H. Ogren⁶³, A. Oh⁸⁶, S. H. Oh⁴⁷, C. C. Ohm¹⁶, H. Ohman¹⁶⁹, H. Oide³², H. Okawa¹⁶⁵, Y. Okumura¹⁵⁸, T. Okuyama⁶⁸, A. Olariu^{28b}, L. F. Oleiro Seabra^{127a}, S. A. Olivares Pino⁴⁸, D. Oliveira Damazio²⁷, A. Olszewski⁴¹, J. Olszowska⁴¹, A. Onofre^{127a,127e}, K. Onogi¹⁰⁴, P. U. E. Onyisi^{11,w}, M. J. Oreglia³³, Y. Oren¹⁵⁶, D. Orestano^{135a,135b}, N. Orlando^{62b}, R. S. Orr¹⁶², B. Osculati^{52a,52b,*}, R. Ospanov⁸⁶, G. Otero y Garzon²⁹, H. Otono⁷², M. Ouchrif^{136d}, F. Ould-Saada¹²⁰, A. Ouraou¹³⁷, K. P. Oussoren¹⁰⁸, Q. Ouyang^{35a}, M. Owen⁵⁵, R. E. Owen¹⁹, V. E. Ozcan^{20a}, N. Ozturk⁸, K. Pachal¹⁴⁵, A. Pacheco Pages¹³, L. Pacheco Rodriguez¹³⁷, C. Padilla Aranda¹³, M. Pagáčová⁵⁰, S. Pagan Griso¹⁶, F. Paige²⁷, P. Pais⁸⁸, K. Pajchel¹²⁰, G. Palacino^{164b}, S. Palazzo^{39a,39b}, S. Palestini³², M. Palka^{40b}, D. Pallin³⁶, E. St. Panagiotopoulou¹⁰, C. E. Pandini⁸², J. G. Panduro Vazquez⁷⁹, P. Pani^{149a,149b}, S. Panitkin²⁷, D. Pantea^{28b}, L. Paolozzi⁵¹, Th. D. Papadopoulos¹⁰, K. Papageorgiou¹⁵⁷, A. Paramonov⁶, D. Paredes Hernandez¹⁸⁰, A. J. Parker⁷⁴,

- M. A. Parker³⁰, K. A. Parker¹⁴², F. Parodi^{52a,52b}, J. A. Parsons³⁷, U. Parzefall⁵⁰, V. R. Pascuzzi¹⁶², E. Pasqualucci^{133a}, S. Passaggio^{52a}, Fr. Pastore⁷⁹, G. Pásztor^{31,ag}, S. Pataria¹⁷⁹, J. R. Pater⁸⁶, T. Pauly³², J. Pearce¹⁷³, B. Pearson¹¹⁴, L. E. Pedersen³⁸, M. Pedersen¹²⁰, S. Pedraza Lopez¹⁷¹, R. Pedro^{127a,127b}, S. V. Peleganchuk^{110,c}, O. Penc¹²⁸, C. Peng^{35a}, H. Peng⁵⁹, J. Penwell⁶³, B. S. Peralva^{26b}, M. M. Perego¹³⁷, D. V. Perepelitsa²⁷, E. Perez Codina^{164a}, L. Perini^{93a,93b}, H. Pernegger³², S. Perrella^{105a,105b}, R. Peschke⁴⁴, V. D. Peshekhonov⁶⁷, K. Peters⁴⁴, R. F. Y. Peters⁸⁶, B. A. Petersen³², T. C. Petersen³⁸, E. Petit⁵⁷, A. Petridis¹, C. Petridou¹⁵⁷, P. Petroff¹¹⁸, E. Petrolo^{133a}, M. Petrov¹²¹, F. Petrucci^{135a,135b}, N. E. Pettersson⁸⁸, A. Peyaud¹³⁷, R. Pezoa^{34b}, P. W. Phillips¹³², G. Piacquadio^{146,ah}, E. Pianori¹⁷⁴, A. Picazio⁸⁸, E. Piccaro⁷⁸, M. Piccinini^{22a,22b}, M. A. Pickering¹²¹, R. Piegai²⁹, J. E. Pilcher³³, A. D. Pilkington⁸⁶, A. W. J. Pin⁸⁶, M. Pinamonti^{168a,168c,ai}, J. L. Pinfold³, A. Pingel³⁸, S. Pires⁸², H. Pirumov⁴⁴, M. Pitt¹⁷⁶, L. Plazak^{147a}, M. -A. Pleier²⁷, V. Pleskot⁸⁵, E. Plotnikova⁶⁷, P. Plucinski⁹², D. Pluth⁶⁶, R. Poettgen^{149a,149b}, L. Poggioli¹¹⁸, D. Pohl²³, G. Polesello^{122a}, A. Poley⁴⁴, A. Policicchio^{39a,39b}, R. Polifka¹⁶², A. Polini^{22a}, C. S. Pollard⁵⁵, V. Polychronakos²⁷, K. Pommès³², L. Pontecorvo^{133a}, B. G. Pope⁹², G. A. Popeneciu^{28c}, A. Poppleton³², S. Pospisil¹²⁹, K. Potamianos¹⁶, I. N. Potrap⁶⁷, C. J. Potter³⁰, C. T. Potter¹¹⁷, G. Poulard³², J. Poveda³², V. Pozdnyakov⁶⁷, M. E. Pozo Astigarraga³², P. Pralavorio⁸⁷, A. Pranko¹⁶, S. Prell⁶⁶, D. Price⁸⁶, L. E. Price⁶, M. Primavera^{75a}, S. Prince⁸⁹, K. Prokofiev^{62c}, F. Prokoshin^{34b}, S. Protopopescu²⁷, J. Proudfoot⁶, M. Przybycien^{40a}, D. Puddu^{135a,135b}, M. Purohit^{27,aj}, P. Puzo¹¹⁸, J. Qian⁹¹, G. Qin⁵⁵, Y. Qin⁸⁶, A. Quadl⁵⁶, W. B. Quayle^{168a,168b}, M. Queitsch-Maitland⁸⁶, D. Quilty⁵⁵, S. Raddum¹²⁰, V. Radeka²⁷, V. Radescu¹²¹, S. K. Radhakrishnan¹⁵¹, P. Radloff¹¹⁷, P. Rados⁹⁰, F. Ragusa^{93a,93b}, G. Rahal¹⁸², J. A. Raine⁸⁶, S. Rajagopalan²⁷, M. Rammensee³², C. Rangel-Smith¹⁶⁹, M. G. Ratti^{93a,93b}, F. Rauscher¹⁰¹, S. Rave⁸⁵, T. Ravenscroft⁵⁵, I. Ravinovich¹⁷⁶, M. Raymond³², A. L. Read¹²⁰, N. P. Readioff⁷⁶, M. Reale^{75a,75b}, D. M. Rebuffi^{122a,122b}, A. Redelbach¹⁷⁸, G. Redlinger²⁷, R. Reece¹³⁸, K. Reeves⁴³, L. Rehnisch¹⁷, J. Reichert¹²³, H. Reisin²⁹, C. Rembser³², H. Ren^{35a}, M. Rescigno^{133a}, S. Resconi^{93a}, O. L. Rezanova^{110,c}, P. Reznicek¹³⁰, R. Rezvani⁹⁶, R. Richter¹⁰², S. Richter⁸⁰, E. Richter-Was^{40b}, O. Ricken²³, M. Ridel⁸², P. Rieck¹⁷, C. J. Riegel¹⁷⁹, J. Rieger⁵⁶, O. Rifki¹¹⁴, M. Rijssenbeek¹⁵¹, A. Rimoldi^{122a,122b}, M. Rimoldi¹⁸, L. Rinaldi^{22a}, B. Ristic⁵¹, E. Ritsch³², I. Riu¹³, F. Rizatdinova¹¹⁵, E. Rizvi⁷⁸, C. Rizzi¹³, S. H. Robertson^{89,m}, A. Robichaud-Veronneau⁸⁹, D. Robinson³⁰, J. E. M. Robinson⁴⁴, A. Robson⁵⁵, C. Roda^{125a,125b}, Y. Rodina^{87,ak}, A. Rodriguez Perez¹³, D. Rodriguez Rodriguez¹⁷¹, S. Roe³², C. S. Rogan⁵⁸, O. Røhne¹²⁰, A. Romaniouk⁹⁹, M. Romano^{22a,22b}, S. M. Romano Saez³⁶, E. Romero Adam¹⁷¹, N. Rompotis¹³⁹, M. Ronzani⁵⁰, L. Roos⁸², E. Ros¹⁷¹, S. Rosati^{133a}, K. Rosbach⁵⁰, P. Rose¹³⁸, O. Rosenthal¹⁴⁴, N. -A. Rosien⁵⁶, V. Rossetti^{149a,149b}, E. Rossi^{105a,105b}, L. P. Rossi^{52a}, J. H. N. Rosten³⁰, R. Rosten¹³⁹, M. Rotaru^{28b}, I. Roth¹⁷⁶, J. Rothberg¹³⁹, D. Rousseau¹¹⁸, C. R. Royon¹³⁷, A. Rozanov⁸⁷, Y. Rozen¹⁵⁵, X. Ruan^{148c}, F. Rubbo¹⁴⁶, M. S. Rudolph¹⁶², F. Rühr⁵⁰, A. Ruiz-Martinez³¹, Z. Rurikova⁵⁰, N. A. Rusakovich⁶⁷, A. Ruschke¹⁰¹, H. L. Russell¹³⁹, J. P. Rutherford⁷, N. Ruthmann³², Y. F. Ryabov¹²⁴, M. Rybar¹⁷⁰, G. Rybkin¹¹⁸, S. Ryu⁶, A. Ryzhov¹³¹, G. F. Rzehorz⁵⁶, A. F. Saavedra¹⁵³, G. Sabato¹⁰⁸, S. Sacerdoti²⁹, H. F-W. Sadrozinski¹³⁸, R. Sadykov⁶⁷, F. Safai Tehrani^{133a}, P. Saha¹⁰⁹, M. Sahinsoy^{60a}, M. Saimpert¹³⁷, T. Saito¹⁵⁸, H. Sakamoto¹⁵⁸, Y. Sakurai¹⁷⁵, G. Salamanna^{135a,135b}, A. Salamon^{134a,134b}, J. E. Salazar Loyola^{34b}, D. Salek¹⁰⁸, P. H. Sales De Bruin¹³⁹, D. Salihagic¹⁰², A. Salnikov¹⁴⁶, J. Salt¹⁷¹, D. Salvatore^{39a,39b}, F. Salvatore¹⁵², A. Salvucci^{62a}, A. Salzburger³², D. Sammel⁵⁰, D. Sampsonidis¹⁵⁷, J. Sánchez¹⁷¹, V. Sanchez Martinez¹⁷¹, A. Sanchez Pineda^{105a,105b}, H. Sandaker¹²⁰, R. L. Sandbach⁷⁸, H. G. Sander⁸⁵, M. Sandhoff¹⁷⁹, C. Sandoval²¹, R. Sandstroem¹⁰², D. P. C. Sankey¹³², M. Sannino^{52a,52b}, A. Sansoni⁴⁹, C. Santoni³⁶, R. Santonicio^{134a,134b}, H. Santos^{127a}, I. Santoyo Castillo¹⁵², K. Sapp¹²⁶, A. Sapronov⁶⁷, J. G. Saraiva^{127a,127d}, B. Sarrazin²³, O. Sasaki⁶⁸, Y. Sasaki¹⁵⁸, K. Sato¹⁶⁵, G. Sauvage^{5,*}, E. Sauvan⁵, G. Savage⁷⁹, P. Savard^{162,d}, N. Savic¹⁰², C. Sawyer¹³², L. Sawyer^{81,r}, J. Saxon³³, C. Sbarra^{22a}, A. Sbrizzi^{22a,22b}, T. Scanlon⁸⁰, D. A. Scannicchio¹⁶⁷, M. Scarcella¹⁵³, V. Scarfone^{39a,39b}, J. Schaarschmidt¹⁷⁶, P. Schacht¹⁰², B. M. Schachtner¹⁰¹, D. Schaefer³², L. Schaefer¹²³, R. Schaefer⁴⁴, J. Schaeffer⁸⁵, S. Schaepe²³, S. Schaetzel^{60b}, U. Schäfer⁸⁵, A. C. Schaffer¹¹⁸, D. Schaile¹⁰¹, R. D. Schamberger¹⁵¹, V. Scharf^{60a}, V. A. Schegelsky¹²⁴, D. Scheirich¹³⁰, M. Schernau¹⁶⁷, C. Schiavi^{52a,52b}, S. Schier¹³⁸, C. Schillo⁵⁰, M. Schioppa^{39a,39b}, S. Schlenker³², K. R. Schmidt-Sommerfeld¹⁰², K. Schmieden³², C. Schmitt⁸⁵, S. Schmitt⁴⁴, S. Schmitz⁸⁵, B. Schneider^{164a}, U. Schnoor⁵⁰, L. Schoeffel¹³⁷, A. Schoening^{60b}, B. D. Schoenrock⁹², E. Schopf²³, M. Schott⁸⁵, J. Schovancova⁸, S. Schramm⁵¹, M. Schreyer¹⁷⁸, N. Schuh⁸⁵, A. Schulte⁸⁵, M. J. Schultens²³, H. -C. Schultz-Coulon^{60a}, H. Schulz¹⁷, M. Schumacher⁵⁰, B. A. Schumm¹³⁸, Ph. Schune¹³⁷, A. Schwartzman¹⁴⁶, T. A. Schwarz⁹¹, H. Schweiger⁸⁶, Ph. Schwemling¹³⁷, R. Schwienhorst⁹², J. Schwindling¹³⁷, T. Schwindt²³, G. Sciolla²⁵, F. Scuri^{125a,125b}, F. Scutti⁹⁰, J. Searcy⁹¹, P. Seema²³, S. C. Seidel¹⁰⁶, A. Seiden¹³⁸, F. Seifert¹²⁹, J. M. Seixas^{26a}, G. Sekhniaidze^{105a}, K. Sekhon⁹¹, S. J. Sekula⁴², D. M. Seliverstov^{124,*}, N. Semprini-Cesari^{22a,22b}, C. Serfon¹²⁰, L. Serin¹¹⁸, L. Serkin^{168a,168b}, M. Sessa^{135a,135b}, R. Seuster¹⁷³, H. Severini¹¹⁴, T. Sfiligoi⁷⁷, F. Sforza³², A. Sfyrta⁵¹, E. Shabalina⁵⁶, N. W. Shaikh^{149a,149b}, L. Y. Shan^{35a}, R. Shang¹⁷⁰, J. T. Shank²⁴, M. Shapiro¹⁶, P. B. Shatalov⁹⁸, K. Shaw^{168a,168b}, S. M. Shaw⁸⁶, A. Shcherbakova^{149a,149b}, C. Y. Shehu¹⁵², P. Sherwood⁸⁰, L. Shi^{154,al}, S. Shimizu⁶⁹, C. O. Shimmin¹⁶⁷, M. Shimojima¹⁰³, M. Shiyakova^{67,am}

A. Shmeleva⁹⁷, D. Shoaleh Saadi⁹⁶, M. J. Shochet³³, S. Shojaii^{93a,93b}, S. Shrestha¹¹², E. Shulga⁹⁹, M. A. Shupe⁷, P. Sicho¹²⁸, A. M. Sickles¹⁷⁰, P. E. Sidebo¹⁵⁰, O. Sidiropoulou¹⁷⁸, D. Sidorov¹¹⁵, A. Sidoti^{22a,22b}, F. Siegert⁴⁶, Dj. Sijacki¹⁴, J. Silva^{127a,127d}, S. B. Silverstein^{149a}, V. Simak¹²⁹, Lj. Simic¹⁴, S. Simion¹¹⁸, E. Simioni⁸⁵, B. Simmons⁸⁰, D. Simon³⁶, M. Simon⁸⁵, P. Sinervo¹⁶², N. B. Sinev¹¹⁷, M. Sioli^{22a,22b}, G. Siragusa¹⁷⁸, S. Yu. Sivoklov¹⁰⁰, J. Sjölin^{149a,149b}, M. B. Skinner⁷⁴, H. P. Skottowe⁵⁸, P. Skubic¹¹⁴, M. Slater¹⁹, T. Slavicek¹²⁹, M. Slawinska¹⁰⁸, K. Sliwa¹⁶⁶, R. Slovak¹³⁰, V. Smakhtin¹⁷⁶, B. H. Smart⁵, L. Smestad¹⁵, J. Smiesko^{147a}, S. Yu. Smirnov⁹⁹, Y. Smirnov⁹⁹, L. N. Smirnova^{100,an}, O. Smirnova⁸³, M. N. K. Smith³⁷, R. W. Smith³⁷, M. Smizanska⁷⁴, K. Smolek¹²⁹, A. A. Snesarev⁹⁷, S. Snyder²⁷, R. Sobie^{173,m}, F. Socher⁴⁶, A. Soffer¹⁵⁶, D. A. Soh¹⁵⁴, G. Sokhrannyi⁷⁷, C. A. Solans Sanchez³², M. Solar¹²⁹, E. Yu. Soldatov⁹⁹, U. Soldevila¹⁷¹, A. A. Solodkov¹³¹, A. Soloshenko⁶⁷, O. V. Solovyanov¹³¹, V. Solovyev¹²⁴, P. Sommer⁵⁰, H. Son¹⁶⁶, H. Y. Song^{59,ao}, A. Sood¹⁶, A. Sopczak¹²⁹, V. Sopko¹²⁹, V. Sorin¹³, D. Sosa^{60b}, C. L. Sotiropoulou^{125a,125b}, R. Soualah^{168a,168c}, A. M. Soukharev^{110,c}, D. South⁴⁴, B. C. Sowden⁷⁹, S. Spagnolo^{75a,75b}, M. Spalla^{125a,125b}, M. Spangenberg¹⁷⁴, F. Spanò⁷⁹, D. Sperlich¹⁷, F. Spettel¹⁰², R. Spighi^{22a}, G. Spigo³², L. A. Spiller⁹⁰, M. Spousta¹³⁰, R. D. St. Denis^{55,*}, A. Stabile^{93a}, R. Stamen^{60a}, S. Stamm¹⁷, E. Stanecka⁴¹, R. W. Stanek⁶, C. Stanescu^{135a}, M. Stanescu-Bellu⁴⁴, M. M. Stanitzki⁴⁴, S. Stapnes¹²⁰, E. A. Starchenko¹³¹, G. H. Stark³³, J. Stark⁵⁷, P. Staroba¹²⁸, P. Starovoitov^{60a}, S. Stärz³², R. Staszewski⁴¹, P. Steinberg²⁷, B. Stelzer¹⁴⁵, H. J. Stelzer³², O. Stelzer-Chilton^{164a}, H. Stenzel⁵⁴, G. A. Stewart⁵⁵, J. A. Stillings²³, M. C. Stockton⁸⁹, M. Stoebe⁸⁹, G. Stoicea^{28b}, P. Stolte⁵⁶, S. Stonjek¹⁰², A. R. Stradling⁸, A. Straessner⁴⁶, M. E. Stramaglia¹⁸, J. Strandberg¹⁵⁰, S. Strandberg^{149a,149b}, A. Strandlie¹²⁰, M. Strauss¹¹⁴, P. Strizenec^{147b}, R. Ströhmer¹⁷⁸, D. M. Strom¹¹⁷, R. Stroynowski⁴², A. Strubig¹⁰⁷, S. A. Stucci²⁷, B. Stugu¹⁵, N. A. Styles⁴⁴, D. Su¹⁴⁶, J. Su¹²⁶, S. Suchek^{60a}, Y. Sugaya¹¹⁹, M. Suk¹²⁹, V. V. Sulin⁹⁷, S. Sultansoy^{4c}, T. Sumida⁷⁰, S. Sun⁵⁸, X. Sun^{35a}, J. E. Sundermann⁵⁰, K. Suruliz¹⁵², G. Susinno^{39a,39b}, M. R. Sutton¹⁵², S. Suzuki⁶⁸, M. Svatos¹²⁸, M. Swiatlowski³³, I. Sykora^{147a}, T. Sykora¹³⁰, D. Ta⁵⁰, C. Taccini^{135a,135b}, K. Tackmann⁴⁴, J. Taenzer¹⁶², A. Taffard¹⁶⁷, R. Tahirout^{164a}, N. Taiblum¹⁵⁶, H. Takai²⁷, R. Takashima⁷¹, T. Takeshita¹⁴³, Y. Takubo⁶⁸, M. Talby⁸⁷, A. A. Talyshv^{110,c}, K. G. Tan⁹⁰, J. Tanaka¹⁵⁸, M. Tanaka¹⁶⁰, R. Tanaka¹¹⁸, S. Tanaka⁶⁸, B. B. Tannenwald¹¹², S. Tapia Araya^{34b}, S. Tapprogge⁸⁵, S. Tarem¹⁵⁵, G. F. Tartarelli^{93a}, P. Tas¹³⁰, M. Tasevsky¹²⁸, T. Tashiro⁷⁰, E. Tassi^{39a,39b}, A. Tavares Delgado^{127a,127b}, Y. Tayalati^{136e}, A. C. Taylor¹⁰⁶, G. N. Taylor⁹⁰, P. T. E. Taylor⁹⁰, W. Taylor^{164b}, F. A. Teischinger³², P. Teixeira-Dias⁷⁹, K. K. Temming⁵⁰, D. Temple¹⁴⁵, H. Ten Kate³², P. K. Teng¹⁵⁴, J. J. Teoh¹¹⁹, F. Tepel¹⁷⁹, S. Terada⁶⁸, K. Terashi¹⁵⁸, J. Terron⁸⁴, S. Terzo¹³, M. Testa⁴⁹, R. J. Teuscher^{162,m}, T. Theveneaux-Pelzer⁸⁷, J. P. Thomas¹⁹, J. Thomas-Wilsker⁷⁹, E. N. Thompson³⁷, P. D. Thompson¹⁹, A. S. Thompson⁵⁵, L. A. Thomsen¹⁸⁰, E. Thomson¹²³, M. Thomson³⁰, M. J. Tibbetts¹⁶, R. E. Ticse Torres⁸⁷, V. O. Tikhomirov^{97,ap}, Yu. A. Tikhonov^{110,c}, S. Timoshenko⁹⁹, P. Tipton¹⁸⁰, S. Tisserant⁸⁷, K. Todome¹⁶⁰, T. Todorov^{5,*}, S. Todorova-Nova¹³⁰, J. Tojo⁷², S. Tokár^{147a}, K. Tokushuku⁶⁸, E. Tolley⁵⁸, L. Tomlinson⁸⁶, M. Tomoto¹⁰⁴, L. Tompkins^{146,aq}, K. Toms¹⁰⁶, B. Tong⁵⁸, E. Torrence¹¹⁷, H. Torres¹⁴⁵, E. Torró Pastor¹³⁹, J. Toth^{87,ar}, F. Touchard⁸⁷, D. R. Tovey¹⁴², T. Trefzger¹⁷⁸, A. Tricoli²⁷, I. M. Trigger^{164a}, S. Trincas-Duvoid⁸², M. F. Tripiana¹³, W. Trischuk¹⁶², B. Trocmé⁵⁷, A. Trofymov⁴⁴, C. Troncon^{93a}, M. Trottier-McDonald¹⁶, M. Trovatelli¹⁷³, L. Truong^{168a,168c}, M. Trzebinski⁴¹, A. Trzupek⁴¹, J. C-L. Tseng¹²¹, P. V. Tsiarshka⁹⁴, G. Tsipolitis¹⁰, N. Tsirintanis⁹, S. Tsiskaridze¹³, V. Tsiskaridze⁵⁰, E. G. Tskhadadze^{53a}, K. M. Tsui^{62a}, I. I. Tsukerman⁹⁸, V. Tsulaia¹⁶, S. Tsuno⁶⁸, D. Tsybychev¹⁵¹, Y. Tu^{62b}, A. Tudorache^{28b}, V. Tudorache^{28b}, A. N. Tuna⁵⁸, S. A. Tupputi^{22a,22b}, S. Turchikhin⁶⁷, D. Turecek¹²⁹, D. Turgeman¹⁷⁶, R. Turra^{93a,93b}, A. J. Turvey⁴², P. M. Tuts³⁷, M. Tyndel¹³², G. Uccchielli^{22a,22b}, I. Ueda¹⁵⁸, M. Ughetto^{149a,149b}, F. Ukegawa¹⁶⁵, G. Unal³², A. Undrus²⁷, G. Unel¹⁶⁷, F. C. Ungaro⁹⁰, Y. Unno⁶⁸, C. Unverdorben¹⁰¹, J. Urban^{147b}, P. Urquijo⁹⁰, P. Urrejola⁸⁵, G. Usai⁸, A. Usanova⁶⁴, L. Vacavant⁸⁷, V. Vacek¹²⁹, B. Vachon⁸⁹, C. Valderanis¹⁰¹, E. Valdes Santurio^{149a,149b}, N. Valencic¹⁰⁸, S. Valentini^{22a,22b}, A. Valero¹⁷¹, L. Valery¹³, S. Valkar¹³⁰, J. A. Valls Ferrer¹⁷¹, W. Van Den Wollenberg¹⁰⁸, P. C. Van Der Deijl¹⁰⁸, H. van der Graaf¹⁰⁸, N. van Eldik¹⁵⁵, P. van Gemmeren⁶, J. Van Nieuwkoop¹⁴⁵, I. van Vulpen¹⁰⁸, M. C. van Woerden³², M. Vanadia^{133a,133b}, W. Vandelli³², R. Vanguri¹²³, A. Vaniachine¹⁶¹, P. Vankov¹⁰⁸, G. Vardanyan¹⁸¹, R. Vari^{133a}, E. W. Varnes⁷, T. Varol⁴², D. Varouchas⁸², A. Vartapetian⁸, K. E. Varvell¹⁵³, J. G. Vasquez¹⁸⁰, F. Vazeille³⁶, T. Vazquez Schroeder⁸⁹, J. Veatch⁵⁶, V. Veeraraghavan⁷, L. M. Veloce¹⁶², F. Veloso^{127a,127c}, S. Veneziano^{133a}, A. Ventura^{75a,75b}, M. Venturi¹⁷³, N. Venturi¹⁶², A. Venturini²⁵, V. Vercesi^{122a}, M. Verducci^{133a,133b}, W. Verkerke¹⁰⁸, J. C. Vermeulen¹⁰⁸, A. Vest^{46,as}, M. C. Vetterli^{145,d}, O. Viazlo⁸³, I. Vichou^{170,*}, T. Vickey¹⁴², O. E. Vickey Boeriu¹⁴², G. H. A. Viehhauser¹²¹, S. Viel¹⁶, L. Vigani¹²¹, M. Villa^{22a,22b}, M. Villaplana Perez^{93a,93b}, E. Vilucchi⁴⁹, M. G. Vinciter³¹, V. B. Vinogradov⁶⁷, C. Vittori^{22a,22b}, I. Vivarelli¹⁵², S. Vlachos¹⁰, M. Vlasak¹²⁹, M. Vogel¹⁷⁹, P. Vokac¹²⁹, G. Volpi^{125a,125b}, M. Volpi⁹⁰, H. von der Schmitt¹⁰², E. von Toerne²³, V. Vorobel¹³⁰, K. Vorobev⁹⁹, M. Vos¹⁷¹, R. Voss³², J. H. Vossebeld⁷⁶, N. Vranjes¹⁴, M. Vranjes Milosavljevic¹⁴, V. Vrba¹²⁸, M. Vreeswijk¹⁰⁸, R. Vuillermet³², I. Vukotic³³, Z. Vykydal¹²⁹, P. Wagner²³, W. Wagner¹⁷⁹, H. Wahlberg⁷³, S. Wahrmond⁴⁶, J. Wakabayashi¹⁰⁴, J. Walder⁷⁴, R. Walker¹⁰¹, W. Walkowiak¹⁴⁴, V. Wallangen^{149a,149b}, C. Wang^{35b}, C. Wang^{87,140}, F. Wang¹⁷⁷, H. Wang¹⁶, H. Wang⁴², J. Wang⁴⁴

J. Wang¹⁵³, K. Wang⁸⁹, R. Wang⁶, S. M. Wang¹⁵⁴, T. Wang²³, T. Wang³⁷, W. Wang⁵⁹, X. Wang¹⁸⁰, C. Wanotayaroj¹¹⁷, A. Warburton⁸⁹, C. P. Ward³⁰, D. R. Wardrope⁸⁰, A. Washbrook⁴⁸, P. M. Watkins¹⁹, A. T. Watson¹⁹, M. F. Watson¹⁹, G. Watts¹³⁹, S. Watts⁸⁶, B. M. Waugh⁸⁰, S. Webb⁸⁵, M. S. Weber¹⁸, S. W. Weber¹⁷⁸, J. S. Webster⁶, A. R. Weidberg¹²¹, B. Weinert⁶³, J. Weingarten⁵⁶, C. Weiser⁵⁰, H. Weits¹⁰⁸, P. S. Wells³², T. Wenaus²⁷, T. Wengler³², S. Wenig³², N. Wermes²³, M. Werner⁵⁰, M. D. Werner⁶⁶, P. Werner³², M. Wessels^{60a}, J. Wetter¹⁶⁶, K. Whalen¹¹⁷, N. L. Whallon¹³⁹, A. M. Wharton⁷⁴, A. White⁸, M. J. White¹, R. White^{34b}, D. Whiteson¹⁶⁷, F. J. Wickens¹³², W. Wiedenmann¹⁷⁷, M. Wielers¹³², P. Wienemann²³, C. Wiglesworth³⁸, L. A. M. Wiik-Fuchs²³, A. Wildauer¹⁰², F. Wilk⁸⁶, H. G. Wilkens³², H. H. Williams¹²³, S. Williams¹⁰⁸, C. Willis⁹², S. Willocq⁸⁸, J. A. Wilson¹⁹, I. Wingerter-Seetz⁵, F. Winklmeier¹¹⁷, O. J. Winston¹⁵², B. T. Winter²³, M. Wittgen¹⁴⁶, J. Wittkowski¹⁰¹, T. M. H. Wolf¹⁰⁸, M. W. Wolter⁴¹, H. Wolters^{127a,127c}, S. D. Worm¹³², B. K. Wosiek⁴¹, J. Wotschack³², M. J. Woudstra⁸⁶, K. W. Wozniak⁴¹, M. Wu⁵⁷, M. Wu³³, S. L. Wu¹⁷⁷, X. Wu⁵¹, Y. Wu⁹¹, T. R. Wyatt⁸⁶, B. M. Wynne⁴⁸, S. Xella³⁸, D. Xu^{35a}, L. Xu²⁷, B. Yabsley¹⁵³, S. Yacoub^{148a}, D. Yamaguchi¹⁶⁰, Y. Yamaguchi¹¹⁹, A. Yamamoto⁶⁸, S. Yamamoto¹⁵⁸, T. Yamanaka¹⁵⁸, K. Yamauchi¹⁰⁴, Y. Yamazaki⁶⁹, Z. Yan²⁴, H. Yang¹⁴¹, H. Yang¹⁷⁷, Y. Yang¹⁵⁴, Z. Yang¹⁵, W.-M. Yao¹⁶, Y. C. Yap⁸², Y. Yasu⁶⁸, E. Yatsenko⁵, K. H. Yau Wong²³, J. Ye⁴², S. Ye²⁷, I. Yeletsikh⁶⁷, A. L. Yen⁵⁸, E. Yildirim⁸⁵, K. Yorita¹⁷⁵, R. Yoshida⁶, K. Yoshihara¹²³, C. Young¹⁴⁶, C. J. S. Young³², S. Youssef²⁴, D. R. Yu¹⁶, J. Yu⁸, J. M. Yu⁹¹, J. Yu⁶⁶, L. Yuan⁶⁹, S. P. Yuen²³, I. Yusuff^{30,at}, B. Zabinski⁴¹, R. Zaidan⁶⁵, A. M. Zaitsev^{131,ae}, N. Zakharchuk⁴⁴, J. Zalieckas¹⁵, A. Zaman¹⁵¹, S. Zambito⁵⁸, L. Zanello^{133a,133b}, D. Zanzi⁹⁰, C. Zeitnitz¹⁷⁹, M. Zeman¹²⁹, A. Zemla^{40a}, J. C. Zeng¹⁷⁰, Q. Zeng¹⁴⁶, K. Zengel²⁵, O. Zenin¹³¹, T. Ženiš^{147a}, D. Zerwas¹¹⁸, D. Zhang⁹¹, F. Zhang¹⁷⁷, G. Zhang^{59,ao}, H. Zhang^{35b}, J. Zhang⁶, L. Zhang⁵⁰, R. Zhang²³, R. Zhang^{59,au}, X. Zhang¹⁴⁰, Z. Zhang¹¹⁸, X. Zhao⁴², Y. Zhao¹⁴⁰, Z. Zhao⁵⁹, A. Zhemchugov⁶⁷, J. Zhong¹²¹, B. Zhou⁹¹, C. Zhou⁴⁷, L. Zhou³⁷, L. Zhou⁴², M. Zhou¹⁵¹, N. Zhou^{35c}, C. G. Zhu¹⁴⁰, H. Zhu^{35a}, J. Zhu⁹¹, Y. Zhu⁵⁹, X. Zhuang^{35a}, K. Zhukov⁹⁷, A. Zibell¹⁷⁸, D. Zieminska⁶³, N. I. Zimine⁶⁷, C. Zimmermann⁸⁵, S. Zimmermann⁵⁰, Z. Zinonos⁵⁶, M. Zinser⁸⁵, M. Ziolkowski¹⁴⁴, L. Živković¹⁴, G. Zobernig¹⁷⁷, A. Zoccoli^{22a,22b}, M. zur Nedden¹⁷, L. Zwalinski³²

¹ Department of Physics, University of Adelaide, Adelaide, Australia

² Physics Department, SUNY Albany, Albany, NY, USA

³ Department of Physics, University of Alberta, Edmonton, AB, Canada

⁴ (a) Department of Physics, Ankara University, Ankara, Turkey; (b) Istanbul Aydin University, Istanbul, Turkey; (c) Division of Physics, TOBB University of Economics and Technology, Ankara, Turkey

⁵ LAPP, CNRS/IN2P3 and Université Savoie Mont Blanc, Annecy-le-Vieux, France

⁶ High Energy Physics Division, Argonne National Laboratory, Argonne, IL, USA

⁷ Department of Physics, University of Arizona, Tucson, AZ, USA

⁸ Department of Physics, The University of Texas at Arlington, Arlington, TX, USA

⁹ Physics Department, University of Athens, Athens, Greece

¹⁰ Physics Department, National Technical University of Athens, Zografou, Greece

¹¹ Department of Physics, The University of Texas at Austin, Austin, TX, USA

¹² Institute of Physics, Azerbaijan Academy of Sciences, Baku, Azerbaijan

¹³ Institut de Física d'Altes Energies (IFAE), The Barcelona Institute of Science and Technology, Barcelona, Spain

¹⁴ Institute of Physics, University of Belgrade, Belgrade, Serbia

¹⁵ Department for Physics and Technology, University of Bergen, Bergen, Norway

¹⁶ Physics Division, Lawrence Berkeley National Laboratory, University of California, Berkeley, CA, USA

¹⁷ Department of Physics, Humboldt University, Berlin, Germany

¹⁸ Albert Einstein Center for Fundamental Physics and Laboratory for High Energy Physics, University of Bern, Bern, Switzerland

¹⁹ School of Physics and Astronomy, University of Birmingham, Birmingham, UK

²⁰ (a) Department of Physics, Bogazici University, Istanbul, Turkey; (b) Department of Physics Engineering, Gaziantep University, Gaziantep, Turkey; (c) Faculty of Engineering and Natural Sciences, Istanbul Bilgi University, Istanbul, Turkey; (d) Faculty of Engineering and Natural Sciences, Bahcesehir University, Istanbul, Turkey

²¹ Centro de Investigaciones, Universidad Antonio Narino, Bogota, Colombia

²² (a) INFN Sezione di Bologna, Bologna, Italy; (b) Dipartimento di Fisica e Astronomia, Università di Bologna, Bologna, Italy

²³ Physikalisches Institut, University of Bonn, Bonn, Germany

²⁴ Department of Physics, Boston University, Boston, MA, USA

²⁵ Department of Physics, Brandeis University, Waltham, MA, USA

- 26 (a)Universidade Federal do Rio De Janeiro COPPE/EE/IF, Rio de Janeiro, Brazil; (b)Electrical Circuits Department, Federal University of Juiz de Fora (UFJF), Juiz de Fora, Brazil; (c)Federal University of Sao Joao del Rei (UFSJ), Sao Joao del Rei, Brazil; (d)Instituto de Fisica, Universidade de Sao Paulo, Sao Paulo, Brazil
- 27 Physics Department, Brookhaven National Laboratory, Upton, NY, USA
- 28 (a)Transilvania University of Brasov, Brasov, Romania; (b)National Institute of Physics and Nuclear Engineering, Bucharest, Romania; (c)Physics Department, National Institute for Research and Development of Isotopic and Molecular Technologies, Cluj Napoca, Romania; (d)University Politehnica Bucharest, Bucharest, Romania; (e)West University in Timisoara, Timisoara, Romania
- 29 Departamento de Física, Universidad de Buenos Aires, Buenos Aires, Argentina
- 30 Cavendish Laboratory, University of Cambridge, Cambridge, UK
- 31 Department of Physics, Carleton University, Ottawa, ON, Canada
- 32 CERN, Geneva, Switzerland
- 33 Enrico Fermi Institute, University of Chicago, Chicago, IL, USA
- 34 (a)Departamento de Física, Pontificia Universidad Católica de Chile, Santiago, Chile; (b)Departamento de Física, Universidad Técnica Federico Santa María, Valparaíso, Chile
- 35 (a)Institute of High Energy Physics, Chinese Academy of Sciences, Beijing, China; (b)Department of Physics, Nanjing University, Jiangsu, China; (c)Physics Department, Tsinghua University, Beijing 100084, China
- 36 Laboratoire de Physique Corpusculaire, Clermont Université and Université Blaise Pascal and CNRS/IN2P3, Clermont-Ferrand, France
- 37 Nevis Laboratory, Columbia University, Irvington, NY, USA
- 38 Niels Bohr Institute, University of Copenhagen, Copenhagen, Denmark
- 39 (a)INFN Gruppo Collegato di Cosenza, Laboratori Nazionali di Frascati, Rende, Italy; (b)Dipartimento di Fisica, Università della Calabria, Rende, Italy
- 40 (a)Faculty of Physics and Applied Computer Science, AGH University of Science and Technology, Kraków, Poland ; (b)Marian Smoluchowski Institute of Physics, Jagiellonian University, Kraków, Poland
- 41 Institute of Nuclear Physics , Polish Academy of Sciences, Kraków, Poland
- 42 Physics Department, Southern Methodist University, Dallas, TX, USA
- 43 Physics Department, University of Texas at Dallas, Richardson, TX, USA
- 44 DESY, Hamburg and Zeuthen, Germany
- 45 Lehrstuhl für Experimentelle Physik IV, Technische Universität Dortmund, Dortmund, Germany
- 46 Institut für Kern-und Teilchenphysik, Technische Universität Dresden, Dresden, Germany
- 47 Department of Physics, Duke University, Durham, NC, USA
- 48 SUPA-School of Physics and Astronomy, University of Edinburgh, Edinburgh, UK
- 49 INFN Laboratori Nazionali di Frascati, Frascati, Italy
- 50 Fakultät für Mathematik und Physik, Albert-Ludwigs-Universität, Freiburg, Germany
- 51 Section de Physique, Université de Genève, Geneva, Switzerland
- 52 (a)INFN Sezione di Genova, Genoa, Italy; (b)Dipartimento di Fisica, Università di Genova, Genoa, Italy
- 53 (a)E. Andronikashvili Institute of Physics, Iv. Javakhishvili Tbilisi State University, Tbilisi, Georgia; (b)High Energy Physics Institute, Tbilisi State University, Tbilisi, Georgia
- 54 II Physikalisches Institut, Justus-Liebig-Universität Giessen, Giessen, Germany
- 55 SUPA-School of Physics and Astronomy, University of Glasgow, Glasgow, UK
- 56 II Physikalisches Institut, Georg-August-Universität, Göttingen, Germany
- 57 Laboratoire de Physique Subatomique et de Cosmologie, Université Grenoble-Alpes, CNRS/IN2P3, Grenoble, France
- 58 Laboratory for Particle Physics and Cosmology, Harvard University, Cambridge, MA, USA
- 59 Department of Modern Physics, University of Science and Technology of China, Anhui, China
- 60 (a)Kirchhoff-Institut für Physik, Ruprecht-Karls-Universität Heidelberg, Heidelberg, Germany; (b)Physikalisches Institut, Ruprecht-Karls-Universität Heidelberg, Heidelberg, Germany; (c)ZITI Institut für technische Informatik, Ruprecht-Karls-Universität Heidelberg, Mannheim, Germany
- 61 Faculty of Applied Information Science, Hiroshima Institute of Technology, Hiroshima, Japan
- 62 (a)Department of Physics, The Chinese University of Hong Kong, Shatin, NT, Hong Kong; (b)Department of Physics, The University of Hong Kong, Pokfulam, Hong Kong; (c)Department of Physics and Institute for Advanced Study, The Hong Kong University of Science and Technology, Clear Water Bay, Kowloon, Hong Kong, China
- 63 Department of Physics, Indiana University, Bloomington, IN, USA

- ⁶⁴ Institut für Astro- und Teilchenphysik, Leopold-Franzens-Universität, Innsbruck, Austria
- ⁶⁵ University of Iowa, Iowa City, IA, USA
- ⁶⁶ Department of Physics and Astronomy, Iowa State University, Ames, IA, USA
- ⁶⁷ Joint Institute for Nuclear Research, JINR Dubna, Dubna, Russia
- ⁶⁸ KEK, High Energy Accelerator Research Organization, Tsukuba, Japan
- ⁶⁹ Graduate School of Science, Kobe University, Kobe, Japan
- ⁷⁰ Faculty of Science, Kyoto University, Kyoto, Japan
- ⁷¹ Kyoto University of Education, Kyoto, Japan
- ⁷² Department of Physics, Kyushu University, Fukuoka, Japan
- ⁷³ Instituto de Física La Plata, Universidad Nacional de La Plata and CONICET, La Plata, Argentina
- ⁷⁴ Physics Department, Lancaster University, Lancaster, UK
- ⁷⁵ ^(a)INFN Sezione di Lecce, Lecce, Italy; ^(b)Dipartimento di Matematica e Fisica, Università del Salento, Lecce, Italy
- ⁷⁶ Oliver Lodge Laboratory, University of Liverpool, Liverpool, UK
- ⁷⁷ Department of Physics, Jožef Stefan Institute and University of Ljubljana, Ljubljana, Slovenia
- ⁷⁸ School of Physics and Astronomy, Queen Mary University of London, London, UK
- ⁷⁹ Department of Physics, Royal Holloway University of London, Surrey, UK
- ⁸⁰ Department of Physics and Astronomy, University College London, London, UK
- ⁸¹ Louisiana Tech University, Ruston, LA, USA
- ⁸² Laboratoire de Physique Nucléaire et de Hautes Energies, UPMC and Université Paris-Diderot and CNRS/IN2P3, Paris, France
- ⁸³ Fysiska institutionen, Lunds universitet, Lund, Sweden
- ⁸⁴ Departamento de Física Teórica C-15, Universidad Autónoma de Madrid, Madrid, Spain
- ⁸⁵ Institut für Physik, Universität Mainz, Mainz, Germany
- ⁸⁶ School of Physics and Astronomy, University of Manchester, Manchester, UK
- ⁸⁷ CPPM, Aix-Marseille Université and CNRS/IN2P3, Marseille, France
- ⁸⁸ Department of Physics, University of Massachusetts, Amherst, MA, USA
- ⁸⁹ Department of Physics, McGill University, Montreal, QC, Canada
- ⁹⁰ School of Physics, University of Melbourne, Victoria, Australia
- ⁹¹ Department of Physics, The University of Michigan, Ann Arbor, MI, USA
- ⁹² Department of Physics and Astronomy, Michigan State University, East Lansing, MI, USA
- ⁹³ ^(a)INFN Sezione di Milano, Milan, Italy; ^(b)Dipartimento di Fisica, Università di Milano, Milan, Italy
- ⁹⁴ B.I. Stepanov Institute of Physics, National Academy of Sciences of Belarus, Minsk, Republic of Belarus
- ⁹⁵ National Scientific and Educational Centre for Particle and High Energy Physics, Minsk, Republic of Belarus
- ⁹⁶ Group of Particle Physics, University of Montreal, Montreal, QC, Canada
- ⁹⁷ P.N. Lebedev Physical Institute of the Russian Academy of Sciences, Moscow, Russia
- ⁹⁸ Institute for Theoretical and Experimental Physics (ITEP), Moscow, Russia
- ⁹⁹ National Research Nuclear University MEPhI, Moscow, Russia
- ¹⁰⁰ D.V. Skobeltsyn Institute of Nuclear Physics, M.V. Lomonosov Moscow State University, Moscow, Russia
- ¹⁰¹ Fakultät für Physik, Ludwig-Maximilians-Universität München, Munich, Germany
- ¹⁰² Max-Planck-Institut für Physik (Werner-Heisenberg-Institut), Munich, Germany
- ¹⁰³ Nagasaki Institute of Applied Science, Nagasaki, Japan
- ¹⁰⁴ Graduate School of Science and Kobayashi-Maskawa Institute, Nagoya University, Nagoya, Japan
- ¹⁰⁵ ^(a)INFN Sezione di Napoli, Naples, Italy; ^(b)Dipartimento di Fisica, Università di Napoli, Naples, Italy
- ¹⁰⁶ Department of Physics and Astronomy, University of New Mexico, Albuquerque, NM, USA
- ¹⁰⁷ Institute for Mathematics Astrophysics and Particle Physics, Radboud University Nijmegen/Nikhef, Nijmegen, The Netherlands
- ¹⁰⁸ Nikhef National Institute for Subatomic Physics and University of Amsterdam, Amsterdam, The Netherlands
- ¹⁰⁹ Department of Physics, Northern Illinois University, DeKalb, IL, USA
- ¹¹⁰ Budker Institute of Nuclear Physics, SB RAS, Novosibirsk, Russia
- ¹¹¹ Department of Physics, New York University, New York, NY, USA
- ¹¹² Ohio State University, Columbus, OH, USA
- ¹¹³ Faculty of Science, Okayama University, Okayama, Japan
- ¹¹⁴ Homer L. Dodge Department of Physics and Astronomy, University of Oklahoma, Norman, OK, USA

- 115 Department of Physics, Oklahoma State University, Stillwater, OK, USA
- 116 Palacký University, RCPTM, Olomouc, Czech Republic
- 117 Center for High Energy Physics, University of Oregon, Eugene, OR, USA
- 118 LAL, Univ. Paris-Sud, CNRS/IN2P3, Université Paris-Saclay, Orsay, France
- 119 Graduate School of Science, Osaka University, Osaka, Japan
- 120 Department of Physics, University of Oslo, Oslo, Norway
- 121 Department of Physics, Oxford University, Oxford, UK
- 122 (a) INFN Sezione di Pavia, Pavia, Italy; (b) Dipartimento di Fisica, Università di Pavia, Pavia, Italy
- 123 Department of Physics, University of Pennsylvania, Philadelphia, PA, USA
- 124 National Research Centre “Kurchatov Institute” B.P. Konstantinov Petersburg Nuclear Physics Institute, St. Petersburg, Russia
- 125 (a) INFN Sezione di Pisa, Pisa, Italy; (b) Dipartimento di Fisica E. Fermi, Università di Pisa, Pisa, Italy
- 126 Department of Physics and Astronomy, University of Pittsburgh, Pittsburgh, PA, USA
- 127 (a) Laboratório de Instrumentação e Física Experimental de Partículas-LIP, Lisbon, Portugal; (b) Faculdade de Ciências, Universidade de Lisboa, Lisbon, Portugal; (c) Department of Physics, University of Coimbra, Coimbra, Portugal; (d) Centro de Física Nuclear da Universidade de Lisboa, Lisbon, Portugal; (e) Departamento de Física, Universidade do Minho, Braga, Portugal; (f) Departamento de Física Teórica y del Cosmos and CAFPE, Universidad de Granada, Granada, Spain; (g) Dep Física and CEFITEC of Faculdade de Ciências e Tecnologia, Universidade Nova de Lisboa, Caparica, Portugal
- 128 Institute of Physics, Academy of Sciences of the Czech Republic, Prague, Czech Republic
- 129 Czech Technical University in Prague, Prague, Czech Republic
- 130 Faculty of Mathematics and Physics, Charles University in Prague, Prague, Czech Republic
- 131 State Research Center Institute for High Energy Physics Protvino, Protvino, Russia
- 132 Particle Physics Department, Rutherford Appleton Laboratory, Didcot, UK
- 133 (a) INFN Sezione di Roma, Rome, Italy; (b) Dipartimento di Fisica, Sapienza Università di Roma, Rome, Italy
- 134 (a) INFN Sezione di Roma Tor Vergata, Rome, Italy; (b) Dipartimento di Fisica, Università di Roma Tor Vergata, Rome, Italy
- 135 (a) INFN Sezione di Roma Tre, Rome, Italy; (b) Dipartimento di Matematica e Fisica, Università Roma Tre, Rome, Italy
- 136 (a) Faculté des Sciences Ain Chock, Réseau Universitaire de Physique des Hautes Energies-Université Hassan II, Casablanca, Morocco; (b) Centre National de l’Energie des Sciences Techniques Nucleaires, Rabat, Morocco; (c) Faculté des Sciences Semlalia, Université Cadi Ayyad, LPHEA-Marrakech, Marrakesh, Morocco; (d) Faculté des Sciences, Université Mohamed Premier and LPTPM, Oujda, Morocco; (e) Faculté des , Sciences, Université Mohammed V, Rabat, Morocco
- 137 DSM/IRFU (Institut de Recherches sur les Lois Fondamentales de l’Univers), CEA Saclay (Commissariat à l’Energie Atomique et aux Energies Alternatives), Gif-sur-Yvette, France
- 138 Santa Cruz Institute for Particle Physics, University of California Santa Cruz, Santa Cruz, CA, USA
- 139 Department of Physics, University of Washington, Seattle, WA, USA
- 140 School of Physics, Shandong University, Shandong, China
- 141 Department of Physics and Astronomy (also affiliated with PKU-CHEP), Shanghai Key Laboratory for Particle Physics and Cosmology, Shanghai Jiao Tong University, Shanghai, China
- 142 Department of Physics and Astronomy, University of Sheffield, Sheffield, UK
- 143 Department of Physics, Shinshu University, Nagano, Japan
- 144 Fachbereich Physik, Universität Siegen, Siegen, Germany
- 145 Department of Physics, Simon Fraser University, Burnaby, BC, Canada
- 146 SLAC National Accelerator Laboratory, Stanford, CA, USA
- 147 (a) Faculty of Mathematics, Physics and Informatics, Comenius University, Bratislava, Slovakia; (b) Department of Subnuclear Physics, Institute of Experimental Physics of the Slovak Academy of Sciences, Kosice, Slovak Republic
- 148 (a) Department of Physics, University of Cape Town, Cape Town, South Africa; (b) Department of Physics, University of Johannesburg, Johannesburg, South Africa; (c) School of Physics, University of the Witwatersrand, Johannesburg, South Africa
- 149 (a) Department of Physics, Stockholm University, Stockholm, Sweden; (b) The Oskar Klein Centre, Stockholm, Sweden
- 150 Physics Department, Royal Institute of Technology, Stockholm, Sweden
- 151 Departments of Physics and Astronomy and Chemistry, Stony Brook University, Stony Brook, NY, USA

- 152 Department of Physics and Astronomy, University of Sussex, Brighton, UK
 - 153 School of Physics, University of Sydney, Sydney, Australia
 - 154 Institute of Physics, Academia Sinica, Taipei, Taiwan
 - 155 Department of Physics, Technion: Israel Institute of Technology, Haifa, Israel
 - 156 Raymond and Beverly Sackler School of Physics and Astronomy, Tel Aviv University, Tel Aviv, Israel
 - 157 Department of Physics, Aristotle University of Thessaloniki, Thessaloniki, Greece
 - 158 International Center for Elementary Particle Physics and Department of Physics, The University of Tokyo, Tokyo, Japan
 - 159 Graduate School of Science and Technology, Tokyo Metropolitan University, Tokyo, Japan
 - 160 Department of Physics, Tokyo Institute of Technology, Tokyo, Japan
 - 161 Tomsk State University, Tomsk, Russia, Russia
 - 162 Department of Physics, University of Toronto, Toronto, ON, Canada
 - 163 ^(a)INFN-TIFPA, Povo, Italy; ^(b)University of Trento, Trento, Italy, Italy
 - 164 ^(a)TRIUMF, Vancouver, BC, Canada; ^(b)Department of Physics and Astronomy, York University, Toronto, ON, Canada
 - 165 Faculty of Pure and Applied Sciences, Center for Integrated Research in Fundamental Science and Engineering, University of Tsukuba, Tsukuba, Japan
 - 166 Department of Physics and Astronomy, Tufts University, Medford, MA, USA
 - 167 Department of Physics and Astronomy, University of California Irvine, Irvine, CA, USA
 - 168 ^(a)INFN Gruppo Collegato di Udine, Sezione di Trieste, Udine, Italy; ^(b)ICTP, Trieste, Italy; ^(c)Dipartimento di Chimica, Fisica e Ambiente, Università di Udine, Udine, Italy
 - 169 Department of Physics and Astronomy, University of Uppsala, Uppsala, Sweden
 - 170 Department of Physics, University of Illinois, Urbana, IL, USA
 - 171 Instituto de Física Corpuscular (IFIC) and Departamento de Física Atomica, Molecular y Nuclear and Departamento de Ingeniería Electrónica and Instituto de Microelectrónica de Barcelona (IMB-CNM), University of Valencia and CSIC, Valencia, Spain
 - 172 Department of Physics, University of British Columbia, Vancouver, BC, Canada
 - 173 Department of Physics and Astronomy, University of Victoria, Victoria, BC, Canada
 - 174 Department of Physics, University of Warwick, Coventry, UK
 - 175 Waseda University, Tokyo, Japan
 - 176 Department of Particle Physics, The Weizmann Institute of Science, Rehovot, Israel
 - 177 Department of Physics, University of Wisconsin, Madison, WI, USA
 - 178 Fakultät für Physik und Astronomie, Julius-Maximilians-Universität, Würzburg, Germany
 - 179 Fakultät für Mathematik und Naturwissenschaften, Fachgruppe Physik, Bergische Universität Wuppertal, Wuppertal, Germany
 - 180 Department of Physics, Yale University, New Haven, CT, USA
 - 181 Yerevan Physics Institute, Yerevan, Armenia
 - 182 Centre de Calcul de l'Institut National de Physique Nucléaire et de Physique des Particules (IN2P3), Villeurbanne, France
- ^a Also at Department of Physics, King's College London, London, UK
- ^b Also at Institute of Physics, Azerbaijan Academy of Sciences, Baku, Azerbaijan
- ^c Also at Novosibirsk State University, Novosibirsk, Russia
- ^d Also at TRIUMF, Vancouver, BC, Canada
- ^e Also at Department of Physics & Astronomy, University of Louisville, Louisville, KY, USA
- ^f Also at Physics Department, An-Najah National University, Nablus, Palestine
- ^g Also at Department of Physics, California State University, Fresno, CA, USA
- ^h Also at Department of Physics, University of Fribourg, Fribourg, Switzerland
- ⁱ Also at Departament de Física de la Universitat Autònoma de Barcelona, Barcelona, Spain
- ^j Also at Departamento de Física e Astronomia, Faculdade de Ciências, Universidade do Porto, Portugal
- ^k Also at Tomsk State University, Tomsk, Russia, Russia
- ^l Also at Università di Napoli Parthenope, Naples, Italy
- ^m Also at Institute of Particle Physics (IPP), Canada
- ⁿ Also at National Institute of Physics and Nuclear Engineering, Bucharest, Romania
- ^o Also at Department of Physics, St. Petersburg State Polytechnical University, St. Petersburg, Russia
- ^p Also at Department of Physics, The University of Michigan, Ann Arbor, MI, USA

- ^q Also at Centre for High Performance Computing, CSIR Campus, Rosebank, Cape Town, South Africa
- ^r Also at Louisiana Tech University, Ruston, LA, USA
- ^s Also at Institutio Catalana de Recerca i Estudis Avancats, ICREA, Barcelona, Spain
- ^t Also at Graduate School of Science, Osaka University, Osaka, Japan
- ^u Also at Department of Physics, National Tsing Hua University, Hsinchu City, Taiwan
- ^v Also at Institute for Mathematics, Astrophysics and Particle Physics, Radboud University Nijmegen/Nikhef, Nijmegen, The Netherlands
- ^w Also at Department of Physics, The University of Texas at Austin, Austin, TX, USA
- ^x Also at CERN, Geneva, Switzerland
- ^y Also at Georgian Technical University (GTU), Tbilisi, Georgia
- ^z Also at Ochadai Academic Production, Ochanomizu University, Tokyo, Japan
- ^{aa} Also at Manhattan College, New York, NY, USA
- ^{ab} Also at Academia Sinica Grid Computing, Institute of Physics, Academia Sinica, Taipei, Taiwan
- ^{ac} Also at School of Physics, Shandong University, Shandong, China
- ^{ad} Also at Department of Physics, California State University, Sacramento, CA, USA
- ^{ae} Also at Moscow Institute of Physics and Technology State University, Dolgoprudny, Russia
- ^{af} Also at Section de Physique, Université de Genève, Geneva, Switzerland
- ^{ag} Also at Eotvos Lorand University, Budapest, Hungary
- ^{ah} Also at Departments of Physics and Astronomy and Chemistry, Stony Brook University, Stony Brook, NY, USA
- ^{ai} Also at International School for Advanced Studies (SISSA), Trieste, Italy
- ^{aj} Also at Department of Physics and Astronomy, University of South Carolina, Columbia, SC, USA
- ^{ak} Also at Institut de Física d'Altes Energies (IFAE), The Barcelona Institute of Science and Technology, Barcelona, Spain
- ^{al} Also at School of Physics and Engineering, Sun Yat-sen University, Guangzhou, China
- ^{am} Also at Institute for Nuclear Research and Nuclear Energy (INRNE) of the Bulgarian Academy of Sciences, Sofia, Bulgaria
- ^{an} Also at Faculty of Physics, M.V. Lomonosov Moscow State University, Moscow, Russia
- ^{ao} Also at Institute of Physics, Academia Sinica, Taipei, Taiwan
- ^{ap} Also at National Research Nuclear University MEPhI, Moscow, Russia
- ^{aq} Also at Department of Physics, Stanford University, Stanford, CA, USA
- ^{ar} Also at Institute for Particle and Nuclear Physics, Wigner Research Centre for Physics, Budapest, Hungary
- ^{as} Also at Flensburg University of Applied Sciences, Flensburg, Germany
- ^{at} Also at University of Malaya, Department of Physics, Kuala Lumpur, Malaysia
- ^{au} Also at CPPM, Aix-Marseille Université and CNRS/IN2P3, Marseille, France
- * Deceased